PHYSICO-CHEMICAL STUDIES OF GLASS FORMING MELTS

ABSTRACT

THESIS SUBMITTED FOR THE DEGREE OF
DOCTOR OF PHILOSOPHY
IN
CHEMISTRY

BY
KAMAL DHAWAN

Department of Chemistry
Aligarh Muslim University Aligarh
April, 1980

PHYSICO-CHEMICAL STUDIES OF GLASS FORMING MELTS

THESIS SUBMITTED FOR THE DEGREE OF
DOCTOR OF PHILOSOPHY
IN
CHEMISTRY

BY
KAMAL DHAWAN

Department of Chemistry
Aligarh Muslim University Aligarh
April, 1980

Department of Chemistry
Aligarh Muslim University
Aligarh

This is to certify that the thesis entitled "Physico-Chemical Studies of Glass Forming Melts" is the original work carried out by Kamal Dhawan under my supervision and is suitable for submission for the award of Ph.D. degree in Chemistry.

(NURUL ISLAM)
Ph.D. (New York)
READER

ACKNOWLEDGEMENT

I express my sincere gratitude to Dr. Nurul Islam, Ph.D. (New York) for his valuable guidance and encouragement during the progress of this work. To Prof. W. Rahman, Head, Department of Chemistry for providing research facilities and to C.S.I.R., New Delhi for financial assistance.

In the last I am also indebted to Dr. N. R. Islam for the suggestions and help and to my research colleagues for their cooperation.

Kamal Dhawan
(KAMAL DHAWAN)

C O N T E N T S

A B S T R A C T

ABSTRACT

The temperature dependence of densities, viscosities and equivalent conductances of molten calcium nitrate tetrahydrate - cobalt(II) nitrate hexahydrate, calcium nitrate tetrahydrate - manganese(II) chloride, cadmium nitrate tetrahydrate - manganese(II) chloride and nickel(II) nitrate hexahydrate - magnesium nitrate hexahydrate systems have been measured at several temperatures for each of the concentrations studied. The logarithmic plots of transport properties against the reciprocal of temperature have been analysed as composed of two regions, i.e. the Arrhenius and the non-Arrhenius region. Such an analysis has been supported by the independent fits for the two regions. A successful applicability of the three current models (the free volume; the Doolittle and the Vogel-Tammann-Fulcher equations; the configurational entropy or the cooperative rearrangement and the Environmental Relaxation models) in explaining the temperature dependence of flow properties of these systems has been demonstrated. This has been achieved by least-squares fitting the data to these models and comparing the best fit parameters which regenerated the experimental data reasonably well. The suitability of these models has been viewed by comparing the energies of activation based

on the computed parameters of each of these models with those of the experimental ones.

The non-linearity of the Arrhenius plots has been accounted for by introducing the ideal glass-transition temperature, T_o whose value reflects the extent of deviation from linearity. This is the only parameter common to the three current models employed and is found to be a linear function of concentration. The opposing trends encountered in the variation of E_γ values with successive increase in solute concentration in the systems studied appear to be guided by the corresponding T_o values which either increase with concentration as a result of increase in the compactness and rigidity of the system or show a downward trend in order to achieve the lower T_o values of the solute as anticipated on the basis of the additive nature of T_o.

The concentration dependence of flow properties of the above melts has been explained by an isoenergic and an apparently isoentropic equations both based on the constant (T/T_o) values in which T is the corresponding temperature in Kelvin. These equations are obtained from the Vogel-Tammann-Fulcher and the Adam-Gibbs configurational entropy model equations. The advantage of these equations lies in their applicability to systems independently of the T_o

values of the two components. They, however, require the linear dependence of the pre-exponential parameter, A_T and the T_0 values.

In addition to the linear dependence of T_0 and A_T on concentration those of A_T and the corrected energies of activation, E_{corr} on T_0 have also been demonstrated. Similarly, in view of the linear dependence of V_0, the intrinsic molar volume at T_0, E_{corr} has been found to vary linearly with V_0.

PART I

TEMPERATURE DEPENDENCE OF TRANSPORT PROPERTIES OF GLASS FORMING MELTS

INTRODUCTION

Even though tremendous amount of work[1-9] has been carried out in the field of electrochemistry of molten salt systems, still unabated interest persists to understand the temperature as well as concentration dependence of transport properties in molecular liquids, ionic liquids, supercooled liquids[10] and many anhydrous and hydrated melts.[11-20] The inability of the rate process theory in explaining the typical transport phenomena in the above systems led many to propose various theories[1,5,9,20] to solve them. In addition to explaining them, these theories have been found to correlate the transport phenomena with the liquid structure particularly in the low temperature region. The three current models employed for this purpose are (1) Cohen and Turnbull's free volume model,[9] (2) Adam and Gibb's configurational entropy model[5] and (3) Simmon and Macedo's environmental relaxation model.[20]

In the case of ordinary liquids the temperature dependence of transport properties was first explained by the Andrade equation,

$$Y = A_{1Y} \exp\left[-k_{1Y}/RT\right] \qquad \ldots (1)$$

where Y may be either viscosity, η , conductance, Λ or

diffusion, D; $A_{\eta Y}$ and $k_{\eta Y}$ are the intercept and slope values, respectively, of Y versus reciprocal of absolute temperature plot and R is the gas constant. Equation (1) is essentially the Arrhenius equation based on the theory of rate process. This equation was found to fail in explaining the temperature dependence of transport properties of associated liquids, supercooled liquids and glass forming melts. The deviation from the Arrhenius behaviour in such liquids was attributed to the relaxation process associated with the temperature dependent energy of activation. This equation also failed to account for the temperature dependence of transport properties under conditions of constant volume.[21]

However, Batchinski[3] studied the pressure dependence of fluidity of liquids and suggested that the appropriate variable which should be related to the viscosity of liquids is the volume expansion and not the temperature. On this basis Batchinski suggested an equation of the form,

$$\eta = B/(V - b) \qquad \ldots (2)$$

where B and b are constants and V is the molar volume of the liquid. The constant b is analogous to that of the van der Walls' equation. This equation was found to explain the temperature dependence of viscosity of associated

liquids over a temperature range of about hundred degrees. However, Hildebrand[22] proposed that the fluidity of a simple liquid at the atmospheric pressure and a given temperature is directly proportional to the free volume, V_f $(= v - v_o)$ and inversely proportional to its intrinsic volume, v_o. Consequently, the Batchinski equation was modified to the form,

$$\phi = B'(v - v_o)/v_o \qquad \ldots (3)$$

where B' is the proportionality constant. This equation too has limited applicability in explaining the temperature dependence of viscosity of associated and supercooled liquids.

These difficulties led Doolittle[7] to develop an expression for the viscous flow of liquids employing the concept of free volume. The resulting Doolittle expression is,

$$\phi = A_{2Y} \exp\left[-B''V_o/V_f\right] \qquad \ldots (4)$$

which accurately represents many viscosity data in the non-Arrhenius region. In equation (4) A_{2Y} and B" are constants. The latter is of the order of unity and V_f is the free volume which is defined as, $V_f = (V - V_o)$ where V is the specific volume mentioned above while V_o is the

limiting specific volume of the liquid at 0 K. Doolittle considered V_f/V_o as the relative free space which is defined as the space arising from the total thermal expansion of the liquid without change of phase. At a fixed pressure, V_f/V_o is a function of temperature only. It is, therefore, evident that the Doolittle's equation predicts an abrupt decrease in fluidity in narrow temperature range where V_f becomes very small. Equation (4) may further be modified to[18]

$$Y = A_{2Y} \exp\left[-k_{2Y}/(V - V_o)\right] \qquad \ldots (5)$$

where A_{2Y} and k_{2Y} are the empirical constants, V_o is defined as the molar intrinsic volume of the substance at the glass transition temperature, T_o, and V is the molar volume at the test temperature.

The Free Volume Model (FVM)

This model was proposed by Cohen and Turnbull.[9] It suggests that the molecular transport in liquids takes place through the process of diffusive displacement of molecular particles into the voids. A void which is assumed to possess a critical size greater than that of the particle is created by the redistribution of "free volume" in the liquid structure without any energy change. Such a void

permits a neighbouring molecule to jump into it thereby hindering the return of the first particle. The probability of finding a void of volume exceeding the critical size has been found to be an exponential function of the ratio of the critical void volume, v^* to the total free volume, V_f. Consequently, the expression for the diffusion coefficient has been derived as

$$D = g\, a\, u \exp\left(-\gamma v^*/V_f\right) \qquad \ldots (6)$$

where g is a geometric factor of the order of $1/6$, 'a' is the particle diameter, u is the velocity of the particle and γ is a correction factor for the overlap of the free volume. The free volume may, further, be taken as approximately equal to the total thermal expansion above the temperature T_0 at which it originates, then

$$V_f = \alpha \bar{V}_m (T - T_0) \qquad \ldots (7)$$

where α is the mean expansion coefficient in the range $T - T_0$ and $\bar{V}_m$ is the mean molecular volume derived from the molar volume. The resulting expression for the diffusion coefficient is given by,

$$D = g\, a\, (3kT/m)^{1/2} \exp\left[-\gamma v^*/\alpha \bar{V}_m (T - T_0)\right] \ldots (8)$$

Since the diffusion coefficient, D is proportional to the

fluidity, ϕ and the electrical conductance, Λ , the above expression has been employed[11-13,23] to describe their behaviour in terms of the relation

$$Y\ (= D, \phi, \Lambda) = A_{5Y} T^{-\gamma/2} \exp\left[-k_{5Y}/(T - T_0)\right] \quad \ldots (9)$$

where $A_{5Y} = g\ a\ (3k/m)^{\gamma/2}$ and $k_{5Y} = \gamma v^*/\alpha \bar{v}_m$. This equation is referred to as the Vogel-Tammann-Fulcher (VTF) equation. It not only takes into account the temperature dependence of transport properties but also the glass forming phenomenon of the test liquids or mixtures and has been adequately employed to describe the temperature dependence of fluidity and conductance in many melts, concentrated electrolytic solutions whether they are glass forming or not within the temperature range T_0 to $2T_0$. However, it fails to explain the transport behaviour in the temperature range, $T/T_0 > 1.3$. Recently, Moynihan and co-workers have shown that the above equation (9) could explain quite accurately the temperature dependence of viscosity of hydrogenated organic liquids and may be employed in the modified form for explaining the concentration dependence also (the latter is to be given in a separate chapter).

The Configurational Entropy Model (CEM)

The plot of entropy versus temperature on extrapolation to the glass transition temperature resulted in

entropy less than the value of the crystalline solid above 0 K. This paradox was later cleared by Gibbs and Dimarzio who resolved that the configurational entropy at the glass transition temperature, T_g vanishes and below T_g its value remains zero. This concept was quantitatively given by Adam and Gibbs.[5] It, therefore, seems that the Cohen and Turnbull's concept of the disappearance of the free volume at T_o resemble that of the Adam and Gibbs' zero configurational entropy at the T_o. They had considered the relaxation properties of the glass-forming liquids and the transition of the cooperatively rearranging groups and suggested an expression for the transition probability, $\bar{\omega}(T)$,

$$\bar{\omega}(T) = \bar{A} \exp \left[- \Delta \mu \, S_c^*/kTS_c \right] \qquad \ldots (10)$$

where $\bar{A}$ is a frequency factor, $\Delta \mu$ is the free energy barrier per mol of particles opposing the cooperative rearrangement, S_c^* is the minimum configurational entropy possessed by the region of a liquid in order to undergo cooperative rearrangement, k is the Boltzmann constant and S_c is the configurational entropy of the system.

The above equation may be simplified by making an approximation,

$$S_c \cong \Delta C_p \ln T/T_o$$

where ΔC_p is the change in heat capacity at the glass transition and its substitution results in the expression,

$$\bar{\omega}(T) = \bar{A} \exp\left[-\Delta\mu S^*_c/kT\,\Delta C_p \ln (T/T_o)\right]$$

which may be rearranged to the form,

$$\bar{\omega}(T) = \bar{A} \exp\left[-k'/T \ln (T/T_o)\right] \qquad \ldots (11)$$

where $k' = \Delta\mu S^*_c/k\,\Delta C_p$.

Since the transition probability, $\bar{\omega}(T)$ is directly related to the mass transport like diffusion, viscosity and conductance, accordingly, equation (11) may be rewritten as,

$$Y = A_{4Y} \exp\left[-k_{4Y}/T \ln (T/T_o)\right] \qquad \ldots (12)$$

where A_{4Y} and k_{4Y} are the empirical parameters. Equation (12) has been found to be adequate in explaining the temperature dependence of transport properties of many hydrated and anhydrous melts. It may be noted that the VTF and the CSM equations are meant for the non-Arrhenius behaviour only; the inclusion of T_o in the expression measures the extent of deviation from the Arrhenius behaviour.

The Environmental Relaxation Model (ERM)

In the study of temperature dependence of transport properties of molten salts and many glass-forming melts it

has been found that the Arrhenius plot shows three distinct regions: (i) the Arrhenian above the melting point of the parent solvent, i.e., at higher temperatures, (ii) the non-Arrhenian below the melting point of the solvent, i.e., in the intermediate temperature range, and finally (iii) a return to the Arrhenian behaviour in the vicinity of the glass-transition temperature, T_g. In view of the difficulties of the VTF and the CEM equations in explaining the overall behaviour for the temperature dependence of such properties Simmons and Macedo[20] proposed a theoretical model by correlating the supercritical fluctuation theory of Ornstein and Zernike to the distribution of relaxation times and activation energies.

The distribution of relaxation times, $g(\ln\tau)$ was log-gaussian in time, and the distribution of activation energies, $g(E)$ was gaussian. The $g(E)$ and the $g(\ln\tau)$ were narrow in the high temperature Arrhenian region. As the temperature was lowered the distribution broadened markedly, while the average activation energy, $\bar{E}$, remained temperature-independent and the most probable relaxation time, τ', remained Arrhenian. This led to the conclusion that the non-Arrhenian viscosity behaviour was due to the broadening in $g(E)$ and $g(\ln\tau)$ which resulted in the appearance of higher as well as lower activation energies. Both the VTF

and the CEM equations generally relate the onset of a non-Arrhenian behaviour to a loss in certain diffusing degrees of freedom or to some increase in the cooperative behaviour as the temperature is lowered, thereby causing an increase in the average activation energy. According to the ERM, the temperature dependence is determined by the activation energy effects and the structural relaxation time and neither by the free volume nor by the configurational entropy as envisaged in the FVM and the CEM.

On the basis of the above view Simmons and Macedo derived (Appendix) an expression for the viscosities. This equation has also been applied to conductances. Such properties have been therefore expressed as

$$\ln Y = \pm \ln(G_{\infty} A)_Y \pm \left\{ R_Y + \tfrac{1}{2} C_{oY} \left[T_e^4 / (T_o^4 + \theta_{oY}^2 (T-T_o)^4) \right]^{3/2} \right\} / RT \qquad \ldots (13)$$

where Y is either viscosity, η (unlike the FVM and the CEM where it stands for fluidity) or equivalent conductance, Λ; and the positive sign refers to η while negative to Λ. G_{∞} is the shear modulus of the material, A is an empirical parameter and other symbols have their usual meaning (Appendix). The above equation has shown its wide applicability to several molten salt systems.[24,25]

In view of the above consideration, the densities, viscosities, and equivalent conductances of molten calcium nitrate tetrahydrate - cobalt(II) nitrate hexahydrate, calcium nitrate tetrahydrate - manganese(II) chloride, cadmium nitrate tetrahydrate - manganese(II) chloride, and nickel(II) nitrate hexahydrate - magnesium nitrate hexahydrate systems were measured as functions of temperature and concentration. The applicability of the models was examined by least-squares fitting the transport data to the current models. An attempt was made to understand the role of the computed parameters and their relative significance in determining the trend in the transport behaviour.

EXPERIMENTAL

Chemicals: Quinoline (Riedel) was distilled before using it as a reference liquid for the calibration of dilatometer and viscometer. Commercial calcium nitrate tetrahydrate (BDH, M.P. 42.7°C), cadmium nitrate tetrahydrate (Reachim, M.P. 59.4°C) and nickel nitrate hexahydrate (BDH, M.P. 56.7°C) were used as solvents, whereas cobalt nitrate hexahydrate (BDH, M.P. 57.0°C), anhydrous manganese(II) chloride and magnesium nitrate hexahydrate (BDH, M.P. 89.0°C) were used as solutes. Anhydrous manganese(II) chloride was prepared as reported.[26]

Determination of water content in hydrated salts: In the cases of hydrated salts the exact water of crystallization was determined before using them for the preparation of samples. In the cases of tetrahydrates of calcium and cadmium nitrates the exact water of crystallization was determined by comparing the measured density data with those of the reported[27,28] values for several concentrations. Such a comparison gave the actual H_2O/Ca^{2+} ratios as 4.06 and 4.03 for two different samples of hydrated calcium nitrate and that of H_2O/Cd^{2+} ratio as 4.18. On the other hand, the exact water content in the cases of hexahydrates of nickel(II), cobalt(II) and magnesium

nitrates were estimated volumetrically using a standard solution of EDTA as titrant.[29] The values of the ratios, H_2O/Ni^{2+}, H_2O/Co^{2+} and H_2O/Mg^{2+} were found to be 6.01, 6.18, and 6.13, respectively.

Temperature control: Preparation of the samples and the measurements of their density, viscosity and conductance were made in a thermostated bath of liquid paraffin. An immersion heater (250 W), a stirrer, a check and a contact thermometer (TGL 4850 MAV = 0.05A = 250 V; GDR) and a relay (Juma type, NT 15.0, 220 V $\simeq$ 15A; Germany) were employed in order to record any variation in temperature by 0.1°C. The actual temperature was recorded by N.B.S. calibrated thermometer meant to record 0-50°, 50-100°, 100-150° and 150-200°C. Each of them was calibrated to record one-tenth of a degree. The overall temperature stability was within $\pm$ 0.1°.

Preparation of samples: During the preparation of samples all the chemicals used were handled with extra care in an atmosphere of pure and dry nitrogen in a dry box containing P_2O_5 to avoid the absorption of moisture by the sample. Required amounts of the solvents were taken in several air tight stoppered glass tubes and immersed in a thermostated paraffin bath maintained at a temperature approximately 10° above the melting point of the parent solvent. After the prelimi-

nary melting, the sample was cooled in a desiccator and weighed again. Alternate melting and cooling was repeated to ensure the constancy in the weight of the solvent. In addition to this, the cooled melt provides a compact surface which minimises the absorption of moisture through diffusion. A known amount of the solute was then added to the molten solvent. Similarly, solutions of several concentrations were prepared by heating them in jacketted tubes in which an inert atmosphere was maintained by flushing the tubes with dry N_2 gas till clear solutions were obtained. The samples thus prepared were cooled and stored in a vacuum desiccator.

Density measurement: The dilatometer employed for measuring the density had a capacity of approximately 7.0 ml and the stem was graduated for recording the variations in volume by 0.01 ml. The markings on the stem were calibrated using the known densities of pure and dry quinoline at the test temperatures. The known densities were obtained from the equation,

$$d_t = \left[1.1090 + 10^{-3}(-0.7542)t + 10^{-6}(-0.1365)t^2 + 10^{-9}(-0.80)t^3\right] + 10^{-4} \times 2,$$

where d_t is the density at $t^\circ C$. The reported values of the parameters of the above equation for quinoline were taken

from the International Critical Table.

For the purpose of calibrating the dilatometer a known amount of quinoline was transferred to the dilatometer. The lower meniscus of the liquid was made to coincide with each of the marks of the graduated stem by adjusting the temperature of the bath. The thermal expansion of the dilatometer was neglected as being small. This expansion was also compensated in calibration as the markings read the expected volume based on the reported densities at the desired temperature, d_t. The values of the calculated volume of quinoline were plotted against the divisions on the stem of the dilatometer for use. A weighed amount of the molten salt sample was then transferred to the calibrated dilatometer with the help of a vacuum pump. The dilatometer was then immersed in the thermostated bath and the volumes of the melt were recorded at several temperatures. The accuracy of these measurements was within $\pm$ 0.3% as determined by comparing the reported densities of toluene with those obtained experimentally using the calibrated volume based on the densities of the reference liquid, quinoline.

Measurement of viscosity: Cannon-Ubbelohde[30] viscometer was used for the measurement of viscosity of the samples. The viscometer consists of three parallel arms, viz.,

receiving, measuring and auxillary to form the suspended level arrangement in a triangular fashion. The receiving tube forms a 'U' with the measuring tube through a bulb D. Bulb A and another fiducial bulb B slightly below the former were sealed to the measuring tube. Two fiducial marks 'a' and 'b' on the bulbs A and B were used for recording the efflux time. The auxillary tube was sealed to the receiving tube through a bulb C. The bulbs B and C were connected with each other through a capillary tube of appropriate length and diameter. It was designed in such a way that the centres of gravity of the three bulbs A, B and C were aligned vertically to reduce the effect of acceleration due to gravity. Special feature of a suspended level viscometer was that the capillary effects of the two liquid surfaces were neutralized by each other.

To measure the viscosity the viscometer was clamped in a vertical position in a thermostated bath and filled with the required amount of the test liquid. The volume of the liquid taken was adequate to avoid any air bubble being introduced in the capillary while the fiducial bulb B was filled. To avoid the absorption of moisture by the sample, the open ends of the viscometer were attached to the anhydrous calcium chloride tubes. Then the viscometer was allowed to stand in the thermostated bath for about

half an hour before recording the data so that the thermal fluctuation in the viscometer was minimum. The sample was sucked into the measuring bulb A with the help of a vacuum pump and was allowed to stand for a few minutes by closing the calcium chloride tubes with the rubber corks. The rubber cork stoppers were then removed from the tubes and the time of fall of the melt from the upper fiducial mark 'a' to the lower mark 'b' was recorded several times with the help of a stop watch and the mean of almost identical readings was taken. The reproducibility in the time of fall was found to be $\pm$ 0.2 to 0.5% in several samples studied. The viscometer constant, β was determined by using the reported viscosities of quinoline. The β values at the temperature of interest were employed to determine the corresponding viscosity values. The accuracy in the viscosity measurements was therefore, based on those of the density and the time of fall of this sample and was on the average of the order of 0.3% x 0.35 ($= \rho \times t$) $\approx$ 0.11%. The density as well as viscosity measurements were made in a descending order of temperature. Poiseuille's equation was employed for calculating the viscosity. This equation is of the form

$$\eta = \pi h \rho g r^4 t / 8 l V$$

where h is the height of the liquid column in the visco-

meter, ρ the density, g is the acceleration due to gravity, r is the radius of the capillary of the viscometer, l is its length and t is the time of fall for the liquid of volume V. The above relation may also be expressed as

$$\eta = \rho \beta t$$

where $\beta = \pi h r^4 g t / 8 l V$ is termed the viscometer constant and varies from viscometer to viscometer. The unit of viscosity is N m^{-2}s (Newton per square meter-second).

Conductance measurement: The conductance measurements were made with the help of a conductivity bridge (Toshniwal model CL 01-02 A. Sl. No. 939) at a frequency of 50 c/s. The capillary type cells of high cell constant values were used for this purpose. The cell was prepared by sealing two platinum foils of an area of 0.25×10^{-4} m^2 to the ends of the two platinum wires. The foils in turn were sealed to the ends of two corning glass tubes. The two electrodes thus fabricated were properly fixed into the two limbs of the 'U'-shaped corning glass tube having a capillary in its lower part. The cell constant was determined by using a decinormal solution of recrystallised potassium chloride in triply distilled water and was found to be 732.5×10^2 m^{-1}. For the measurement of conductance the melt was filled in the above conductivity cell and suspended in the

thermostated bath. Then the electrodes were properly fixed into the limbs of the capillary cell in such a way that the platinum foils were fully dipped into the molten sample. It was ensured that no air bubble sticked to the surface of the electrode or that of the capillary. At the same time the absorption of moisture by the sample was avoided by keeping the platinum electrodes fixed air tightly into the limbs through the glass joints. The precision of the instrument was within ± 0.2 to 2.5% and the accuracy of the measurements was found to be less than ± 2%. The measured conductance did not show any frequency dependence.

The conductances of the samples were recorded at several temperatures, and the corresponding equivalent conductances calculated.

Details of computation: A non-linear least-squares routine (FITTEM, Sub-routine: FUNCT) was used for fitting the viscosity and conductance data to the five parameter ERM equation (13). The T_0 being thermodynamic quantity was taken from the VTF/CEM fittings while the guess values for the remaining four parameters were close to those found earlier (N. Islam and Ismail Kashi, J. Polymer Sci., Nov. issue 17, 1979) for similar melts. The initial values of the steps for the variation of parameters were given as 1.0 for the lower numerical values of the guess parameters, while 2.0

for those of the higher ones. The set of best fit parameters computed in the first run were fed to the computer for the second run with steps reduced to 0.5 and 1.0 in the above cases. Such a cycle was repeated 25 to 30 times for every set of data in succession so that every time there was an improvement in the values of the standard deviation over the previous ones. The steps for the variation of parameters were eventually reduced to 0.001 and 0.01 in the last few runs. Finally, the best fit parameters thus obtained with remarkably reduced values of the standard deviations were those which reproduced the experimental data reasonably well.

A word of caution may be noted that a low value of the standard deviation is sometimes quite misleading as the corresponding parameters representing that deviation may either be physically unsound or they yield occassionally quite erroneous experimental results, and therefore, they are to be discarded. For example, in the present case some of the sets though showed minimum deviations the values of the parameters, θ_{ss} A turned out to be negative and therefore those sets were rejected.

RESULTS AND DISCUSSION

Solubility of solutes in solvents: Unlike the mixtures of hydrated melts the solubility of anhydrous manganese (II) chloride in molten tetrahydrates of calcium and cadmium nitrates may be viewed through the presence of associated species of the type MNO_3^+, where M = Ca^{2+} and Cd^{2+}, the presence of which has been reported earlier.[31] Addition of these anhydrous solutes to the above hydrated melts appears to facilitate the formation of MNO_3^+ species through the dehydration of an equivalent amount of hydrated cations, $M(H_2O)_4^{2+}$ of the melt in accordance with the explanation given for LiCl or CsCl added to molten calcium nitrate tetrahydrate.[32] The maximum solubility of anhydrous manganese(II) chloride may refer to the optimum concentration of MNO_3^+ species obtainable by dehydration. Therefore, qualitatively a higher solubility may be expected if the association constant for the formation of MNO_3^+ species is higher.

Measurements of density, viscosity and electrical conductance of pure as well as those of the mixtures of calcium nitrate tetrahydrate - cobalt nitrate hexahydrate, calcium nitrate tetrahydrate - manganese(II) chloride and cadmium nitrate tetrahydrate - manganese(II) chloride

system were made as functions of temperature and concentration. Densities and viscosities of various concentrations of mixtures of hexahydrates of nickel(II) and magnesium nitrates were also recorded at several temperatures. Density data of all the systems studied were found to vary linearly with temperature and therefore, were least squares fitted to the equation,

$$\rho = a - bT \quad (K) \qquad \ldots (14)$$

where ρ is the density, a and b are empirical parameters and T is the absolute temperature. The values of the best-fit parameters and the calculated coefficients of thermal expansion, α are listed in Table 1.

The molar volumes (Tables 2-5) were calculated from the corresponding density data for various concentrations at several temperatures. The measured equivalent conductance and fluidity, ϕ (reciprocal of viscosity) of all the systems studied are given in Tables 6-9 as functions of temperature and concentration.

<u>The Free Volume Model (FVM)</u>: In order to explain the temperature dependence of transport properties of the systems under investigation ln Y (Y = ϕ or Λ) were plotted against the reciprocal of temperature (Figs. 1-7). The temperature dependence of transport properties show an

TABLE 1 : Parmeters for Density Equation and Expansivities

Molten salt syetems	mol%	a	b x 10^{-3}	10^4 at 345K deg^{-1}
$Ca(NO_3)_2 \cdot 4.06H_2O$ + $Co(NO_3)_2 \cdot 6.18H_2O$	Co^{2+}			
	0.00	1.9738	0.7691	4.4973
	10.13	2.0029	0.8276	4.8146
	19.55	1.9938	0.7796	4.5158
	29.70	2.0027	0.7992	4.6236
	39.80	1.9884	0.7648	4.4215
	49.56	2.0042	0.8184	4.7375
	59.51	1.9885	0.7721	4.4694
	69.68	1.9970	0.8436	4.9278
$Cd(NO_3)_2 \cdot 4.18H_2O$ + $MnCl_2$	Mn^{2+}			
	0.00	2.6012	1.0739	4.8096
	2.50	2.5619	1.0756	4.9044
	5.35	2.5569	1.0577	4.8169
	7.88	2.5548	1.0802	4.9453
	9.83	2.5621	1.0605	4.8239
	12.49	2.5741	1.0697	4.8464

(continued)

TABLE 1 : (continued)

Molten salt systems	mol%	a	b x 10^{-3}	10^4 at 343K deg^{-1}
$Ca(NO_3)_2.4.05H_2O$ +				
$MnCl_2$	Mn^{2+}			
	0.00	1.9836	0.7977	4.6649
	1.05	1.9831	0.7992	4.6763
	2.02	1.9998	0.8308	4.8446
	3.50	1.9869	0.7775	4.5199
	4.99	1.9819	0.7654	4.4519
	7.02	2.0021	0.8015	4.6406
$Ni(NO_3)_2.6.01H_2O$ +				
$Mg(NO_3)_2.6.15H_2O$	Mg^{2+}			
	0.00	2.1273	0.9070	4.9944
	5.41	2.1292	0.9496	5.2650
	9.64	2.1216	0.9550	5.3230
	14.67	2.1113	0.9587	5.3785
	20.11	2.0844	0.9296	5.2653
	25.43	2.0797	0.9589	5.4748
	30.03	2.0698	0.9585	5.5054

TABLE 2 : Molar Volumes (10^{-6} m^3/mol) as Functions of Temperature and Concentration for $Ca(NO_3)_2.4.06H_2O$ + $Co(NO_3)_2.6.18H_2O$ Molten Salt System

	mol % Co^{2+}							
T/K	0.00	10.13	19.55	29.70	39.80	49.56	59.51	69.68
303.0	136.3	138.7	141.3	144.4	148.0	151.2	-	-
308.0	136.6	139.0	141.6	144.7	148.3	151.5	155.1	-
313.0	136.9	139.4	142.0	145.0	148.6	151.9	155.5	160.0
318.0	137.2	139.7	142.3	145.4	149.0	152.2	155.8	160.4
323.0	137.5	140.0	142.6	145.7	149.3	152.6	156.2	160.8
328.0	137.9	140.4	142.9	146.4	149.6	153.0	156.5	161.2
333.0	138.1	140.7	143.2	146.5	149.9	153.3	156.9	161.6
338.0	138.4	141.0	143.6	146.7	150.3	153.7	157.2	162.0
343.0	138.7	141.4	143.9	147.1	150.6	154.1	157.6	162.4

TABLE 5 : Molar Volumes (10^{-6} m^3/mol) as Functions of Temperature and Concentration for $Ca(NO_3)_2 \cdot 4.05H_2O$ + $MnCl_2$ Molten Salt System

	mol % of Mn^{2+}					
T/K	0.00	1.05	2.02	3.50	4.99	7.02
313.0	136.5	135.9	134.8	133.5	132.7	130.7
318.0	136.8	136.2	135.1	133.8	133.0	131.0
323.0	137.1	136.5	135.4	134.1	133.2	131.3
328.0	137.6	136.9	135.7	134.4	133.6	131.6
333.0	137.8	137.2	136.1	134.7	133.8	131.9
338.0	138.1	137.5	136.4	135.0	134.1	132.2
343.0	138.4	137.8	136.7	135.3	134.4	132.5
348.0	138.7	138.1	137.0	135.6	134.7	132.8
353.0	139.1	138.5	137.4	136.0	135.0	133.1

TABLE 4 : Molar Volumes(10^{-6} m^3/mol) as Functions of Temperature and Concentration for $Cd(NO_3)_2 \cdot 4.18H_2O$ + $MnCl_2$ Molten Salt System

	mol % of Mn^{2+}					
T/K	0.00	2.50	5.35	7.88	9.83	12.49
313.0	137.5	137.9	135.4	133.9	131.5	128.8
318.0	137.9	138.3	135.7	134.3	131.8	129.0
323.0	138.2	138.6	136.1	134.6	132.1	129.4
328.0	138.5	138.9	136.4	134.9	132.5	129.7
333.0	138.9	139.3	136.7	135.3	132.8	130.0
338.0	139.2	139.6	137.0	135.6	133.1	130.3
343.0	139.5	139.9	137.4	135.9	133.4	130.6
348.0	139.9	140.3	137.7	136.3	133.7	131.0

TABLE 5 : Molar Volumes (10^{-6} m^3/mol) as Functions of Temperature and Concentration for $Ni(NO_3)_2.6.01H_2O$ + $Mg(NO_3)_2.6.15H_2O$ Molten Salt System

	mol % of Ni^{2+}						
T/K	0.00	5.41	9.64	14.67	20.11	25.43	30.05
323.0	158.6	158.7	158.8	-	-	-	-
328.0	159.0	159.1	159.2	-	-	-	-
333.0	159.4	159.5	159.6	159.8	160.3	-	-
338.0	159.9	160.0	160.1	160.1	160.7	161.1	161.1
343.0	160.3	160.4	160.5	160.6	161.1	161.5	161.6
348.0	160.7	160.8	160.9	161.0	161.6	162.0	162.0
353.0	161.1	161.2	161.3	161.5	162.0	162.4	162.5
358.0	161.5	161.7	161.8	161.9	162.4	162.9	163.0
363.0	161.9	162.1	162.2	162.4	162.9	163.3	163.4
368.0	162.3	162.5	162.6	162.8	163.3	163.8	163.8
373.0	162.7	163.0	163.1	163.2	163.7	164.2	164.3
378.0	163.1	163.4	163.5	163.7	164.2	164.7	164.8
383.0	163.5	163.8	164.0	164.1	164.6	165.1	165.2

TABLE 6 : Equivalent Conductance ($10^4\Lambda$, S m^2 $equiv^{-1}$) and Fluidity ($10^{-1}\phi$, N^{-1} m^2 s^{-1}) data as Functions of Temperature and Concentration (mol% of Co^{2+}) for $Ca(NO_3)_2 \cdot 4.06H_2O$ + $Co(NO_3)_2 \cdot 6.18H_2O$ molten salt system

T/K	0.00	10.13	19.55	29.70	39.80	49.56	59.51	69.68
303.0	0.4657	0.5214	0.5530	0.5775	0.6314	0.6702	-	-
	(0.5040)	(0.6641)	(0.7775)	(0.8221)	(1.0136)	(1.0310)		
308.0	0.6113	0.6574	0.7081	0.7372	0.7957	0.8398	0.8789	-
	(0.7030)	(0.9249)	(1.1048)	(1.1136)	(1.3099)	(1.3431)	(1.5959)	
313.0	0.7857	0.8518	0.8969	0.9242	0.9755	1.0377	1.0758	1.3443
	(0.9443)	(1.2458)	(1.3691)	(1.4572)	(1.6800)	(1.7314)	(1.9946)	(2.3677)
318.0	0.9977	1.0502	1.1143	1.1505	1.1914	1.2662	1.2846	1.6063
	(1.2539)	(1.6039)	(1.7817)	(1.8783)	(2.0433)	(2.1903)	(2.4846)	(2.8754)
323.0	1.2486	1.2996	1.3571	1.3973	1.4464	1.5039	1.5365	1.9160
	(1.5992)	(2.0318)	(2.1678)	(2.3472)	(2.6009)	(2.6609)	(3.0863)	(3.4975)
328.0	1.5017	1.5518	1.6281	1.6893	1.7376	1.7514	1.7961	2.2418
	(2.0172)	(2.5254)	(2.6812)	(2.9136)	(3.1553)	(3.2210)	(3.7056)	(4.2426)

(continued)

TABLE 6 : (continued)

T/K	0.00	10.13	19.55	29.70	39.80	49.56	59.51	69.68
333.0	1.7843	1.8557	1.8923	1.9174	2.0098	2.0285	2.0423	2.5822
	(2.4699)	(3.0868)	(3.2701)	(3.5061)	(3.7532)	(3.8690)	(4.3354)	(4.9033)
338.0	2.1155	2.2089	2.2965	2.2981	2.3040	2.4566	2.4942	2.9673
	(2.9701)	(3.7005)	(3.9270)	(4.1056)	(4.4207)	(4.6781)	(5.0739)	(5.8109)
343.0	2.4259	2.5068	2.5757	2.6707	2.6956	2.7075	2.7106	3.3878
	(3.5211)	(4.3628)	(4.6471)	(4.9052)	(5.2030)	(5.3870)	(5.9030)	(6.7286)

Fluidity data are given within parentheses.

TABLE 7 : Equivalent Conductance ($10^4\Lambda$, S m^2 $equiv^{-1}$) and Fluidity ($10^{-1}\phi$, N^{-1} m^2 s^{-1}) data as Functions of Temperature and Concentration (mol% of Mn^{2+}) for $Ca(NO_3)_2.4.03H_2O$ + $MnCl_2$ molten salt system

T/K	0.00	1.05	2.01	3.50	4.99	7.02
313.0	0.7377	0.7107	0.6343	0.6052	0.5666	0.4785
	(0.8908)	(0.8272)	(0.7702)	(0.7039)	(0.6256)	(0.5339)
318.0	0.9541	0.9023	0.8007	0.7698	0.6954	0.6395
	(1.1640)	(1.1036)	(1.0426)	(0.9246)	(0.8401)	(0.7390)
323.0	1.1953	1.0947	0.9796	0.9352	0.8595	0.7783
	(1.5050)	(1.4130)	(1.3287)	(1.1928)	(1.1023)	(0.9862)
328.0	1.3898	1.3358	1.1949	1.1482	1.0709	0.9636
	(1.8590)	(1.7799)	(1.6880)	(1.5534)	(1.4637)	(1.2722)
333.0	1.6812	1.6019	1.4468	1.3856	1.3066	1.1498
	(2.3001)	(2.1980)	(2.0903)	(1.9239)	(1.7902)	(1.6121)
338.0	1.9740	1.8833	1.7832	1.5765	1.5434	1.4060
	(2.7802)	(2.6703)	(2.5514)	(2.3680)	(2.2131)	(2.0121)
343.0	2.2682	2.2100	2.0497	1.9345	1.8163	1.6634
	(3.3218)	(3.1914)	(3.0700)	(2.8693)	(2.6815)	(2.4401)
348.0	2.6363	2.5282	2.4011	2.2699	2.1140	1.9452
	(3.9300)	(3.7802)	(3.6516)	(3.4100)	(3.2616)	(2.9552)
353.0	2.9334	2.8720	2.7782	2.5594	2.4012	2.2631
	(4.5651)	(4.4209)	(4.2662)	(3.9976)	(3.7823)	(3.5091)

Fluidity data are given within parentheses.

TABLE 8 : Equivalent Conductance ($10^4\Lambda$, S m^2 $equiv^{-1}$) and Fluidity ($10^{-1}\phi$, N^{-1} m^2 s^{-1}) data as Functions of Temperature and Concentration (mol% of Mn^{2+}) for $Cd(NO_3)_2.4.18H_2O$ + $MnCl_2$ molten salt system

T/K	0.00	2.50	5.35	7.88	9.83	12.49
313.0	1.9163	2.1252	1.8866	1.8096	1.6379	1.3863
	(2.5720)	(3.0622)	(2.7522)	(2.6135)	(2.3363)	(2.0070)
318.0	2.2993	2.4806	2.2635	2.1825	1.9608	1.7166
	(3.1730)	(3.7526)	(3.3929)	(3.2291)	(2.8857)	(2.5107)
323.0	2.7132	3.0132	2.6710	2.5573	2.3292	2.0758
	(3.8404)	(4.5614)	(4.1002)	(3.9168)	(3.5323)	(3.0832)
328.0	3.1291	3.4665	3.0804	2.9623	2.7682	2.4367
	(4.6042)	(5.4210)	(4.9319)	(4.6318)	(4.2665)	(3.7399)
333.0	3.6642	3.9099	3.5783	3.4265	3.1672	2.8131
	(5.4392)	(6.3326)	(5.8001)	(5.4072)	(5.0782)	(4.4467)
338.0	4.1432	4.4794	4.0208	3.8929	3.5682	3.2464
	(6.3719)	(7.3621)	(6.7128)	(6.3428)	(5.9383)	(5.2369)
343.0	4.7123	4.9630	4.5524	4.4765	4.1119	3.6679
	(7.2730)	(8.4819)	(7.7616)	(7.3097)	(6.9011)	(6.1101)
348.0	5.3147	5.6269	5.2028	5.0054	4.6301	4.2296
	(8.3808)	(9.5845)	(8.8553)	(8.3813)	(7.9322)	(7.0462)

Fluidity data are given within parentheses.

TABLE 9 : Fluidity ($10^{-1}\phi$, $N^{-1}\ m^2\ s^{-1}$) data as Functions of Temperature and Concentration (mol% of Mg^{2+}) for $Ni(NO_3)_2.6.01H_2O$ + $Mg(NO_3)_2.6.15H_2O$ molten salt system

T/K	0.00	5.41	9.64	14.67	20.11	25.43	30.03
323.0	1.867	1.890	1.911	-	-	-	-
328.0	2.248	2.280	2.328	-	-	-	-
333.0	2.681	2.712	2.737	2.805	2.964	-	-
338.0	3.127	3.163	3.210	3.404	3.473	3.590	3.641
343.0	3.629	3.660	3.702	3.952	4.014	4.139	4.203
348.0	4.216	4.241	4.278	4.533	4.599	4.740	4.807
353.0	4.815	4.856	4.916	5.162	5.233	5.343	5.460
358.0	5.491	5.547	5.564	5.840	5.923	6.062	6.127
363.0	6.164	6.209	6.272	6.386	6.560	6.752	6.917
368.0	6.942	7.029	7.075	7.328	7.411	7.560	7.705
373.0	7.872	7.882	7.924	8.247	8.313	8.369	8.650
378.0	8.785	8.888	9.029	9.108	9.168	9.356	9.505
383.0	9.602	9.732	9.907	9.984	10.143	10.293	10.497

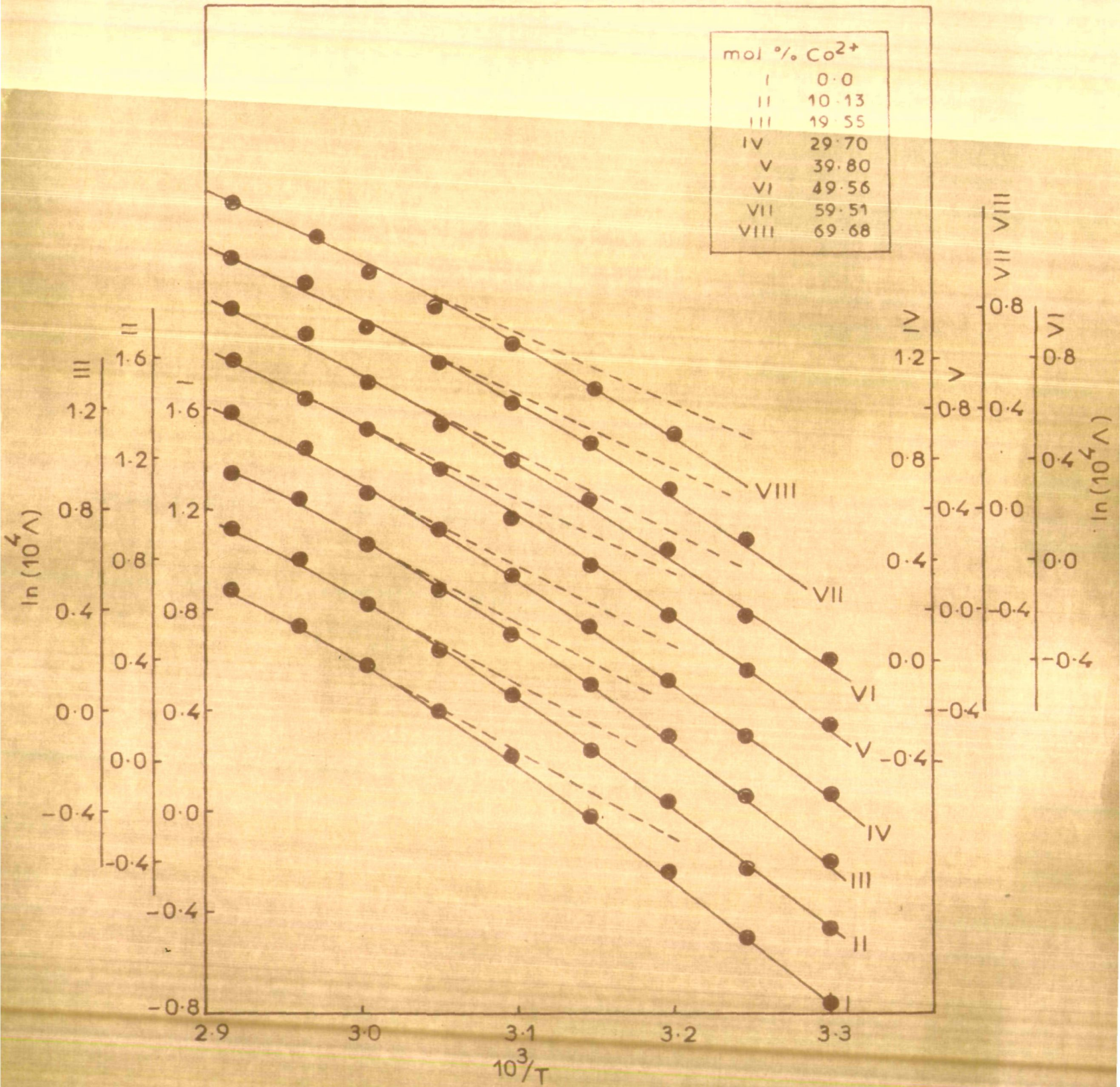

Fig. 1 Arrehenius plots of Equivalent Conductance for $Ca(NO_3)_2 \cdot 4 \cdot 06H_2O - Co(NO_3)_2 \cdot 6 \cdot 18H_2O$ Molten Salt System.

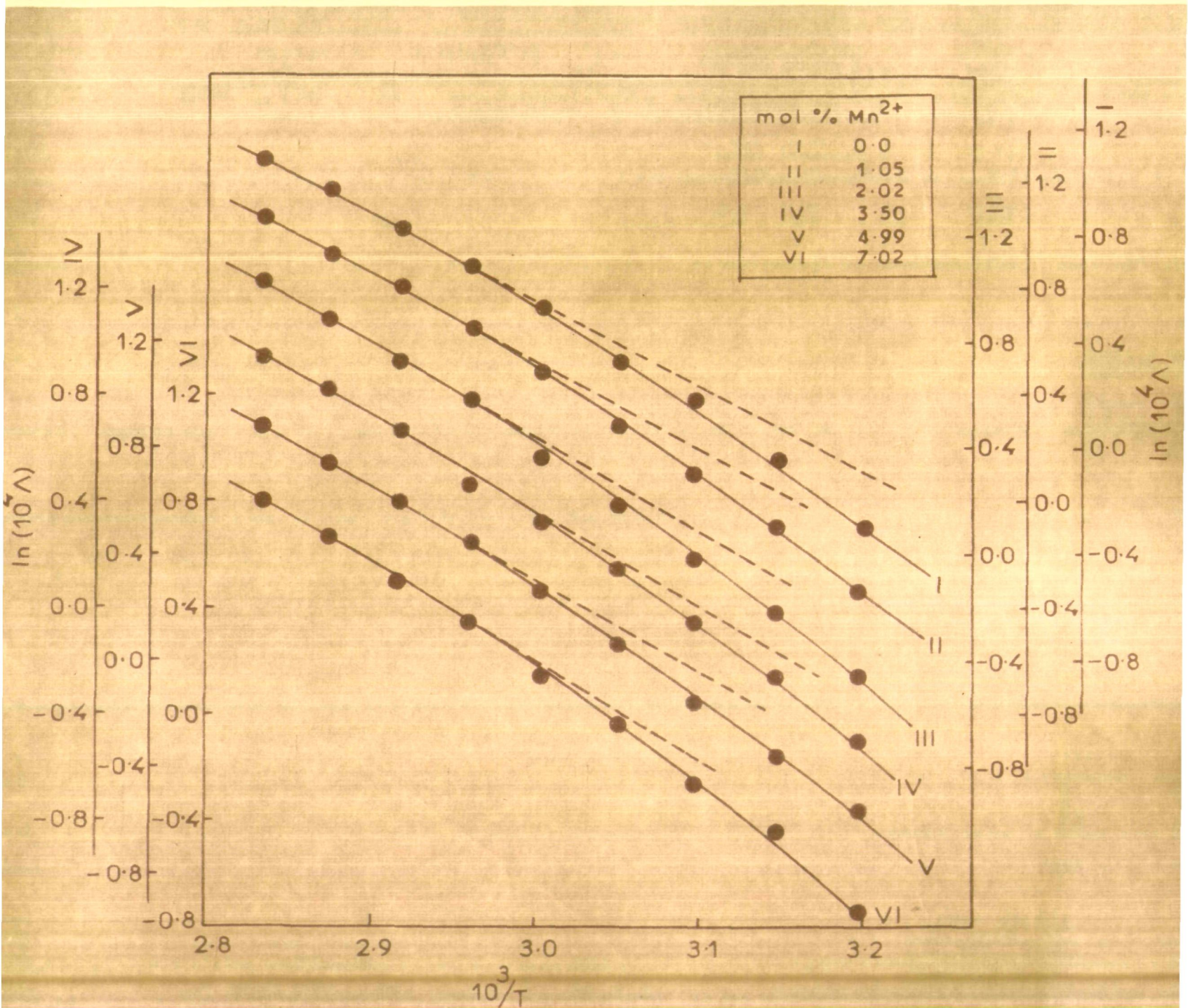

Fig. 2 Arrehenius plots of Equivalent Conductance for $Ca(NO)_3 \cdot 4 \cdot 03H_2O - MnCl_2$ Molten Salt System.

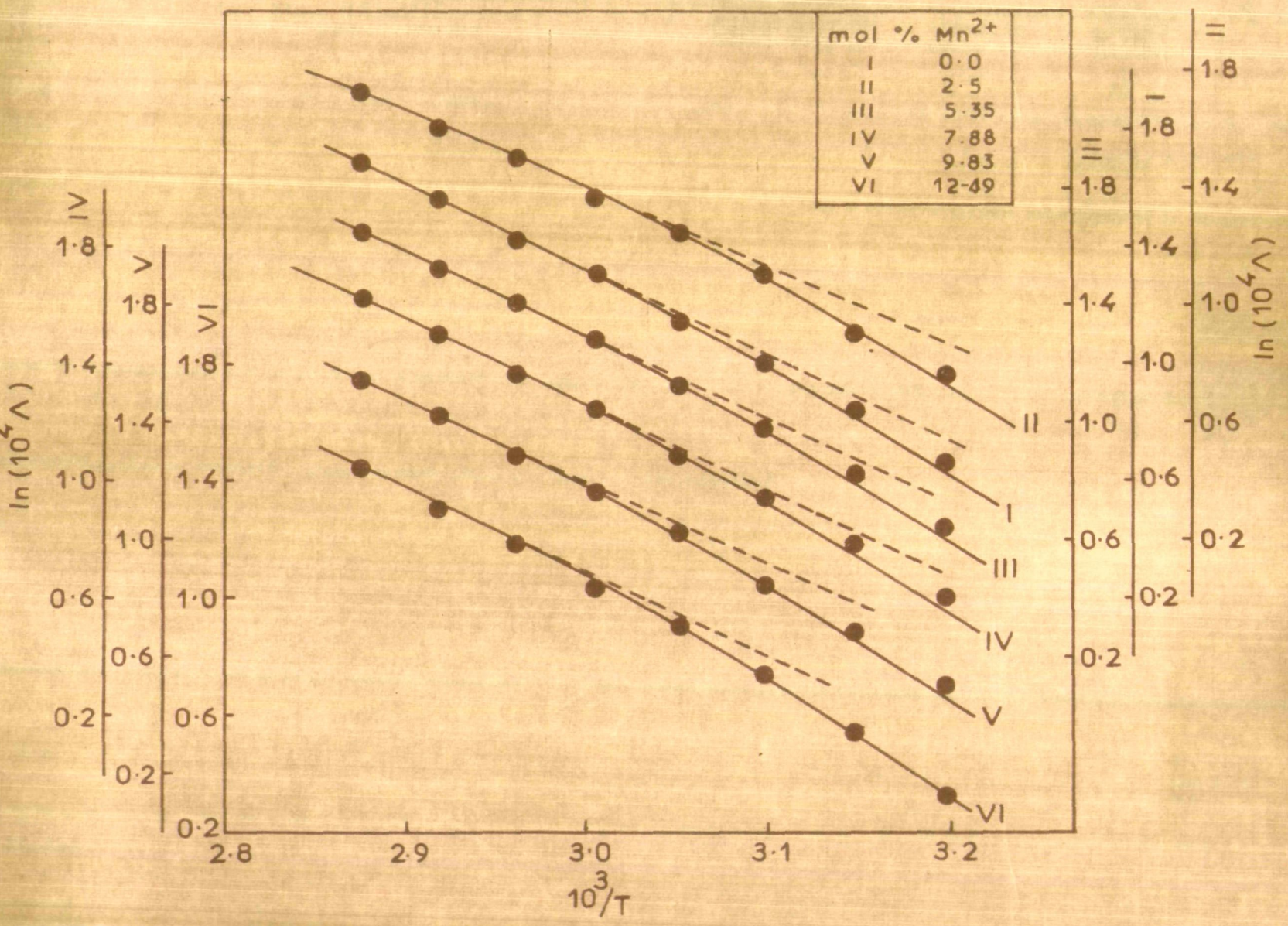

Fig. 3 Arrehenius plots of Equivalent Conductance for $Cd(NO_3)_2 \cdot 4 \cdot 18H_2O - MnCl_2$ Molten Salt System.

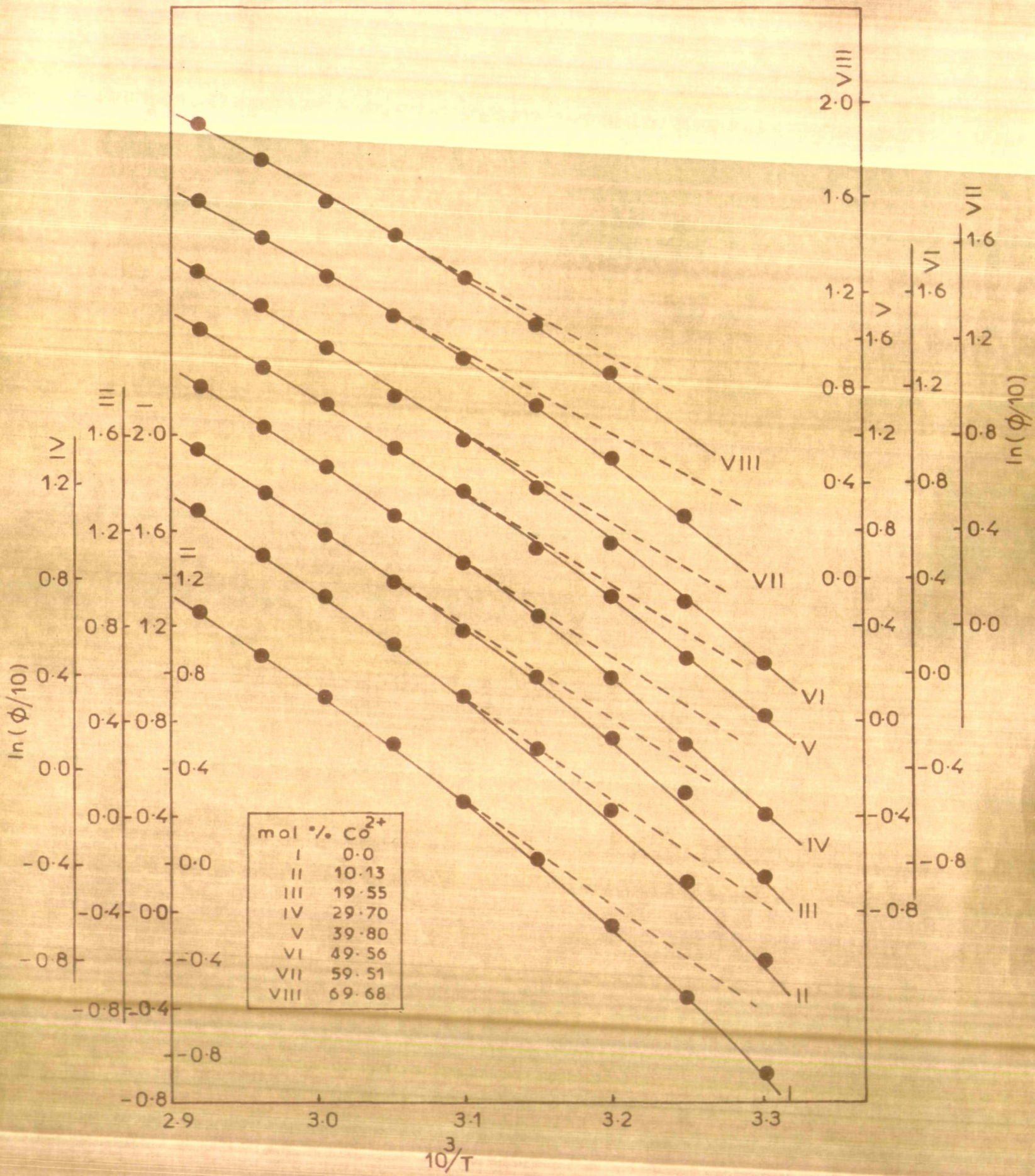

Fig. 4 Arrehenius plots of Fluidity for $Ca(NO_3)_2 \cdot 4{\cdot}06H_2O - Co(NO_3)_2 \cdot 6{\cdot}18H_2O$ Molten Salt System.

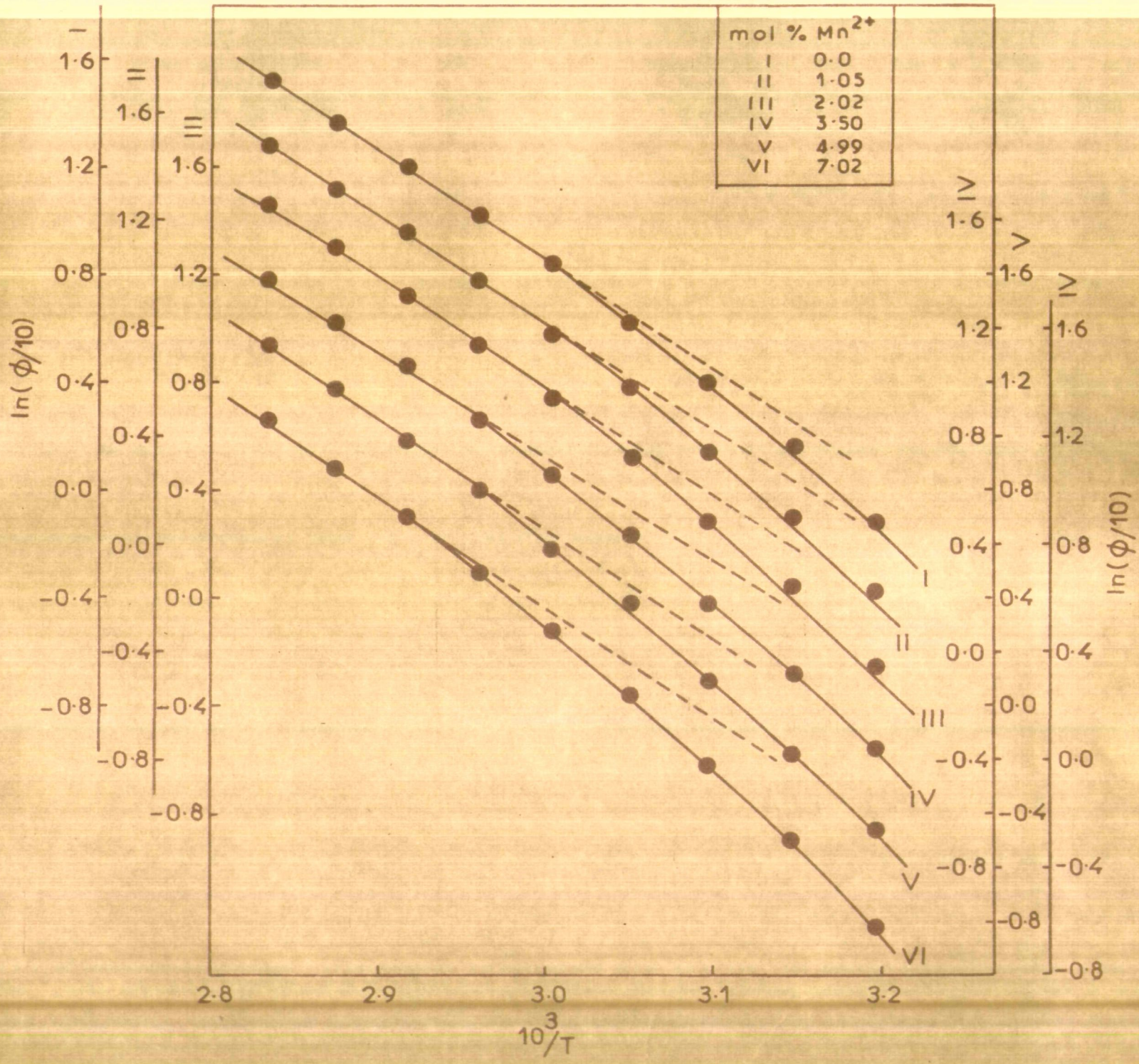

Fig. 5 Arrehenius plors of Fluidity for $Ca(NO_3)_2\ 4{\cdot}03H_2O-MnCl_2$ Molten Salt System.

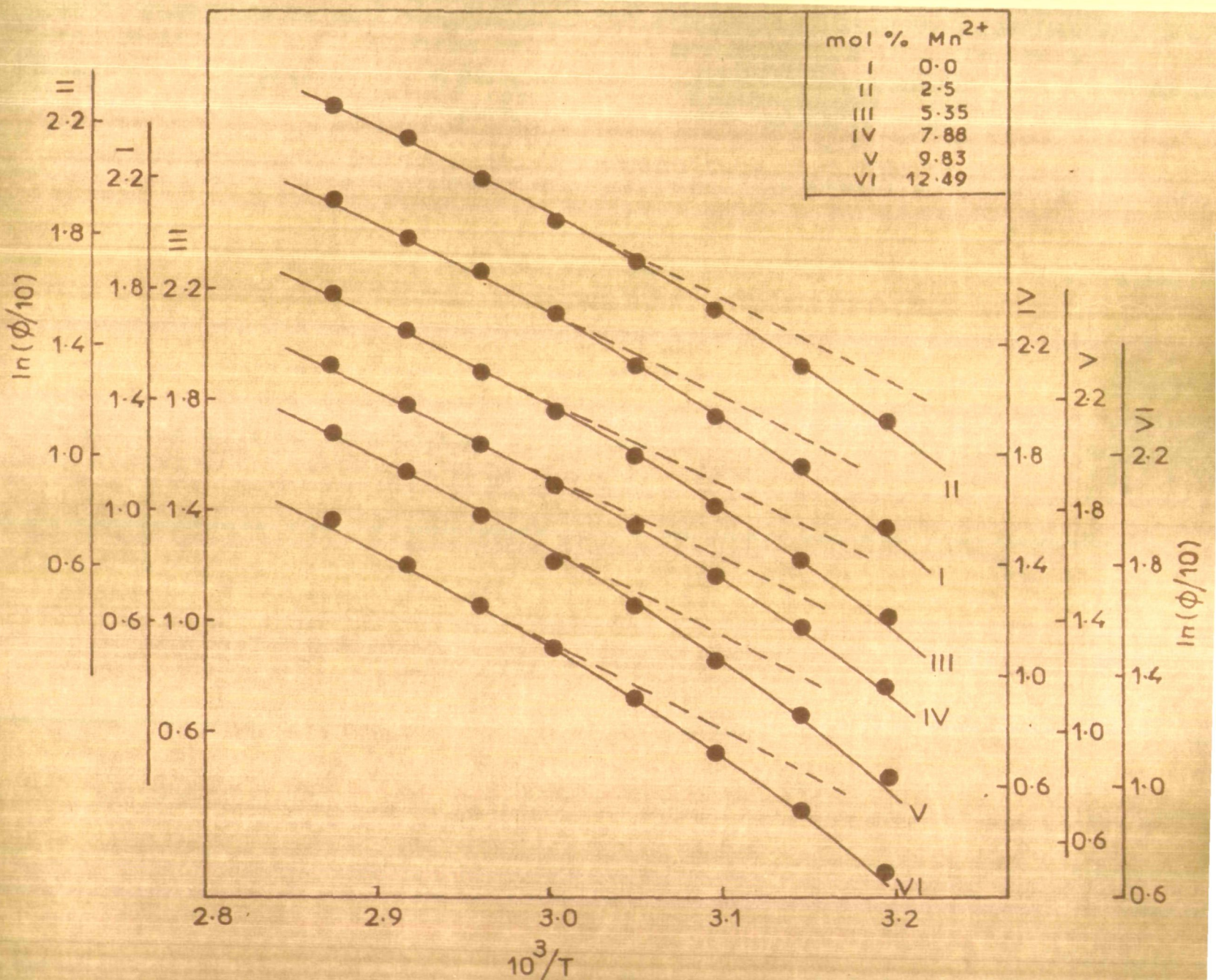

Fig. 6 Arrehenius plots of Fluidity for $Cd(NO_3)_2 \cdot 4{\cdot}18H_2O - MnCl_2$ Molten Salt System.

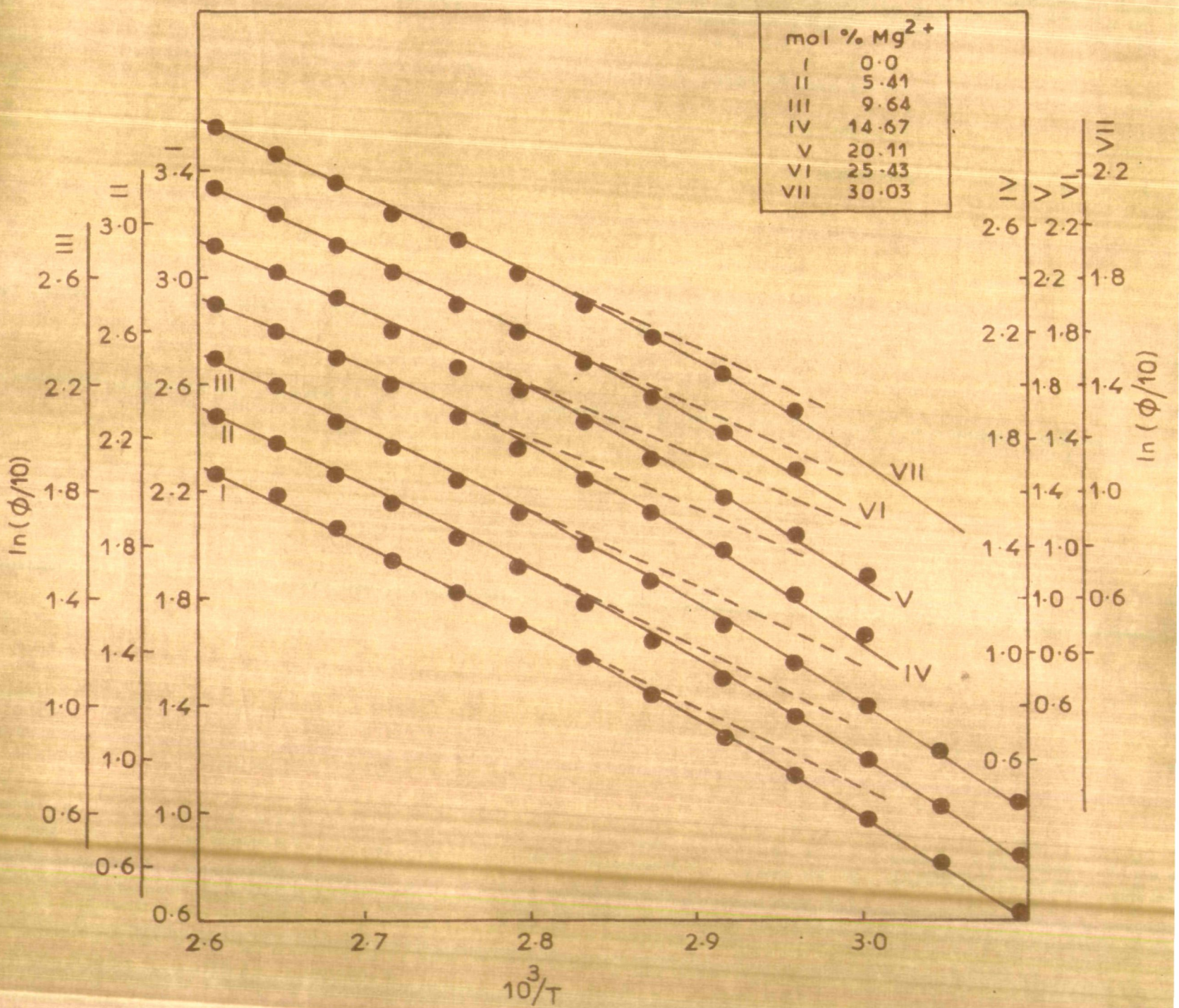

Fig. 7 Arrehenius plots of Fluidity for $Ni(NO_3)_2 \cdot 6\,01H_2O - Mg(NO_3)_2 \cdot 6\,13H_2O$ Molten Salt System.

overall non-Arrhenius behaviour.

In view of the failure of the rate process theory in explaining the temperature dependence of transport properties, the free volume model was employed. Such a model accounts for the non-Arrhenius behaviour. Therefore, the fluidity and the conductance data were least-squares fitted to the three parameters' Vogel-Tammann-Fulcher (VTF) equation, based on the concept of free volume. The best fit parameters thus obtained together with the standard deivations in ln ϕ and ln Λ are given in Table 10-13. The values of these parameters were chosen in a manner similar to those adopted by Moynihan[14,27] and others.[33] Accordingly, the empirical rule regarding the universal constant values of $k_{3\phi} \approx 690$ and $k_{3\Lambda} \approx 600$ were taken into consideration during computation. Thus a constant k_Y value comprising a meaningful set of A_{3Y}, k_{3Y} and T_o giving minimum standard deviation was selected. The linear plots of $\ln(YT^{1/2})$ versus $1/(T-T_o)$ further support the applicability of the VTF equation to such systems as shown in Figs. 8-11. The above best fit parameters were computed considering all the data points of a single plot. However, it appears from Figs. 1-7 that the transport properties exhibit Arrhenius behaviour, particularly in the region above the melting temperature of the parent solvent, and show a tendency for the deviation from

TABLE 10: Computed Parameters for VTF Equation for the Fluidity and Equivalent Conductance of $Ca(NO_3)_2 \cdot 4.06H_2O$ + $Co(NO_3)_2 \cdot 6.18H_2O$ Melts

Mol % Co^{2+}	$A_{3\phi}$	$k_{3\phi}$	$T_{o,\phi}$	Std dev in ln ϕ	$A_{3\Lambda}$	$k_{3\Lambda}$	$T_{o,\Lambda}$	Std dev in ln Λ
0.00	9050.3	670.2	205.0	0.012	2941.6	580.0	204.4	0.012
10.13	9335.0	670.0	202.9	0.012	3073.4	588.9	202.3	0.012
19.55	9670.1	670.0	200.8	0.020	3205.3	584.7	200.3	0.012
29.70	9980.2	679.6	198.8	0.014	3370.2	587.8	198.1	0.018
39.80	10290.0	670.0	196.7	0.014	3468.8	588.9	196.0	0.011
49.56	10600.0	678.3	194.5	0.014	3600.8	585.4	194.0	0.016
59.51	10902.0	681.0	192.4	0.007	3730.5	580.0	191.9	0.021
69.68	11220.0	686.9	190.4	0.008	3860.0	580.0	189.8	0.017

TABLE 11 : Computed Parameters for VTF Equation for the Fluidity and Equivalent Conductance of $Ca(NO_3)_2.4.03H_2O$ + $MnCl_2$ Melts

Mol % Mn^{2+}	$A_{3\phi}$	$k_{3\phi}$	$T_{o,\phi}$	Std dev in ln ϕ	$A_{3\Lambda}$	$k_{3\Lambda}$	$T_{o,\Lambda}$	Std dev in lnΛ
0.00	8005.2	670.6	205.3	0.004	2817.1	579.9	204.8	0.015
1.05	7930.8	670.1	206.3	0.006	2772.4	579.4	205.7	0.005
2.02	7850.5	670.2	207.2	0.010	2727.7	580.0	206.6	0.019
3.50	7695.3	670.0	208.7	0.012	2660.5	578.7	208.5	0.013
4.99	7620.4	670.0	210.1	0.019	2593.3	580.4	209.3	0.016
7.02	7459.6	670.2	212.0	0.018	2503.9	579.3	211.2	0.015

TABLE 12: Computed Parameters for VTF Equation for the Fluidity and Equivalent Conductance of $Cd(NO_3)_2.4.18H_2O + MnCl_2$ Melts

Mol % Mn^{2+}	$A_{3\phi}$	$k_{3\phi}$	$T_{o,\phi}$	Std dev in ln ϕ	$A_{3\Lambda}$	$k_{3\Lambda}$	$T_{o,\Lambda}$	Std dev in ln Λ
0.00	12220.0	666.7	189.3	0.015	4165.2	577.9	189.5	0.013
2.50	11980.0	665.2	190.3	0.004	4030.4	573.8	190.5	0.013
5.35	11730.0	663.8	191.4	0.002	3940.4	580.1	191.6	0.009
7.88	11495.0	666.4	192.5	0.013	3805.6	575.7	192.7	0.007
9.85	11257.0	662.1	193.7	0.007	3715.5	580.0	193.7	0.008
12.49	11030.0	675.1	194.8	0.001	3600.9	574.7	194.8	0.016

TABLE 13 : Computed Parameters for VTF Equation for the Fluidity of $Ni(NO_3)_2.6.01H_2O$ + $Mg(NO_3)_2.6.13H_2O$ Melts

Mol % Mg^{2+}	$A_{3\phi}$	$k_{3\phi}$	$T_{o,\phi}$	Std dev in ln ϕ
0.00	7382.0	694.8	194.6	0.014
5.41	7435.0	696.7	194.1	0.015
9.64	7505.0	695.6	193.5	0.020
14.67	7547.0	695.2	193.1	0.007
20.11	7600.0	694.7	192.5	0.016
25.43	7643.0	697.1	191.8	0.009
30.03	7696.7	696.8	191.4	0.008

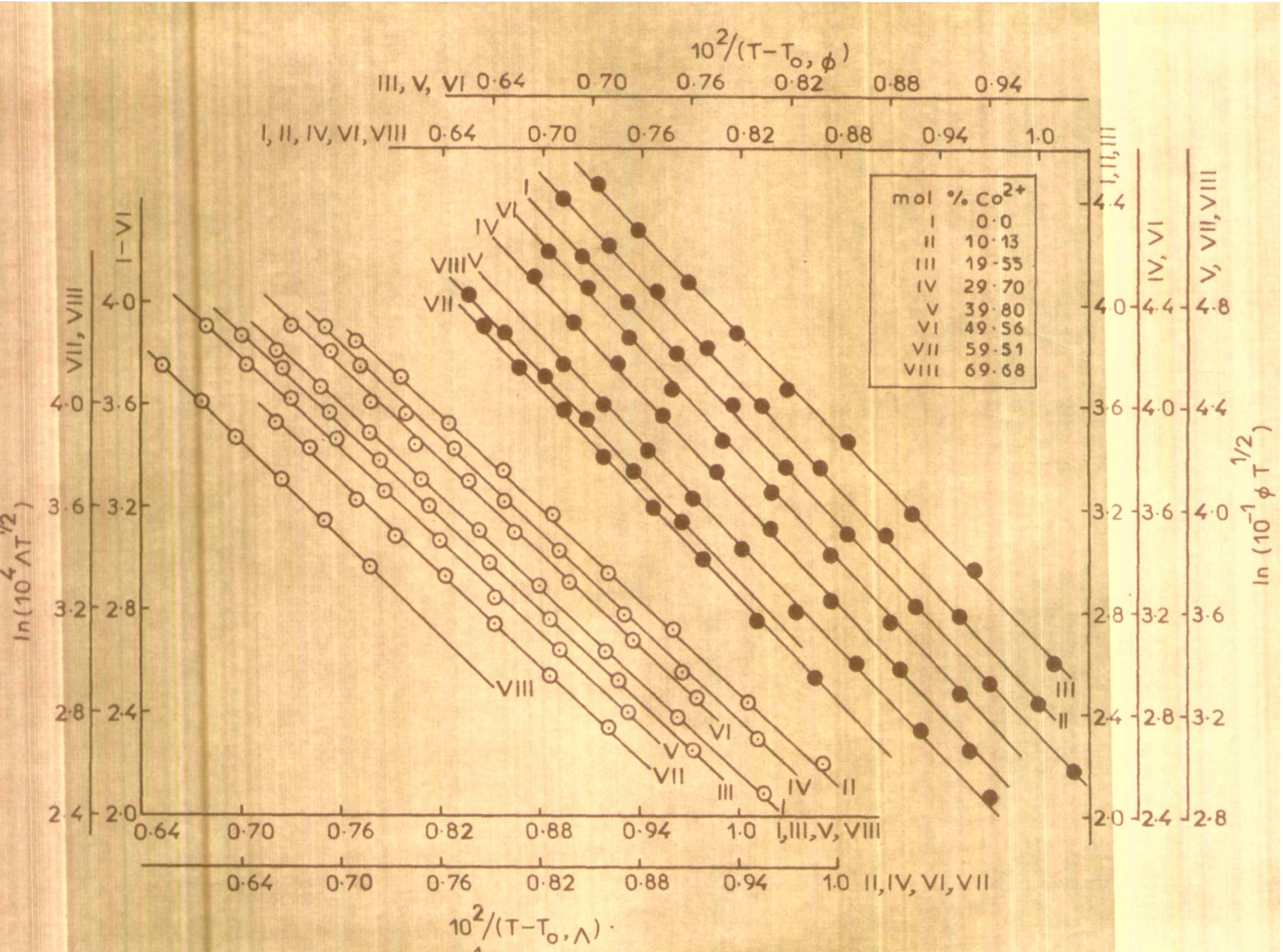

Fig.8 Plots of $\ln \gamma (= \phi \text{ or } \Lambda) T^{1/2}$ Vs. $1/(T-T_o)$ for $Ca(NO_3)_2 \cdot 4 \cdot 06H_2O - Co(NO_3)_2 6 \cdot 18H_2O$ Molten Salt System.

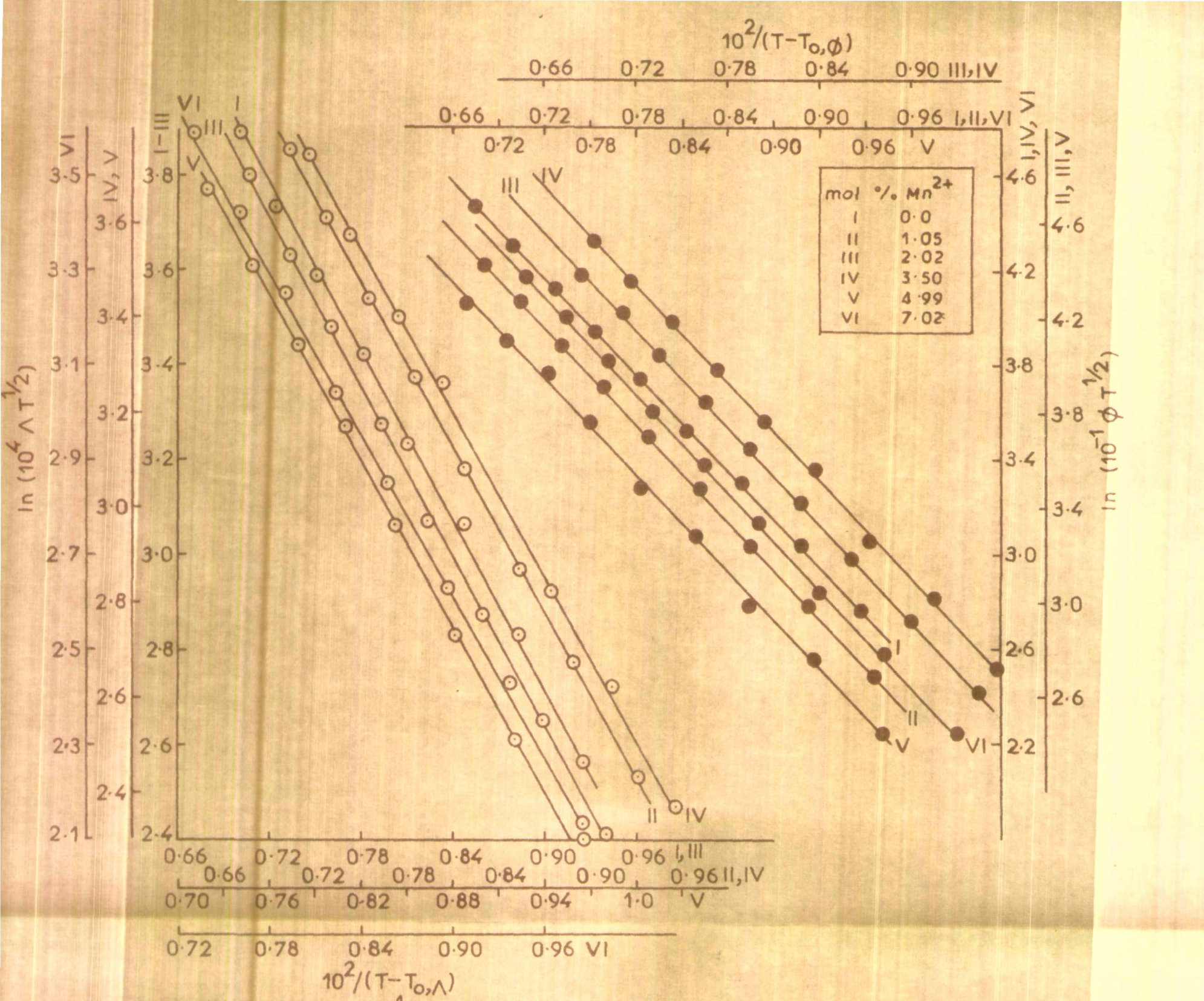

Fig. 9 Plots of $\ln Y (= \phi \text{ or } \Lambda) T^{1/2}$ Vs. $^1/(T-T_o)$ for $Ca(NO_3)_2 \cdot 4{\cdot}03H_2O$–$MnCl_2$ Molten Salt System.

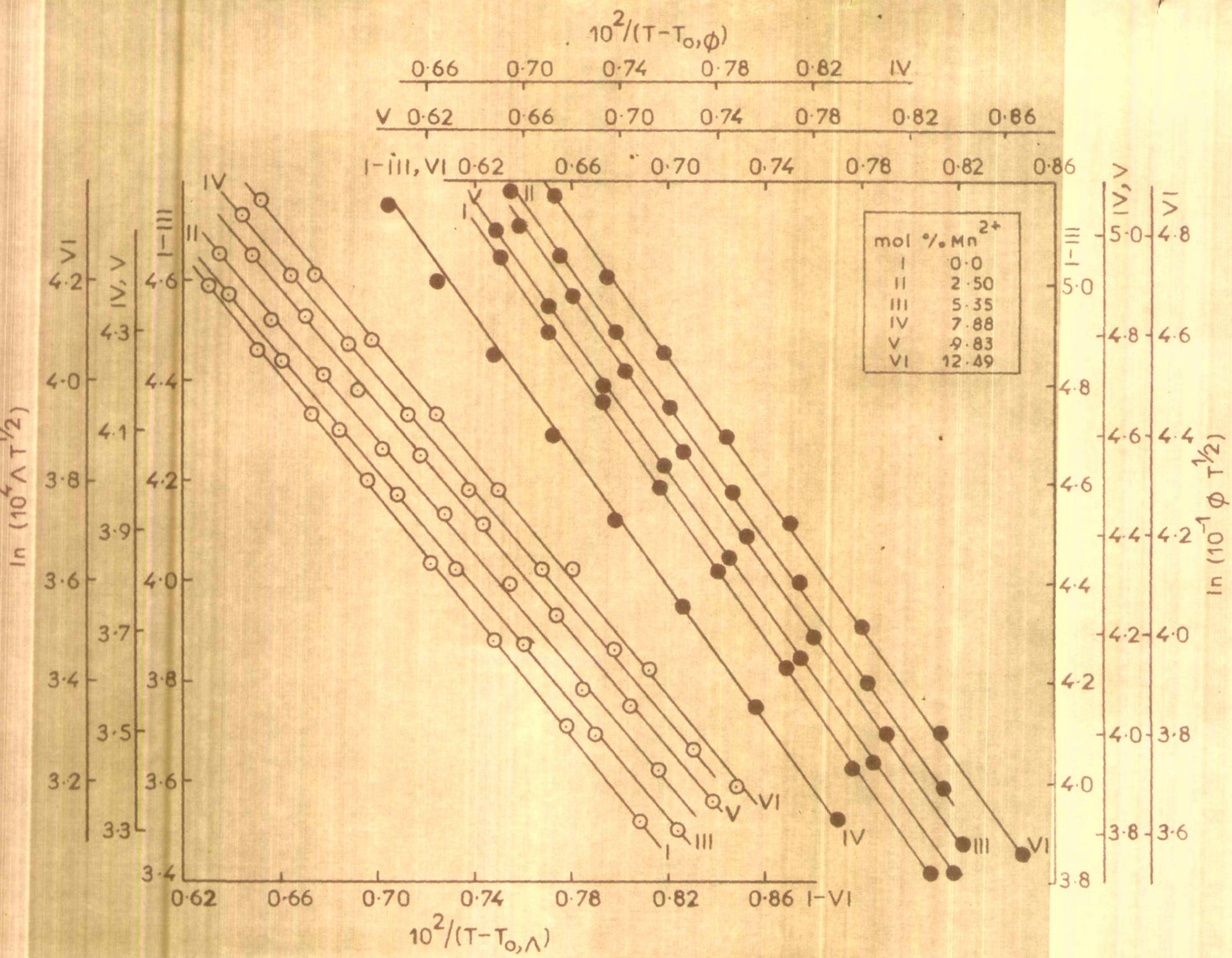

Fig. 10 Plots of $\ln Y (= \phi \text{ or } \Lambda) T^{1/2}$ Vs. $1/(T-T_o)$ for $Cd(NO_3)_2\ 4{\cdot}18H_2O - MnCl_2$ Molten Salt System.

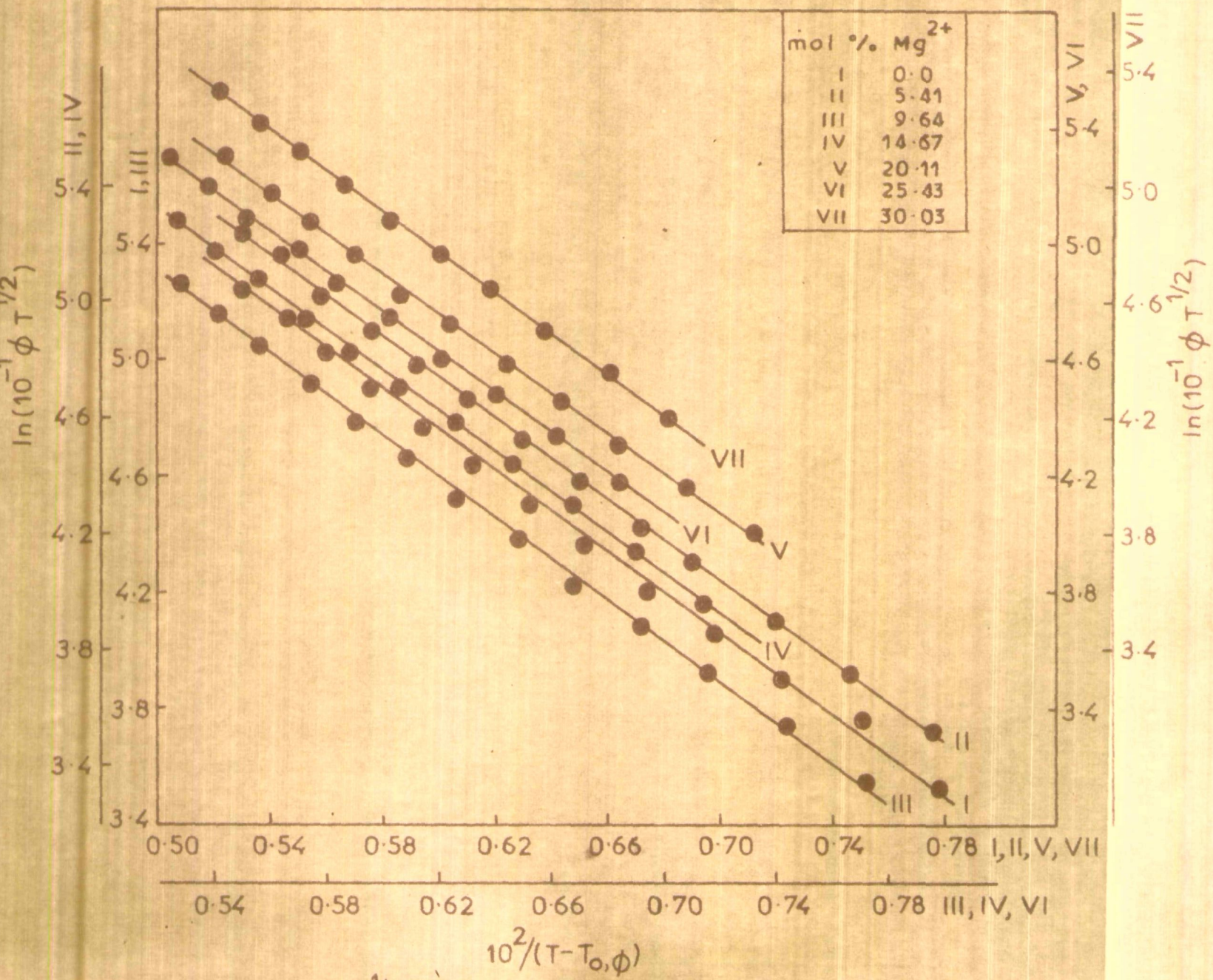

Fig. 11 Plots of $\ln \phi T^{1/2}$ Vs. $1/(T-T_o)$ for $Ni(NO_3)_2 \cdot 6{\cdot}01H_2O - Mg(NO_3)_2 \cdot 6{\cdot}13H_2O$ Molten Salt Sysrem.

the Arrhenian behaviour as the melt is supercooled. Similar results have also been reported earlier.[31] Even though the overall behaviour is best described by the non-linear equations, it is worth while to examine each of these plots as a combination of an (i) Arrhenius and (ii) a non-Arrhenius regions in the vicinity of the melting temperature and the supercooled region, respectively.

Accordingly, the fluidity and conductance data of the two distinct regions were separately least-squares fitted to the Arrhenius' two parameters and the non-Arrhenius' three parameters equations, respectively. The least squares fitted values of the parameters k_{1Y}/R and ln A are given in Tables 14-17 while those of the A_{3Y}, k_{3Y} and T_o are listed in Tables 18-21. Such a consideration results in somewhat reducing the standard deviations for the computed parameters as compared to those based on all the data points in a single fit.

In view of the earlier attempts to explain the variations in fluidities and conductances with temperature in terms of the volume expansion, the above data were examined in the light of the Hildebrand[22] equation, $Y = B'(V-V_o)/V_o$. It is evident from the non-linear plots of Y (= ϕ or Λ) versus $1/(V-V_o)$ shown in Figs. 12-15 that the Hildebrand equation fails to account for the transport behaviour. It

TABLE 14 : Computed Parameters of the Arrhenius Equation for the Fluidity and Equivalent Conductance of $Ca(NO_3)_2.4.06H_2O$ + $Co(NO_3)_2.6.18H_2O$ molten salt system

Mol% Co^{2+}	$k_{1\phi}/R$	ln A	Std. dev. in ln ϕ	$k_{1\Lambda}/R$	ln A	Std. dev. in ln Λ
0.00	4572.04	14.02	0.0028	3441.50	10.92	0.0007
10.13	4242.31	13.85	0.0025	3371.71	10.75	0.0015
19.55	4231.33	13.88	0.0018	3274.88	10.50	0.0024
29.70	3905.48	12.99	0.0027	3711.33	11.80	0.0005
39.80	3826.66	12.81	0.0006	3061.75	9.91	0.0033
49.56	3956.72	13.23	0.0027	3240.04	10.45	0.0042
59.51	3497.41	11.97	0.0002	3226.74	10.42	0.0046
69.68	3546.05	12.24	0.0001	3036.72	10.07	0.0007

TABLE 15: Computed Parameters of the Arrhenius Equation for the Fluidity and Equivalent Conductance of $Ca(NO_3)_2.4.03H_2O$ + $MnCl_2$ molten salt system

Mol% Mn^{2+}	$k_{1\phi}$	ln A	Std. dev. in ln ϕ	$k_{1\Lambda}$	ln A	Std. dev. in ln Λ
0.00	4031.68	12.9470	0.0016	3101.35	10.1251	0.0021
1.05	4006.04	13.0958	0.0012	3300.59	10.4088	0.0009
2.02	4191.23	13.3306	0.0014	3540.97	11.0495	0.0005
3.50	4127.30	13.1240	0.0011	3850.83	11.8669	0.0046
4.99	4095.18	12.9354	0.0014	3522.40	10.8612	0.0017
7.02	4294.61	13.4200	0.0003	3776.28	11.5154	0.0003

TABLE 1@ Computed Parameters of the Arrhenius Equation for the Fluidity and Equivalent Conductance of $Cd(NO_3)_2.4.18H_2O$ + $MnCl_2$ molten salt system

Mol% Mn^{2+}	$k_{1\phi}/R$	ln A	Std. dev. in ln ϕ	$k_{1\Lambda}/R$	ln A	Std. dev. in ln Λ
0.00	3296.07	11.59	0.0000	2870.30	9.92	0.0002
2.50	3197.16	11.45	0.0012	2755.00	9.64	0.0005
5.35	3267.59	11.57	0.0042	2877.26	9.91	0.0017
7.88	3365.84	11.80	0.0006	2942.50	10.07	0.0009
9.85	3431.70	11.93	0.0004	2952.53	10.01	0.0000
12.49	3539.87	12.12	0.0006	3104.18	10.36	0.0011

TABLE 17 : Computed Parameters for Arrhenius Equation for the Fluidity of $Ni(NO_3)_2.6.01H_2O$ - $Mg(NO_3)_2.6.13H_2O$ molten salt system.

Mol% Mg^{2+}	$k_{1\phi}/R$	ln A	Std. dev. in ln ϕ
0.00	3140.95	10.4720	0.0007
5.41	3145.95	10.4953	0.0008
9.64	3193.13	10.6329	0.0005
14.67	2988.60	10.1106	0.0008
20.11	3056.42	10.2455	0.0025
25.43	2910.82	9.9294	0.0004
30.03	2941.61	10.0327	0.0007

TABLE 18 : Computed Parameters for Non-Arrhenius Region of the VTF Equation for $Ca(NO_3)_2 \cdot 4.06H_2O$ - $Co(NO_3)_2 \cdot 6.18H_2O$ molten salt system.

Mol% Co^{2+}	$A_{3\phi}$	$k_{3\phi}$	$T_{o,\lambda}$	Std. dev. in ln ϕ	$A_{3\lambda}$	$k_{3\lambda}$	$T_{o,\lambda}$	Std. dev. in ln λ
0.00	9029.6	677.7	205.3	0.003	2962.0	584.5	204.5	0.009
10.13	9360.1	674.5	203.1	0.013	3097.2	586.2	202.3	0.012
19.55	9691.2	676.8	200.9	0.026	3232.1	584.3	200.2	0.005
29.70	10022.0	680.6	198.9	0.011	3367.2	590.8	198.0	0.013
39.80	10353.0	676.3	196.8	0.026	3502.1	589.6	195.8	0.011
49.56	10684.0	672.3	194.5	0.012	3637.8	588.9	193.8	0.004
59.51	11015.0	692.3	192.3	0.008	3771.3	588.5	191.7	0.003
69.68	11346.0	688.5	190.3	0.008	3906.4	585.6	189.6	0.010

TABLE 19: Computed Parameters for Non-Arrhenius region of the VTF Equation for $Ca(NO_3)_2 \cdot 4.03H_2O$ + $MnCl_2$ molten salt system

Mol% Mn^{2+}	$A_{3\phi}$	$k_{3\phi}$	$T_{o,\phi}$	Std. dev. in ln ϕ	$A_{3\Lambda}$	$k_{3\Lambda}$	$T_{o,\Lambda}$	Std.dev. in ln Λ
0.00	8045.8	670.1	205.5	0.006	2772.8	576.3	205.0	0.018
1.05	8612.3	677.8	206.6	0.004	2638.3	574.4	205.5	0.006
2.02	8504.3	675.6	207.9	0.008	2508.1	577.9	206.2	0.006
3.50	8115.1	674.8	208.0	0.009	2508.5	578.0	206.2	0.007
4.99	8394.3	674.5	211.3	0.011	2347.1	576.8	207.7	0.018
7.02	8526.1	679.6	213.0	0.004	2289.5	575.4	210.0	0.016

TABLE 29: Computed Parameters for Non-Arrhenius region of the VTF Equation for $Cd(NO_3)_2.4.18H_2O$ + $MnCl_2$ molten salt system

Mol% Mn^{2+}	$A_{3\phi}$	$k_{3\phi}$	$T_{o,\phi}$	Std. dev. in ln ϕ	$A_{3\lambda}$	$k_{3\lambda}$	$T_{o,\lambda}$	Std. dev. in ln λ
0.00	12200.0	669.2	189.3	0.0086	4142.0	577.9	189.7	0.0040
2.50	11958.0	668.3	190.3	0.0024	4003.2	579.6	190.6	0.0130
5.35	11729.0	670.2	191.4	0.0025	3864.3	578.2	191.5	0.0052
7.88	11472.0	664.8	192.5	0.0071	3725.2	572.5	192.7	0.0070
9.83	11237.0	669.0	193.7	0.0030	3586.7	575.2	193.8	0.0070
12.49	11011.0	678.2	194.8	0.0011	3447.6	581.9	194.8	0.0161

TABLE 21 : Computed Parameters for Non-Arrhenius Region of the VTF Equation for $Ni(NO_3)_2.6.01H_2O$ - $Mg(NO_3)_2.6.15H_2O$ molten salt system.

Mol% Mg^{2+}	$A_{3\phi}$	$k_{3\phi}$	T_o	Std. dev. in ln ϕ
0.00	7375.2	695.2	194.5	0.014
5.41	7428.0	697.3	194.0	0.014
9.64	7498.7	699.3	193.5	0.015
14.67	7540.2	694.8	193.1	0.005
20.11	7553.5	695.3	192.5	0.007
25.43	7636.5	696.1	191.9	0.010
30.03	7689.1	697.1	191.5	0.006

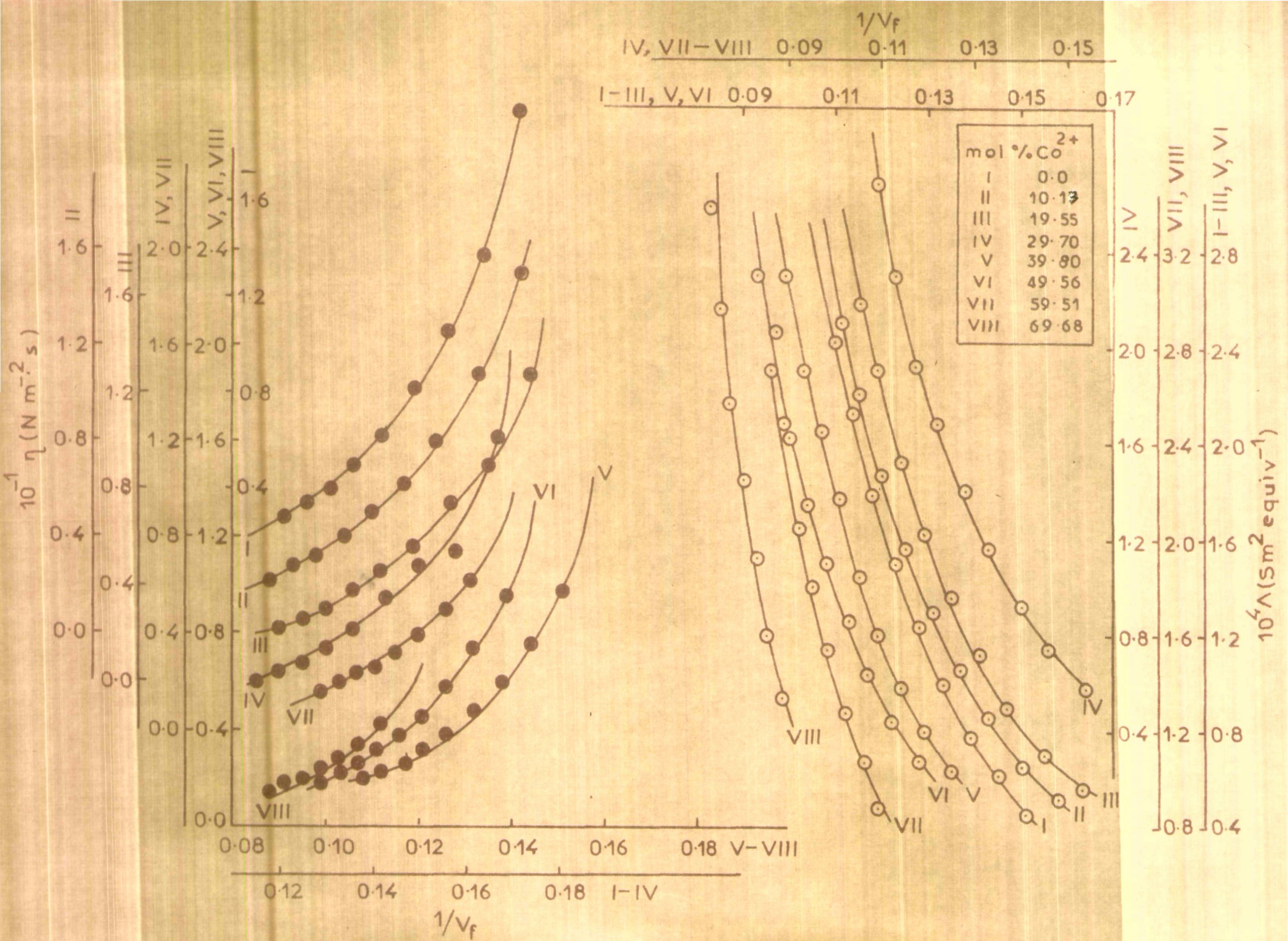

Fig 12 Plots of Viscosity and Conductance Vs. $1/V_f$ for $Ca(NO_3)_2 4{\cdot}6H_2O - Co(NO_3)_2 6{\cdot}18H_2O$ Molten Salt System.

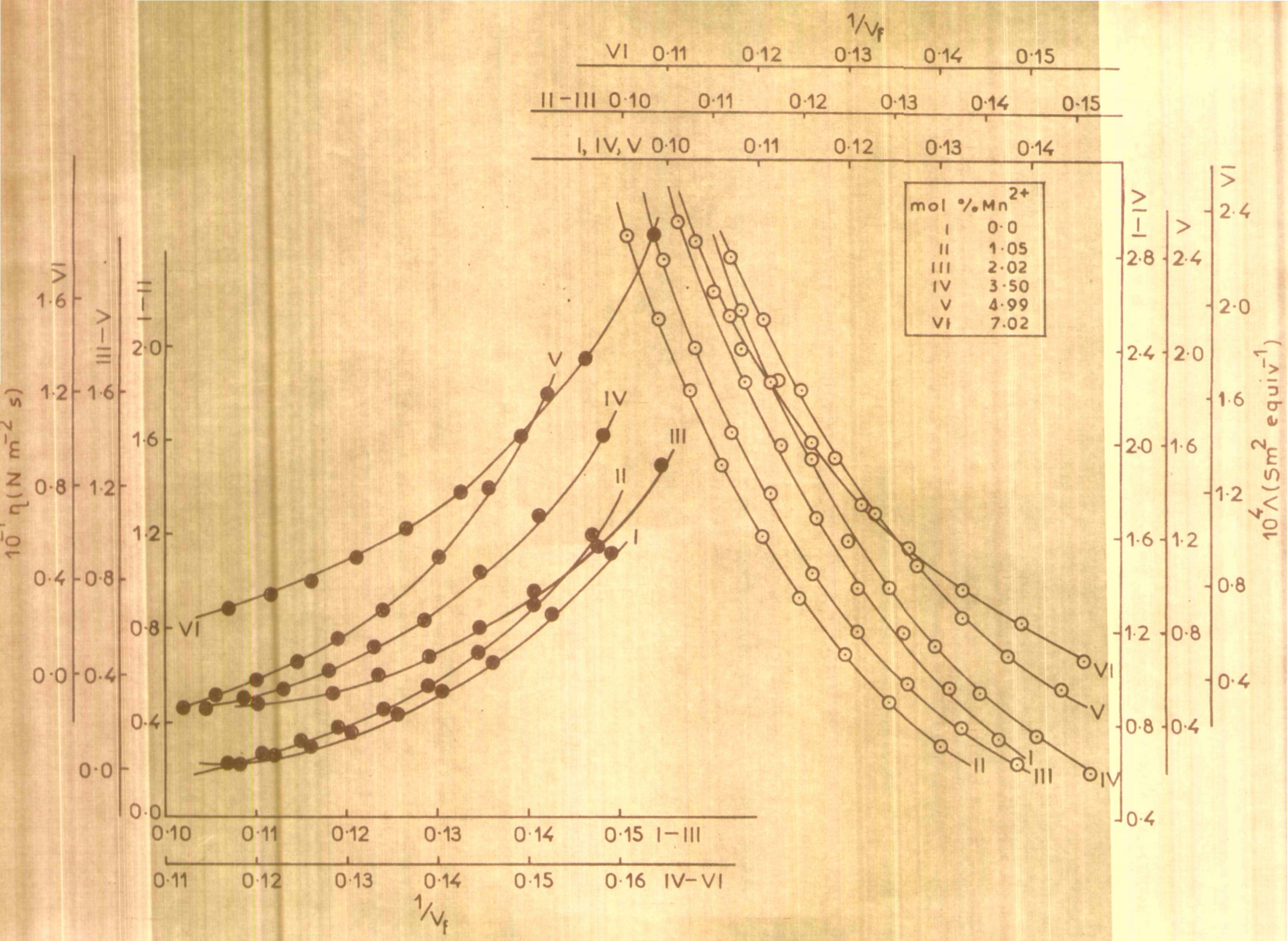

Fig.13 Plots of Viscosity and Conductance Vs. $^1/V_f$ for $Ca(NO_3)_2 \cdot 4 \cdot 03H_2O - MnCl_2$ Molten Salt System.

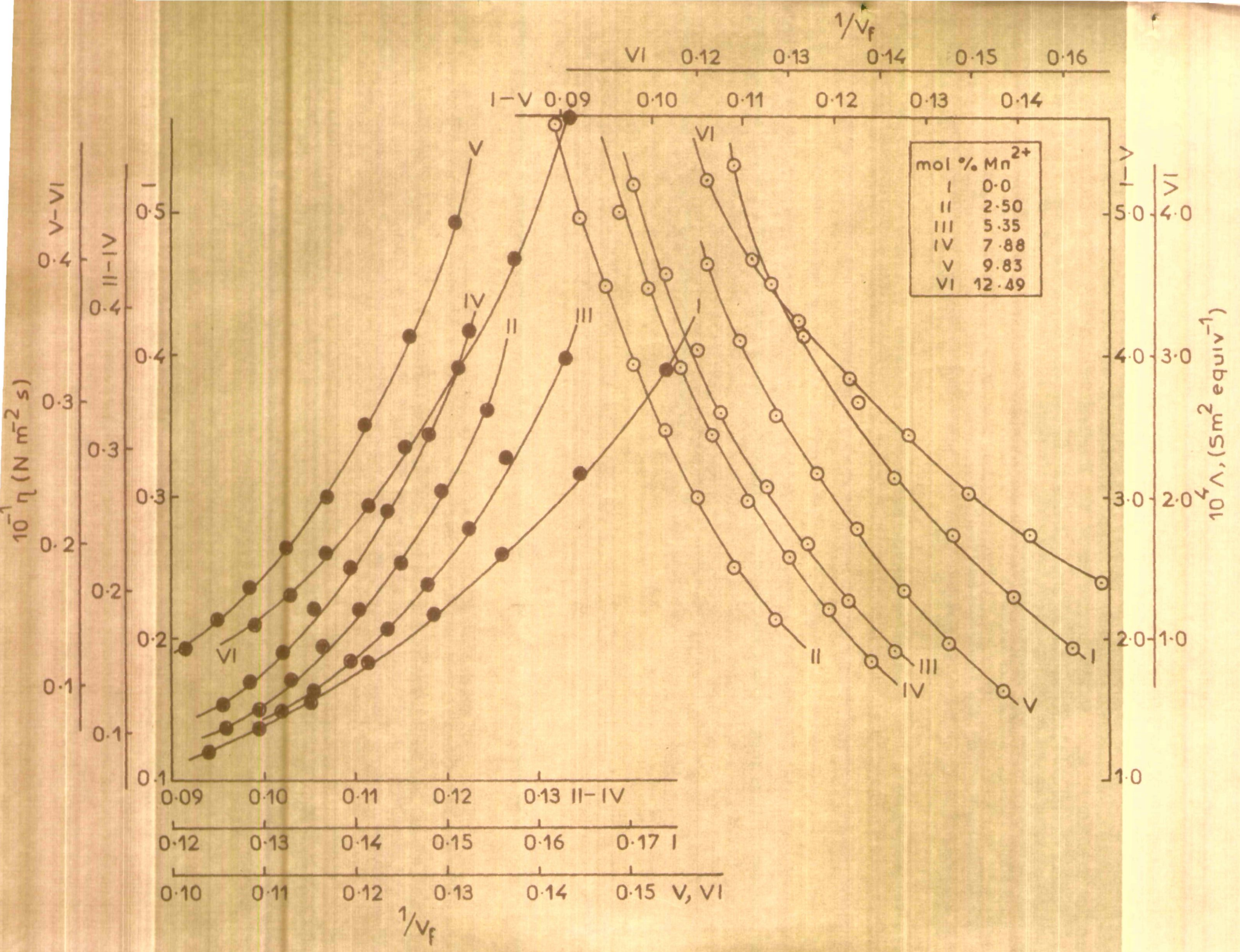

Fig. 14 Plots of Viscosity and Conducrance Vs. $^1/V_f$ for $Cd(NO_3)_2 \cdot 4 \cdot 18H_2O - MnCl_2$ Molten Salt System.

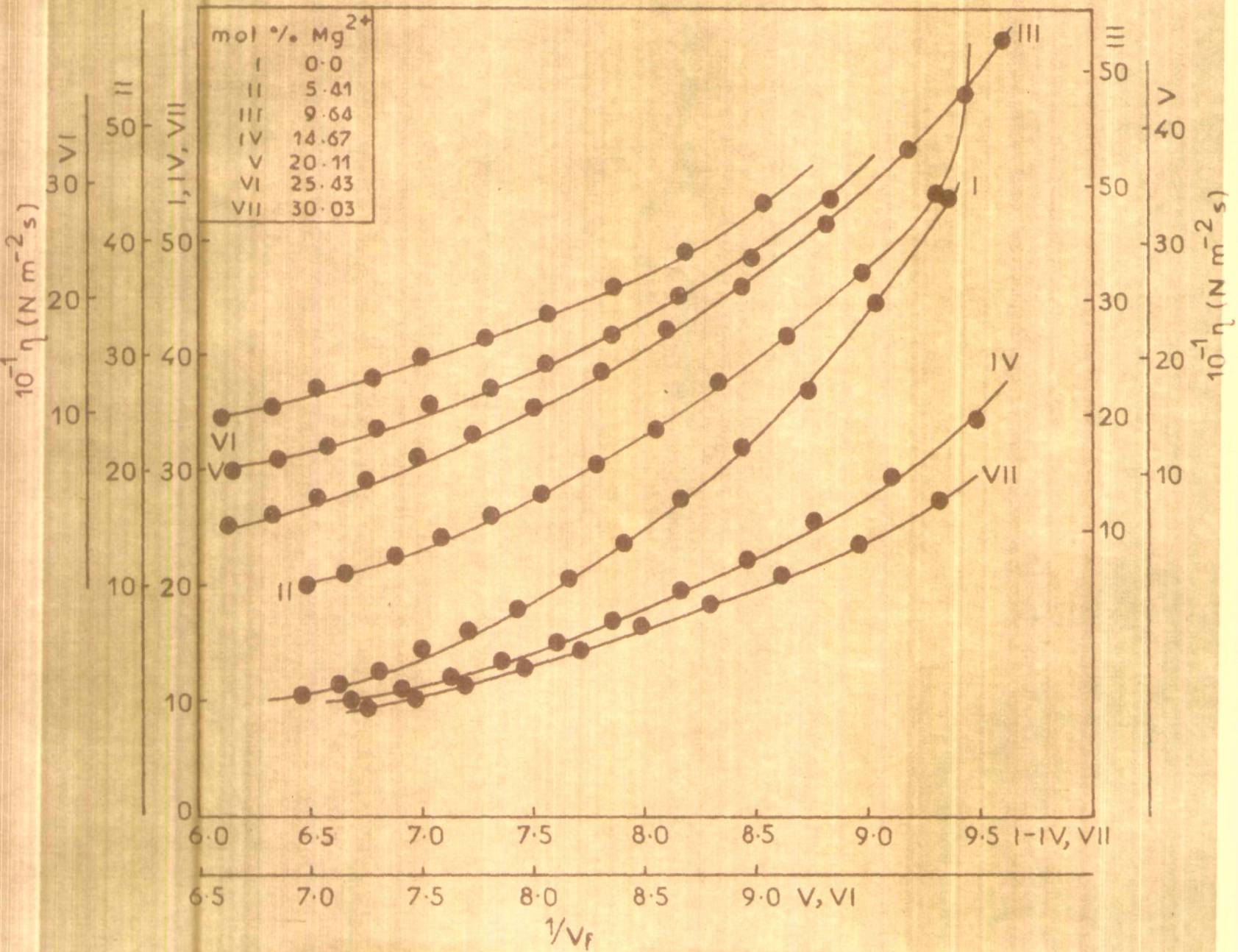

Fig. 15 Plots of Viscosity Vs. $1/V_f$ for $Ni(NO_3)_2 \cdot 6.01H_2O - Mg(NO_3)_2 \cdot 6.13H_2O$ Molten Salt System.

may, however, be noted that these data were best explained by the Doolittle equation as apparent from the least-squares fitted values to equation (4). The best fit parameters for the Doolittle's equation, A_{2Y}, k_{2Y} and V_o along with the standard deviations in ln ϕ and ln Λ are listed in Tables 22-25. The linear plots of ln Y (= ϕ or Λ) versus $1/(V-V_o)$ shown in Figs. 16-19 support the applicability of Doolittle's equation to such systems.

The Configurational Entropy Model (CEM): The non-Arrhenius temperature dependence of transport properties have also been explained by the configurational entropy model in several cases.[34,35] Therefore, the fluidity and conductance data were least-squares fitted to the three parameter CEM equation. The computed parameters A_{4Y}, k_{4Y} and T_o along with the standard deviations in ln ϕ and ln Λ are given in Tables 26-29. It is noted that the computed parameters of the VTF equation are comparable with those of the CEM equation except for the pre-exponential factors. For instance the k_Y and the T_o values computed from these two models are essentially same as has been suggested earlier.[17-19] Nevertheless, the VTF and the CEM equations are based on different theoretical considerations. These equations appear to approach each other at higher temperatures. The parameters for the CEM were chosen in a manner

TABLE 22: Computed Parameters for Doolittle's Equation for the Fluidity and Equivalent Conductance of $Ca(NO_3)_2.4.06H_2O$ + $Co(NO_3)_2.6.18H_2O$ Melts

Mol % Co^{2+}	$A_{2\phi}$	$k_{2\phi}$	$V_{o,\phi}$	Std dev in ln ϕ	$A_{2\Lambda}$	$k_{2\Lambda}$	$V_{o,\Lambda}$	Std dev in ln Λ
0.00	220.2	34.6	130.5	0.057	110.1	35.2	129.7	0.073
10.13	230.2	33.2	133.0	0.009	120.7	34.5	132.4	0.011
19.55	242.5	32.9	135.6	0.019	131.3	33.8	135.2	0.023
29.70	255.1	34.4	138.4	0.061	141.9	36.0	137.9	0.033
39.80	270.1	36.7	141.4	0.021	152.5	40.4	140.6	0.013
49.56	282.4	40.1	144.0	0.022	163.1	43.1	143.4	0.034
59.51	290.5	42.7	146.8	0.055	172.4	47.8	146.0	0.021
69.68	300.8	50.8	149.3	0.066	183.0	54.2	148.8	0.026

TABLE 25: Computed Parameters of the Doolittle's Equation for the Fluidity and Equivalent Conductance of $Ca(NO_3)_2.4.03H_2O$ + $MnCl_2$ molten salt system

Mol% Mn^{2+}	$A_{2\phi}$	$k_{2\phi}$	$V_{o,\phi}$	Std. dev. in ln ϕ	$A_{2\Lambda}$	$k_{2\Lambda}$	$V_{o,\Lambda}$	Std. dev. in ln Λ
0.00	380.1	40.7	120.8	0.015	177.1	40.0	120.2	0.025
1.05	373.2	41.5	120.1	0.006	168.4	40.4	128.5	0.007
2.02	366.4	40.0	128.3	0.029	159.9	38.7	127.8	0.019
3.50	360.0	39.3	127.2	0.012	151.5	38.0	126.7	0.013
4.99	352.1	41.0	126.1	0.053	142.2	38.3	125.7	0.027
7.02	345.7	39.3	124.6	0.017	135.6	36.2	124.3	0.013

TABLE 24: Computed Parameters for Doolittle's Equation for the Fluidity and Equivalent Conductance of $Cd(NO_3)_2 \cdot 4.18H_2O$ + $MnCl_2$ Melts

Mol % Mn^{2+}	$A_{2\phi}$	$k_{2\phi}$	$V_{o,\phi}$	Std dev in ln ϕ	$A_{2\Lambda}$	$k_{2\Lambda}$	$V_{o,\Lambda}$	Std dev in ln Λ
0.00	350.6	29.1	131.8	0.096	200.0	32.5	130.7	0.064
2.50	346.4	37.6	129.9	0.025	190.2	39.5	129.1	0.014
5.35	342.1	36.0	127.9	0.019	180.4	36.1	127.5	0.010
7.88	338.5	39.2	125.8	0.031	170.7	36.6	125.9	0.005
9.85	334.2	37.4	123.9	0.041	160.2	33.3	124.3	0.018
12.49	330.1	35.4	121.8	0.014	150.2	28.9	122.7	0.058

TABLE 25: Computed Parameters of the Doolittle's Equation for the Fluidity of $Ni(NO_3)_2.6.01H_2O$ + $Mg(NO_3)_2.6.13H_2O$ molten salt system

Mol% Mg^{2+}	$A_{2\phi}$	$k_{2\phi}$	$V_{o,\phi}$	Std. dev. in ln ϕ
0.00	279.1	51.4	148.0	0.044
5.41	260.1	46.8	148.4	0.044
9.64	242.1	48.0	148.8	0.023
14.67	225.2	48.2	149.2	0.035
20.11	207.0	46.7	149.6	0.019
25.43	188.2	44.3	150.0	0.012
30.03	171.1	47.5	150.4	0.055

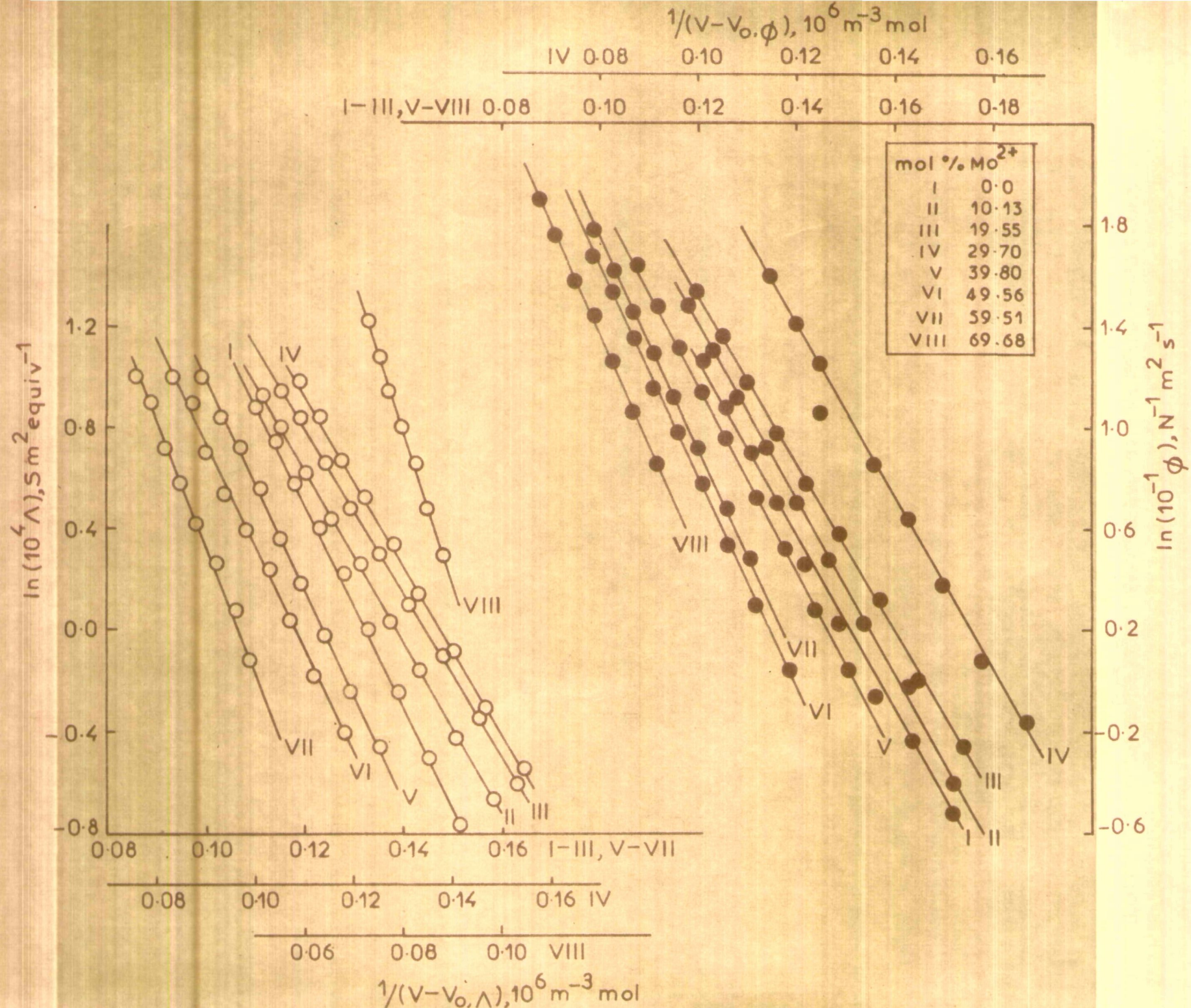

Fig.16 Plots of ln Y (= ϕ or Λ) Vs. $1/(V-V_o)$ for $Ca(NO_3)_2\,4{\cdot}06\,H_2O - Co(NO_3)_2\cdot 6{\cdot}18\,H_2O$ Molten Salt System.

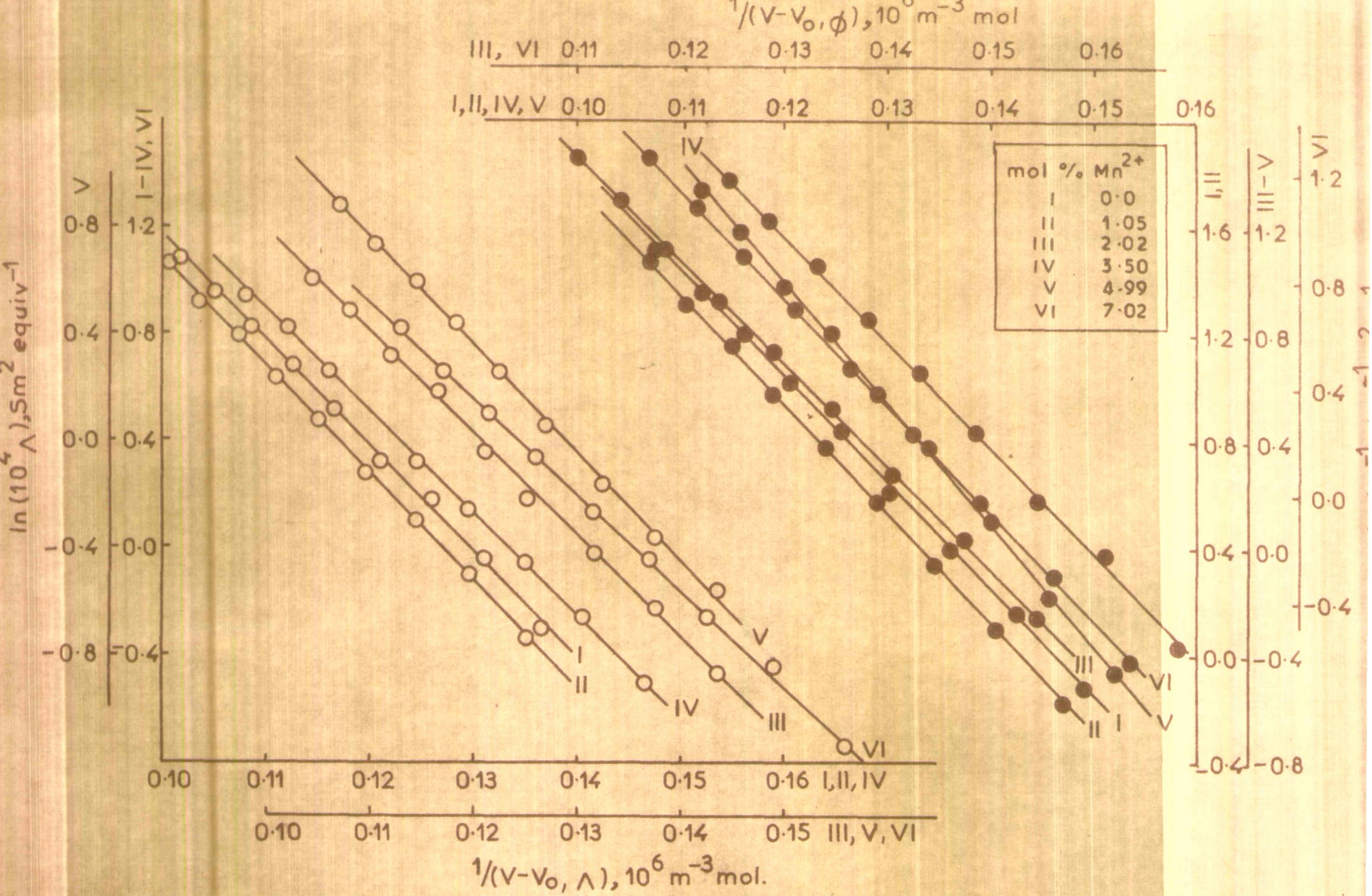

Fig. 17 Plots of $\ln Y (= \phi$ or $\Lambda)$ Vs. $^1/(V-V_o)$ for $Ca(NO_3)_2$ $4{\cdot}03H_2O$–$MnCl_2$ Molten Salt System.

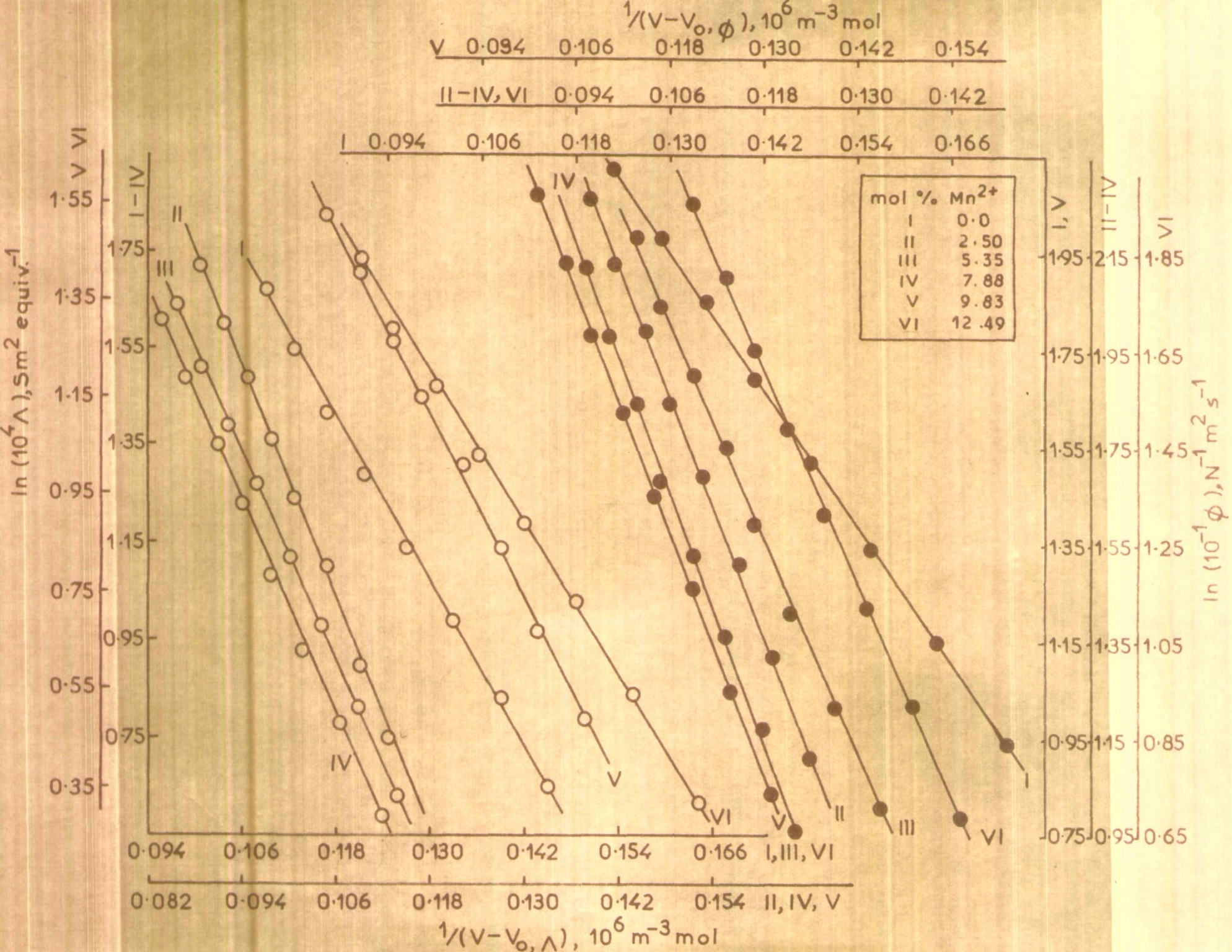

Fig.18 Plots of ln Y(= ϕ or Λ) Vs. $1/(V-V_o)$ for $Cd(NO_3)_2 \cdot 4{\cdot}18H_2O$–$MnCl_2$ Molten Salt System.

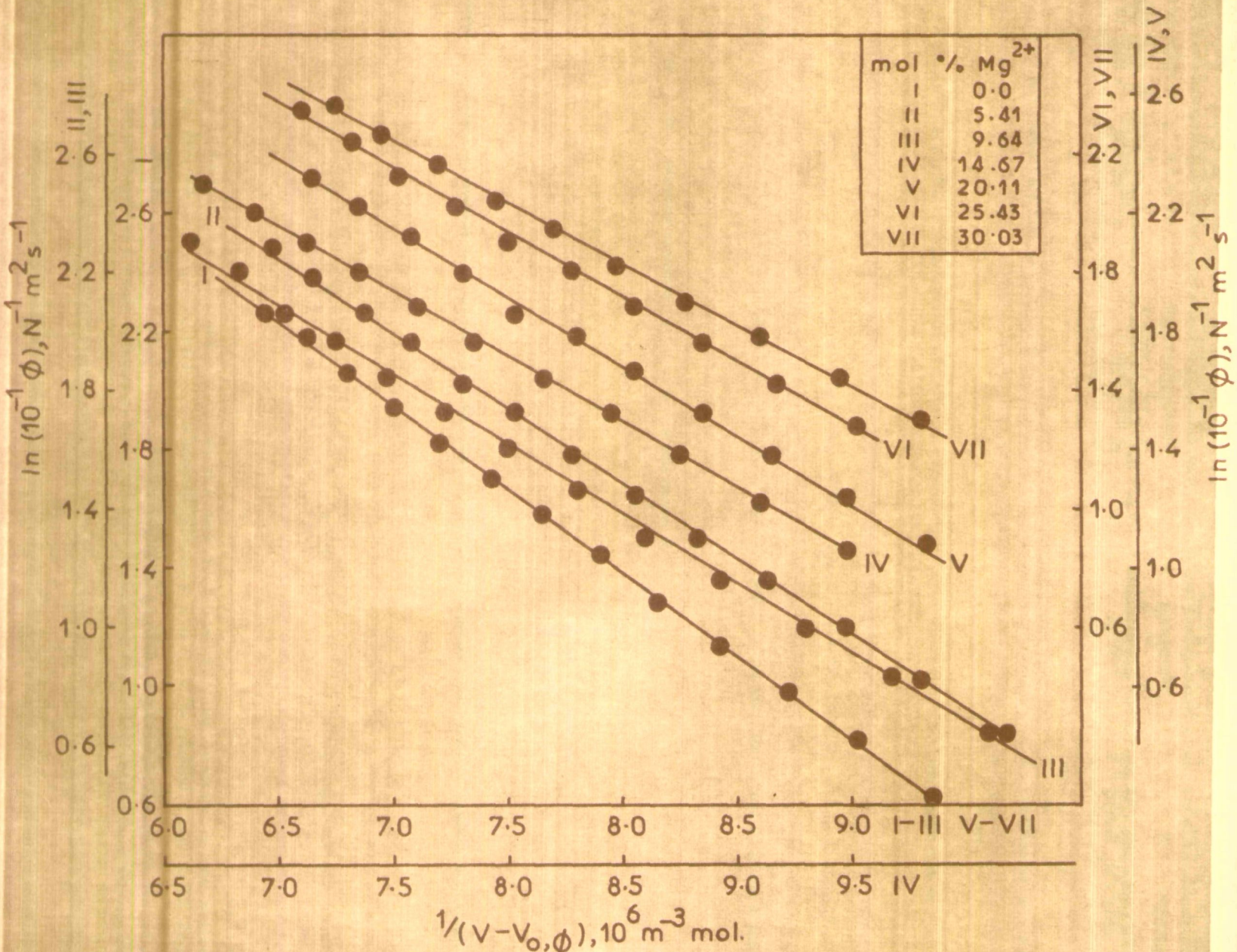

Fig.19 Plots of $\ln \phi$ Vs. $1/(V-V_o)$ for $Ni(NO_3)_2\ 6{\cdot}01H_2O - Mg(NO_3)_2\ 6{\cdot}13H_2O$ Molten Salt System.

TABLE 26: Computed Parameters of the CWM Equation for the Fluidity and Equivalent Conductance of $Ca(NO_3)_2.4.06H_2O$ + $Co(NO_3)_2.6.18H_2O$ molten salt system

Mol% Co^{2+}	$A_{4\phi}$	$k_{4\phi}$(K)	$T_{o,\phi}$	Std. dev. in ln ϕ	$A_{4\Lambda}$	$k_{4\Lambda}$	$T_{o,\Lambda}$	Std. dev. in ln Λ
0.00	177.0	680.0	206.6	0.005	59.1	593.1	205.7	0.007
10.13	181.5	667.7	204.0	0.019	61.4	586.3	203.9	0.013
19.55	186.2	671.9	202.0	0.019	63.6	589.8	201.8	0.010
29.70	190.8	683.3	199.8	0.019	65.9	589.9	199.8	0.017
39.80	195.3	684.3	197.8	0.016	67.2	592.3	197.8	0.014
49.56	200.0	696.9	195.8	0.010	69.6	592.6	195.7	0.016
59.51	205.9	697.6	193.4	0.007	71.7	594.5	193.7	0.018
69.68	209.0	687.3	191.8	0.009	73.8	591.6	191.6	0.013

TABLE 27: Computed Parameters of the CEM Equation for the Fluidity and Equivalent Conductance of $Ca(NO_3)_2.4.03H_2O$ + $MnCl_2$ molten salt system

Mol% Mn^{2+}	$A_{4\phi}$	$k_{4\phi\Lambda}$	$T_{o,\phi\Lambda}$	Std. dev. in ln ϕ	$A_{4\Lambda}$	$k_{4\Lambda}$	$T_{o,\Lambda}$	Std. dev. in ln Λ
0.00	177.4	689.8	206.8	0.010	67.1	589.9	206.0	0.017
1.05	176.6	689.1	207.7	0.006	66.5	589.4	207.0	0.010
2.02	175.7	689.6	208.6	0.006	65.9	594.9	208.1	0.017
3.50	173.4	689.6	210.1	0.009	65.0	591.6	209.6	0.019
4.99	172.1	690.0	211.5	0.010	64.2	590.3	211.2	0.027
7.02	170.4	690.4	213.4	0.003	63.0	589.2	213.3	0.025

TABLE 28: Computed Parameters of the CEM Equation for the Fluidity and Equivalent Conductance of $Cd(NO_3)_2.4.18H_2O$ + $MnCl_2$ molten salt system

Mol% Mn^{2+}	$A_{4\phi}$	$k_{4\phi}$	$T_{o,\phi}$	Std. dev. in ln ϕ	$A_{4\Lambda}$	$k_{4\Lambda}$	$T_{o,\Lambda}$	Std. dev. in ln Λ
0.00	240.1	689.0	191.7	0.004	105.0	500.1	191.9	0.018
2.50	235.4	680.2	192.8	0.011	101.4	589.0	193.0	0.020
5.35	230.0	683.5	193.8	0.011	96.5	592.4	194.0	0.016
7.88	225.0	682.5	194.9	0.022	91.8	583.7	195.1	0.013
9.83	220.1	685.6	196.0	0.008	87.2	583.5	196.2	0.012
12.49	215.2	687.4	197.0	0.006	83.0	589.9	197.2	0.009

TABLE 29: Computed Parameters of the CRM Equation for the Fluidity of $Ni(NO_3)_2.6.01H_2O$ + $Mg(NO_3)_2.6.15H_2O$ molten salt system

Mol% Mg^{2+}	$A_{4\phi}$	$k_{4\phi}$	$T_{o,\phi}$	Std. dev. in ln ϕ
0.00	145.5	692.2	198.0	0.016
5.41	147.5	696.9	197.4	0.017
9.64	148.7	699.2	196.9	0.020
14.67	150.2	696.5	196.3	0.008
20.11	152.0	699.7	195.8	0.018
25.43	153.3	698.9	195.2	0.011
30.03	154.8	701.4	194.7	0.009

similar to that adopted for the VTF equation. The feasibility of this equation in explaining the fluidity and conductance data is also visualised by the linear plots of ln Y versus $1/T \ln (T/T_0)$ shown in Figs. 20-23. Furthermore, the applicability of the CEM equation to the limited number of data points constituting only the non-Arrhenius region of each of the plots signify an improvement over that considering the entire data points of each of the data sets as apparent from much lower values of the standard deviations compared to those of the single fit. Similar conclusions have already been drawn in the cases of such fits to the VTF equation.

The Environmental Relaxation Model (ERM): A careful examination of Figs. 1-7 and a comparison of the standard deviation values for the above data fittings to the two/three parameters (VTF and those of CEM equations) for an apparently linear and non-linear portions of each of the single plots suggest the presence of Arrhenius and non-Arrhenius regions. Even though the VTF and the CEM equations are meant for the non-Arrhenius behaviour of such properties, they describe quite successfully the temperature dependence of transport properties of these systems. In other words, they do not, however, consider the whole region starting from the Arrhenius at higher temperatures to that of the

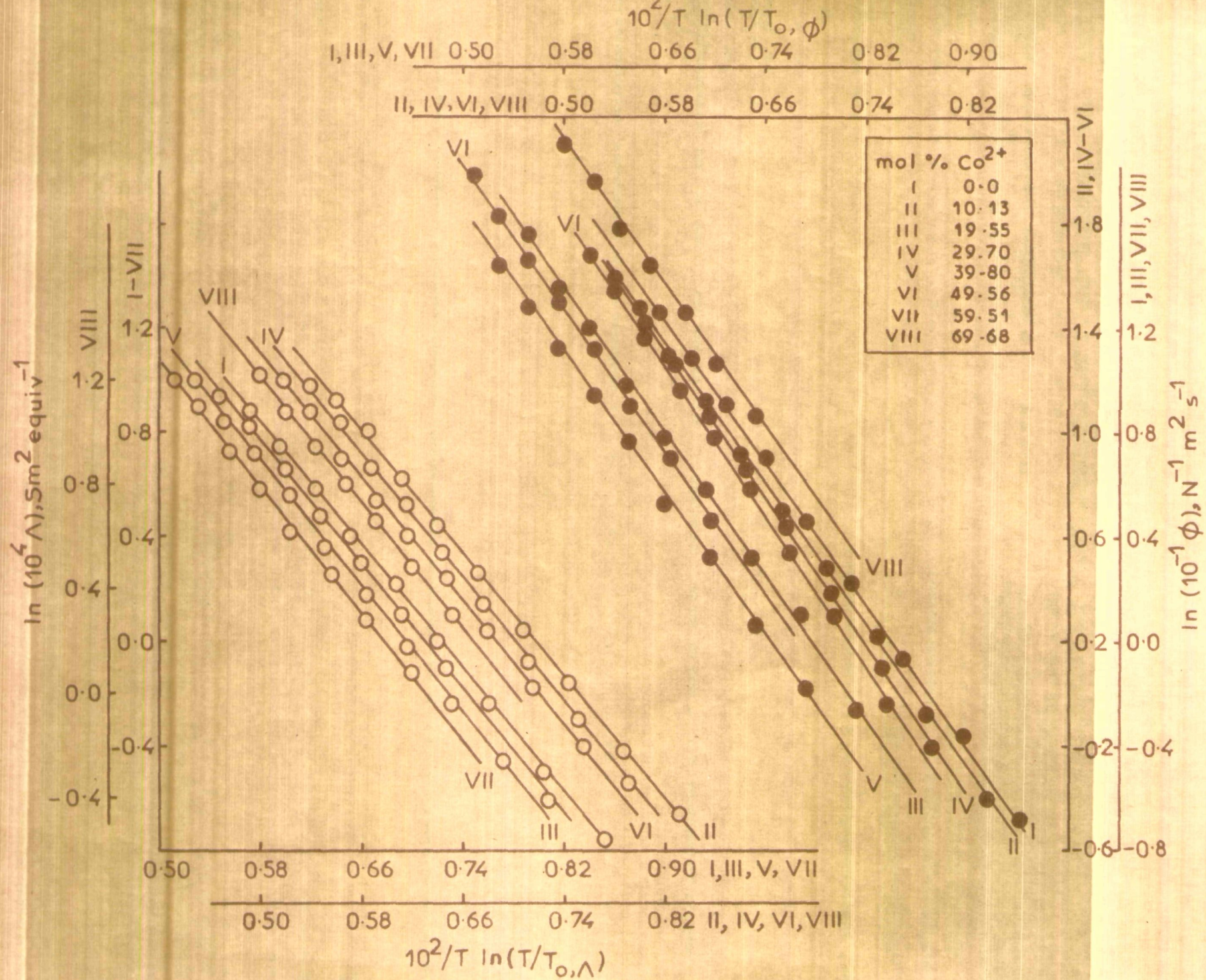

Fig.20 Plots of ln Y(= ϕ or Λ) Vs. $^1/T \ln(T/T_o)$ for $Ca(NO_3)_2 \cdot 4 \cdot 06H_2O - Co(NO_3)_2 \cdot 6 \cdot 18H_2O$ Molten Salt System.

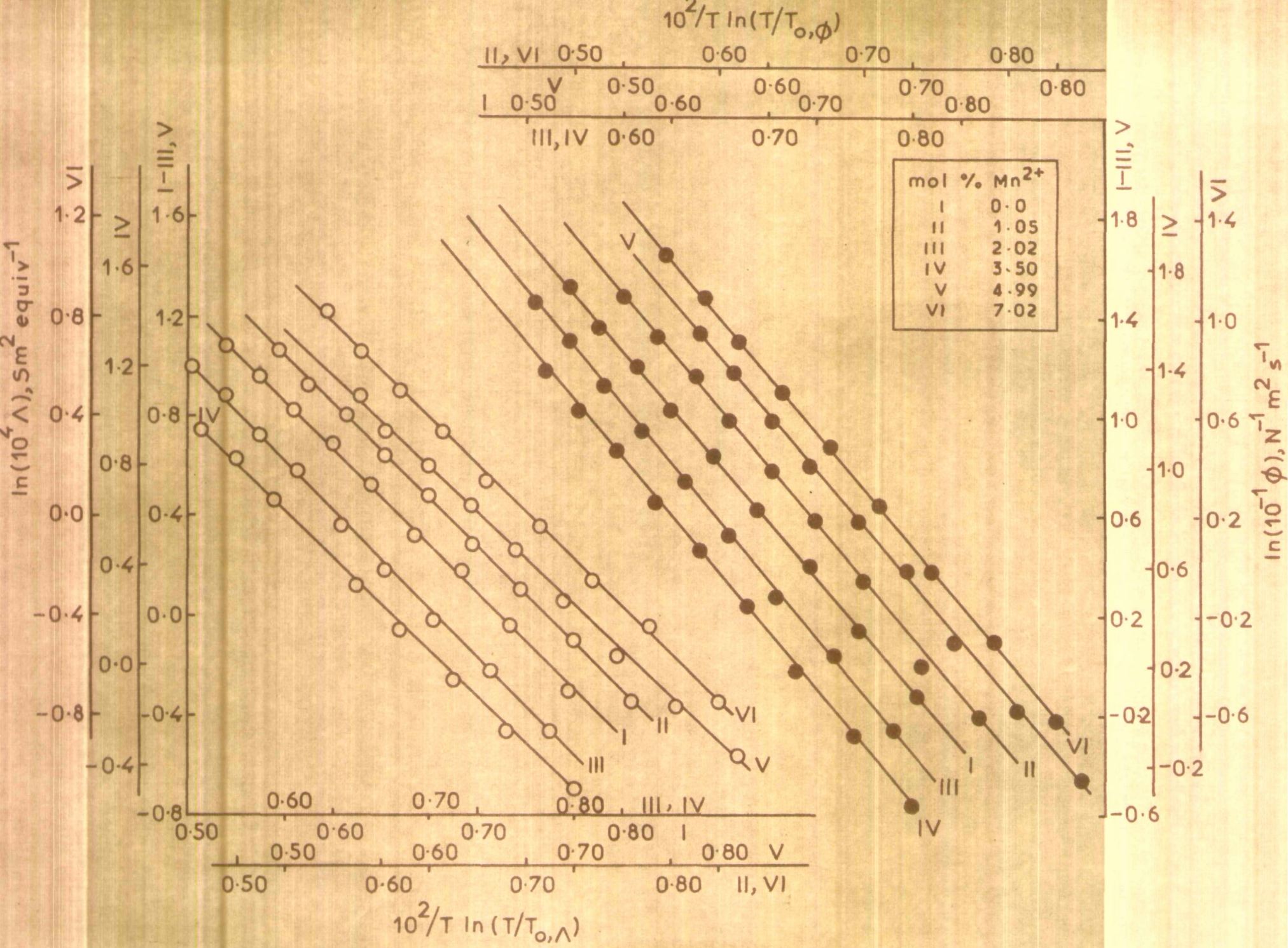

Fig. 21 Plots of $\ln Y (= \phi$ or $\Lambda)$ Vs. $^1/T \ln(T/T_o)$ for $Ca(NO_3)_2 \cdot 4{\cdot}03H_2O$–$MnCl_2$ Molten Salt System.

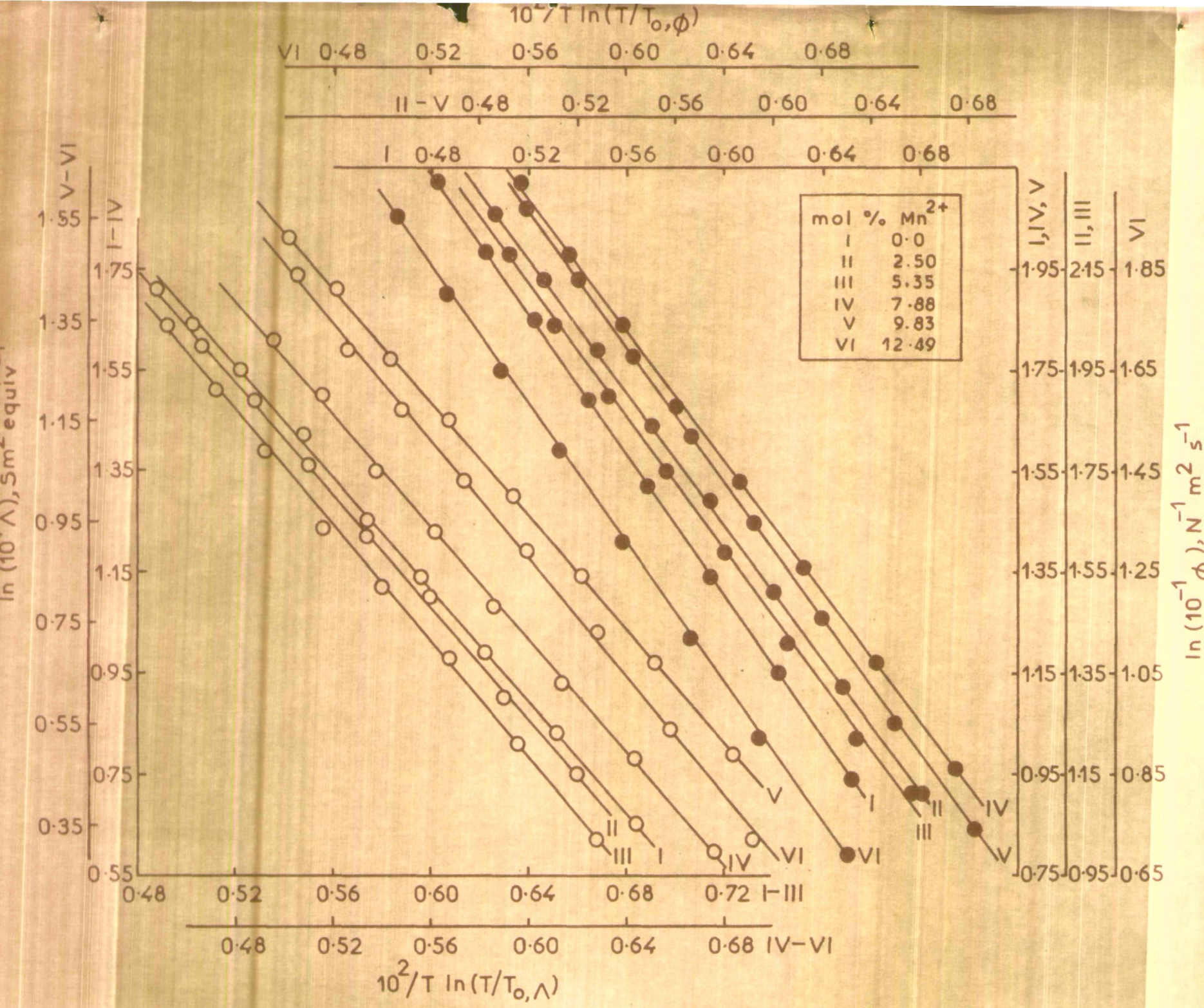

Fig. 22 Plots of $\ln Y (= \phi \text{ or } \Lambda)$ Vs. $^1/T \ln(T/T_o)$ for $Cd(NO_3)_2 \cdot 4{\cdot}18H_2O - MnCl_2$ Molten Salt System.

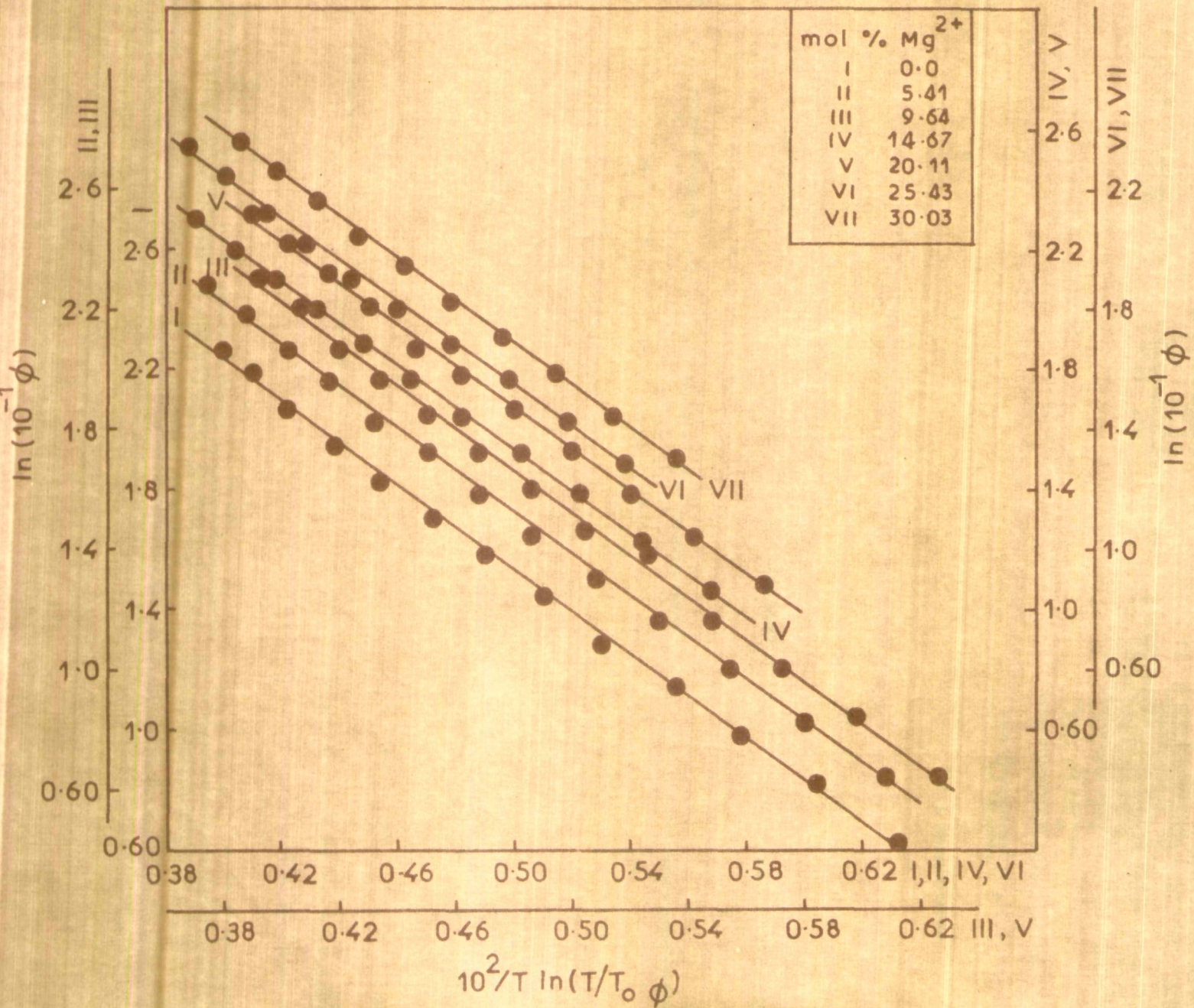

Fig. 23 Plots of $\ln \phi$ Vs. $^1/T \ln(T/T_o)$ for $Ni(NO_3)_2 \cdot 6{\cdot}01H_2O$–$Mg(NO_3)_2 \cdot 6{\cdot}13H_2O$ Molten Salt System.

non-Arrhenius below the melting point of the parent solvent. Sometimes, a return to the Arrhenius behaviour is also recorded in certain cases in which these measurements are possible in the vicinity of T_o values. The consideration of Arrhenius and non-Arrhenius regions in each of the plots is further reinforced indirectly by examining the plots (Figs. 12-15) of conductance/viscosity versus the reciprocal of free volume V_f ($= V-V_o$). Initially rapid decrease in the $\Lambda\eta$ values with decrease in the free volume slows down subsequently showing increasing tendency for the non-linear behaviour due to successive fall in the slope values of these plots. The slope eventually shows a tendency to approach zero as the free volume approaches a minimum or ultimately a zero value. At this point, i.e., near the ideal glass transition temperatures T_o, the curve appears to assume a linear behaviour. Such a behaviour is true of all the systems studied.

In view of the above consideration the environmental relaxation model was employed to explain the temperature dependence of viscosity and conductance data over the entire temperature range. These data were, therefore, least-squares fitted to the EEM equation and the computed values of the best fit parameters together with the standard deviations in $\ln\eta$ or $\ln\Lambda$ were given in Tables 30-32. The

TABLE 30: Computed Parameters of ERM Equation for $Ca(NO_3)_2 \cdot 4.06H_2O$ + $Co(NO_3)_2 \cdot 6.18H_2O$ molten salt system

Mol% Co^{2+}	$(\theta_{\infty} A)_Y$	$\bar{E}_Y$	$(\frac{1}{2})C_{oY}$	$T_{o,Y}(K)$	ℓ_{oY}	Std. dev. in ln Y	$\epsilon^3_{o\lambda}/\epsilon^3_{o\eta}$	$\bar{E}_\eta/\bar{E}_\lambda$
0.00	0.0188	1.617	2.103	204.4	2.82	0.010	1.28	1.27
	(0.4743)	(2.055)	(2.331)	(205.0)	(2.59)	(0.022)		
10.13	0.0196	1.615	2.092	202.3	2.77	0.012	1.26	1.26
	(0.4841)	(2.035)	(2.284)	(202.9)	(2.56)	(0.022)		
19.55	0.0198	1.611	2.087	200.3	2.72	0.010	1.25	1.25
	(0.5014)	(2.016)	(2.200)	(200.8)	(2.52)	(0.013)		
29.70	0.0211	1.579	2.079	198.1	2.66	0.015	1.26	1.26
	(0.5131)	(1.996)	(2.154)	(198.8)	(2.47)	(0.025)		
39.80	0.0220	1.570	2.066	196.0	2.61	0.016	1.25	1.25
	(0.5259)	(1.977)	(2.141)	(196.7)	(2.42)	(0.010)		
49.56	0.0231	1.559	2.035	194.0	2.55	0.020	1.25	1.26
	(0.5446)	(1.970)	(2.139)	(194.5)	(2.37)	(0.016)		

(continued)

TABLE 30: (continued)

Mol% Co^{2+}	$(\sigma_{\infty} A)_Y$	$\bar{R}_Y$	$(\frac{1}{2})C_{\sigma Y}$	$T_{\sigma,Y}(K)$	$\epsilon_{\sigma Y}$	Std. dev. in ln Y	$\epsilon^3_{\sigma\lambda}/\epsilon^3_{\sigma\eta}$	$\bar{R}_\eta/\bar{R}_\lambda$
59.51	0.0251	1.546	2.014	192.0	2.51	0.024	1.25	1.25
	(0.5528)	(1.937)	(2.124)	(192.5)	(2.33)	(0.008)		
69.68	0.0271	1.539	2.003	190.0	2.45	0.023	1.25	1.24
	(0.5716)	(1.918)	(2.110)	(190.5)	(2.28)	(0.015)		

Fluidity data are given within parentheses.

TABLE 31 : Computed Parameters of KRM Equations for $Ca(NO_3)_2.4.05H_2O$ + $MnCl_2$ molten salt system

Mol% Mn^{2+}	$(G_{oo}A)_Y$	$\bar{R}_Y$	$(\frac{1}{2})C_{oY}$	$T_{o,Y}(K)$	ℓ_{oY}	Std. dev. in ln Y	$\ell^3_{o\lambda}/\ell^3_{o\eta}$	$\bar{R}_\eta/\bar{R}_\lambda$
0.00	0.0204 (0.5808)	1.615 (2.068)	1.972 (2.209)	204.7 (204.8)	2.76 (2.54)	0.015 (0.007)	1.27	1.28
1.05	0.0188 (0.5703)	1.676 (2.093)	1.982 (2.244)	205.7 (205.7)	2.77 (2.59)	0.006 (0.008)	1.23	1.24
2.02	0.0197 (0.5600)	1.681 (2.118)	1.984 (2.291)	207.1 (206.0)	2.80 (2.60)	0.025 (0.009)	1.26	1.26
3.50	0.0194 (0.5260)	1.693 (2.144)	1.994 (2.300)	208.5 (208.5)	2.83 (2.62)	0.011 (0.010)	1.26	1.26
4.99	0.0188 (0.5210)	1.697 (2.169)	2.018 (2.320)	210.9 (209.3)	2.86 (2.63)	0.021 (0.017)	1.28	1.27
7.02	0.0185 (0.5072)	1.727 (2.104)	2.138 (2.374)	211.2 (211.2)	2.89 (2.66)	0.029 (0.019)	1.27	1.27

Fluidity data are given within parentheses.

TABLE 32 : Computed Parameters of EEM Equations for $Cd(NO_3)_2.4.16H_2O$ - $MnCl_2$ molten salt system.

Mol% Mn^{2+}	$(\epsilon_{\infty} A)_Y$	$\bar{E}_Y$	$(\frac{1}{2})C_{\epsilon Y}$	$T_{\epsilon,Y}^{(k)}$	$\epsilon_{\epsilon Y}$	Std. dev. in ln Y	$\epsilon^3_{\epsilon\Lambda}/\epsilon^3_{\epsilon\eta}$	$\bar{E}_\eta/\bar{E}_\Lambda$
0.00	0.00990 (0.29885)	1.7169 (2.1306)	1.6746 (1.8547)	189.5 (189.1)	2.0421 (1.9015)	0.013 (0.006)	1.25	1.24
2.50	0.01068 (0.30558)	1.6276 (2.0182)	1.6859 (1.8646)	190.5 (190.3)	2.0333 (1.8906)	0.014 (0.011)	1.24	1.23
5.35	0.01297 (0.36149)	1.5645 (1.9556)	1.6906 (1.8724)	191.4 (191.5)	2.0245 (1.8802)	0.009 (0.009)	1.24	1.24
7.88	0.01437 (0.44850)	1.4484 (1.8655)	1.7075 (1.8878)	192.4 (192.8)	2.0157 (1.8525)	0.008 (0.030)	1.28	1.28
9.85	0.01644 (0.50942)	1.3728 (1.7387)	1.7140 (1.9450)	193.8 (193.7)	2.0069 (1.8505)	0.020 (0.005)	1.27	1.26
12.49	0.01953 (0.62994)	1.3186 (1.6142)	1.7234 (2.0058)	195.0 (194.8)	1.9981 (1.8475)	0.020 (0.006)	1.26	1.22

Viscosity data are given within parentheses.

applicability of the ERM equation in the present systems is, however, evidenced by the linear plots of T ln ($\eta / G_\infty A$) and T ln ($1/\Lambda . G_\infty A$) against $(1/1 + \epsilon^2)^{3/2}$ as shown in Figs. 24-26.

The glass transition temperature, T_0: The glass transition temperature, T_0 is an important parameter in the sense that it is the most appropriate reference temperature to describe the limiting flow behaviour of liquid systems. It is characteristic of the system alone, is independent of the type of the flow property measured and is thermodynamic rather than kinetic in nature. Almost identical T_0 values obtained from the conductance and viscosity data for a given system support the view regarding its independence on the type of flow behaviour determined, i.e., it be conductance or viscosity of the systems studied. In addition, it appears to be independent of the model employed for the data analysis as apparent from Tables 10-13, 26-29, and 30-32 for the least-squares fitted parameters of the VTF, CEM and ERM, respectively, in which the best-fit values yield almost identical T_0 values.

For all the systems investigated the T_0 values show linear dependence on concentration. In the cases of $Ca(NO_3)_2.4.03H_2O$ - $MnCl_2$ and $Cd(NO_3)_2.4.18H_2O$ - $MnCl_2$

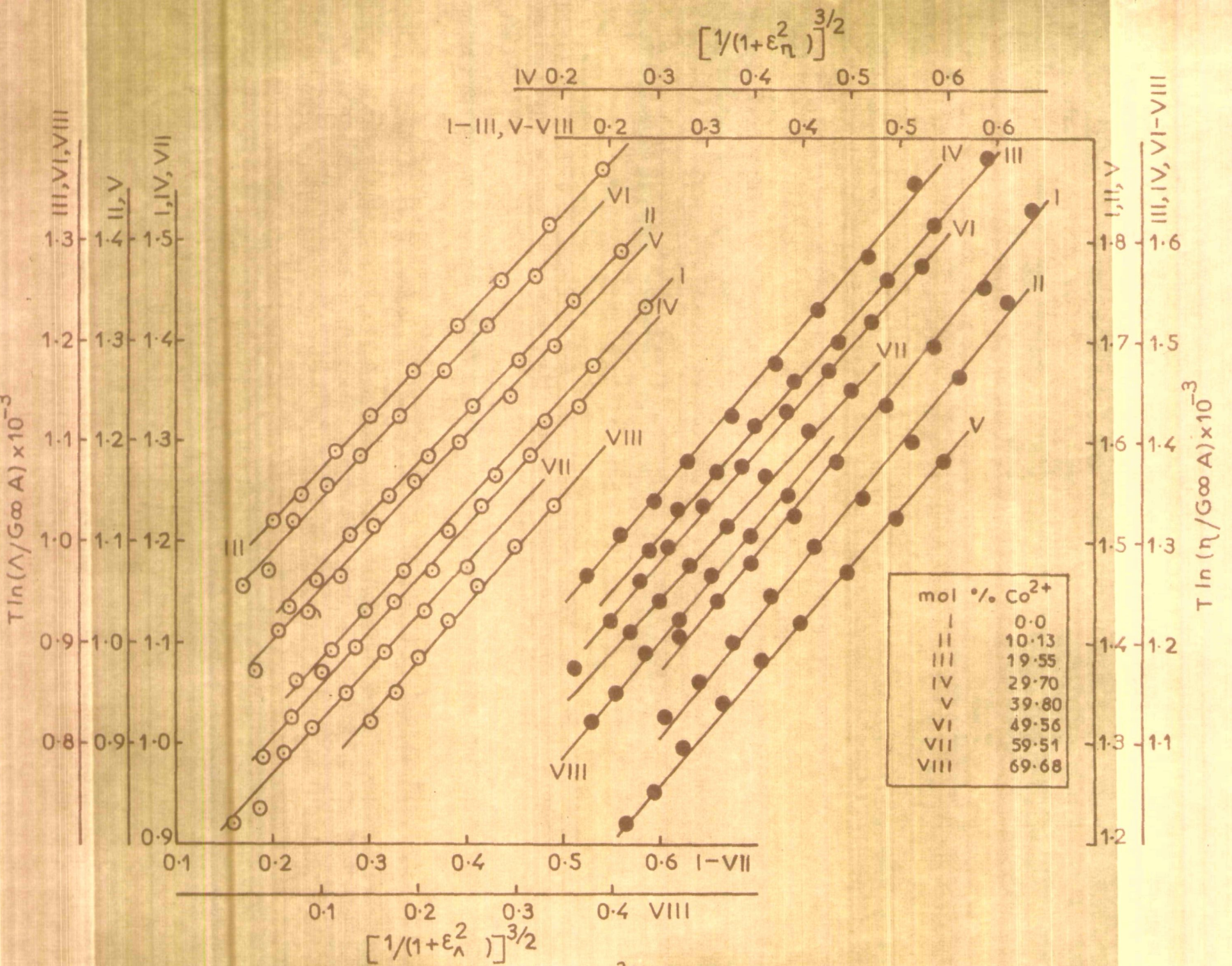

Fig.24 Plots of $T \ln(\eta,\Lambda/G\infty A)$ Vs. $[1/(1+\varepsilon_{\eta,\Lambda}^2)]^{3/2}$ for $Ca(NO_3)_2 \cdot 4.06H_2O + Co(NO_3)_2 \cdot 6.18H_2O$ Molten Salt System.

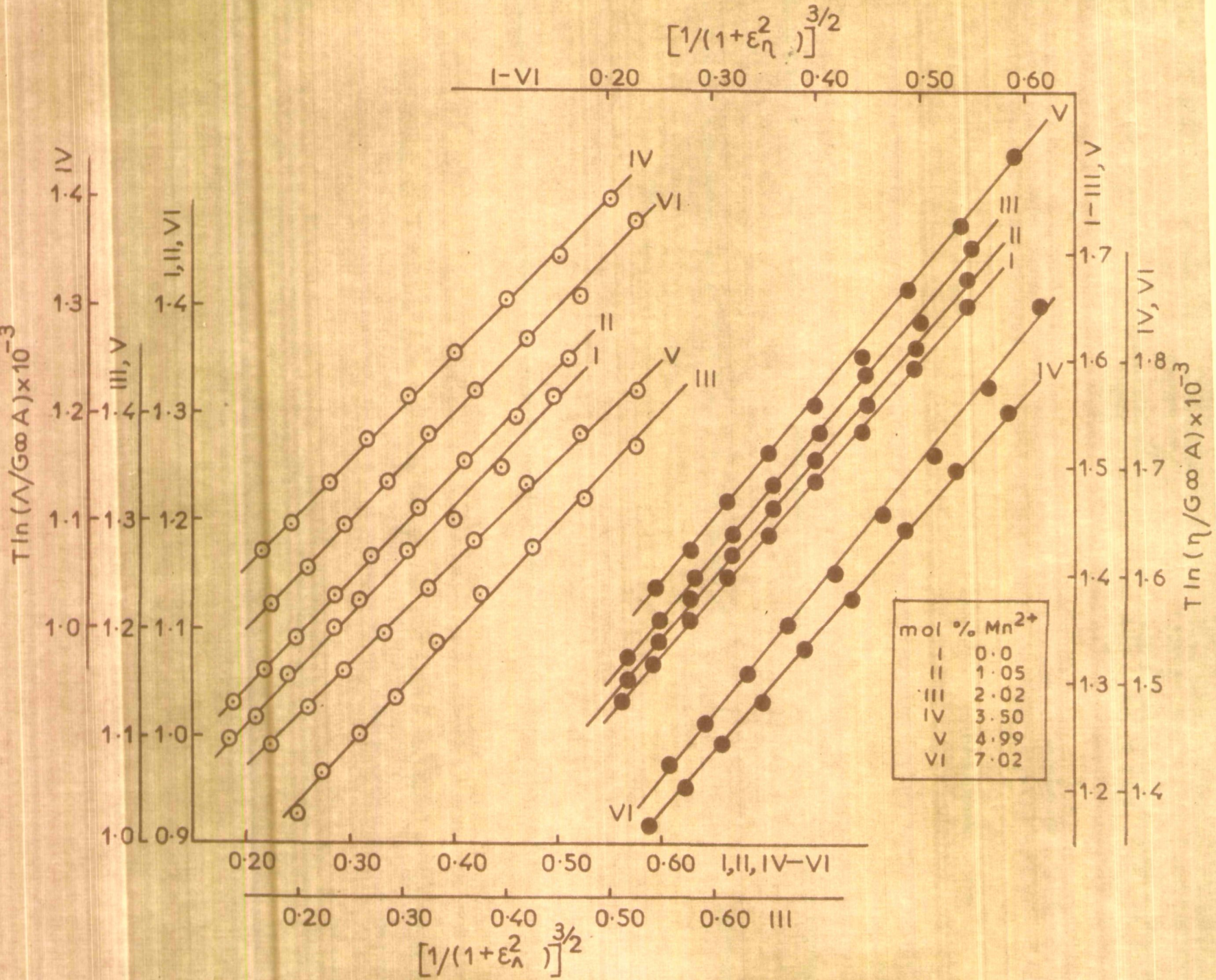

Fig.25 Plots of $T\ln(\eta,\Lambda/G\infty A)$ Vs. $[1/(1+\varepsilon_{\eta,\Lambda}^2)]^{3/2}$ for $Ca(NO_3)_2\cdot4.03H_2O-MnCl_2$ Molten Salt System.

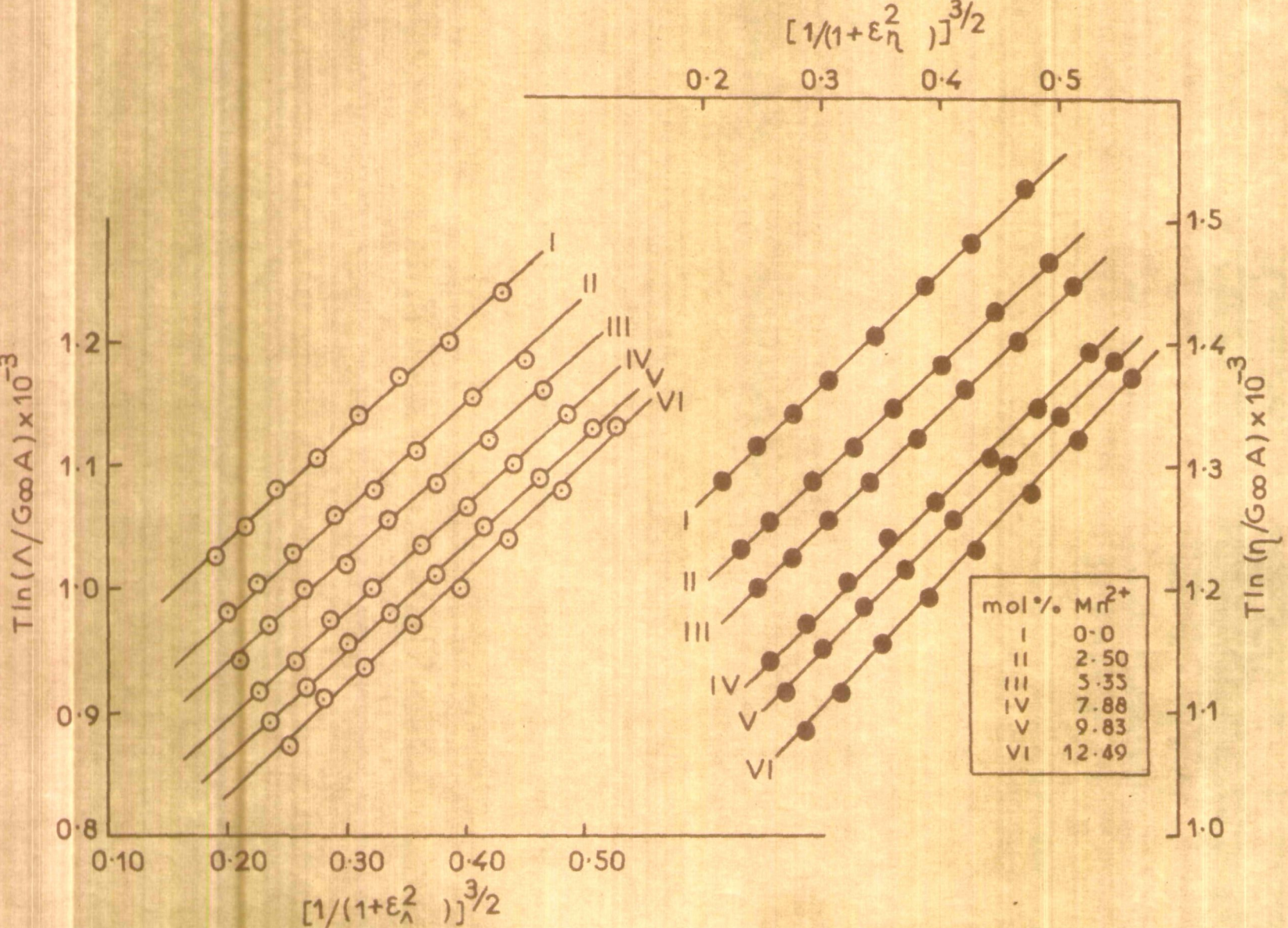

Fig. 26 Plots of $T\ln(\eta,\Lambda/G_\infty A)$ Vs. $[1/(1+\varepsilon_{\eta,\Lambda}^2)]^{3/2}$ for $Cd(NO_3)_2\cdot4\cdot18H_2O$–$MnCl_2$ Molten Salt System.

systems, T_e shows a linear increase with increasing solute concentration, while a linear decrease with increasing solute concentration is observed in those of $Ca(NO_3)_2.4.06 H_2O - Co(NO_3)_2.6.18H_2O$ and $Ni(NO_3)_2.6.01H_2O - Mg(NO_3)_2.6.15H_2O$ systems. This discrepancy in the variation of T_e with the solute concentration may qualitatively be understood in the light of various factors, e.g., the molecular size, the molecular complexity and the causes of supercooling. In most of the molten salts the constituent particles size being very small, the role of molecular complexity in determining the value of T_e appears to be secondary. On the other hand, in systems having small ionic or molecular aggregates the overall cohesive energy of the liquid seems to be the dominant factor in determining the magnitude of T_e. Therefore, it is worthwhile to take into account the role of cohesive energy for this purpose. It may be noted that lower the coulomb energy of a system lower will be the average charge/radius ratios of the cations of the melt. Consequently, the variation of T_e with solute concentration may be explained in terms of the cationic potential which has been defined as $\sum_i N_i Z_i/r_i$, where N_i is the mol fraction, Z_i is the charge and r_i is the radius of the species. In view of such a consideration an increase in the value of T_e with solute concentration in $Ca(NO_3)_2.4.03H_2O - MnCl_2$ and $Cd(NO_3)_2.4.18H_2O - MnCl_2$

systems may be the result of a corresponding increase in the cationic potential of Mn^{2+} which has larger cationic charge/radius ratio. Similar results have also been found[13] for the $Ca(NO_3)_2$ - KNO_3 melt in which the T_g for the pure KNO_3 was obtained as 100 K by extrapolating the plot of T_g versus the cationic potential of Ca^{2+} to zero, i.e., the state of zero cationic potential. Such an extrapolated value of T_g to zero cationic strength is comparable with the T_g values of 80-100 K obtained for simple molecular liquids.[36] This concept of cationic potential may, therefore, be applied to any pure or mixed nitrate system in order to see a reasonable accord in the extrapolated T_g value and that of the observed ones. For the system having halide anions and anions other than the nitrate ions, linear plots with different slopes but similar T_g values corresponding to zero cationic potential may be expected. However, such an extrapolation has not been suggested for systems of mixed anions.

It may be noted that the cationic potential is directly proportional to the cohesive energy of the system, therefore the cohesive force increases with successive additions of solute. This in turn appears to be responsible, for an increase in the T_g values. However, the concept of cationic potential fails to explain the linear

decrease of T_o values with increasing [solute] in the cases of $Ca(NO_3)_2.4.06H_2O$ - $Co(NO_3)_2.6.18H_2O$ and $Ni(NO_3)_2.6.01H_2O$ - $Mg(NO_3)_2.6.13H_2O$ systems contrary to the expected increase in the T_o values with increasing concentrations of Co^{2+} and Mg^{2+} in both the cases due to their higher cationic charge/radius ratios. An alternative interpretation for such variations of T_o with concentration may be made by taking into account the correlation[37] between the T_g or T_o and the characteristic Debye temperature, Θ_D which shows an inverse dependence on the square root of the effective masses (i.e., $m^{-1/2}$ dependence) of the component particles. Thus an increase in T_o with increasing solute concentration in the $Ca(NO_3)_2.4.05H_2O$ - $MnCl_2$ and $Cd(NO_3)_2.4.18H_2O$ - $MnCl_2$ systems may be due to a decrease in the resulting average molecular mass. The same may, further, be applied to $Ca(NO_3)_2.4.06H_2O$ - $Co(NO_3)_2.6.18H_2O$ molten mixtures where an increase in the average molecular mass with the addition of $Co(NO_3)_2.6.18H_2O$ to $Ca(NO_3)_2.4.06H_2O$ causes decrease in the value of T_o. However, such an $m^{-1/2}$ dependence does not apply to $Ni(NO_3)_2.6.01H_2O$ - $Mg(NO_3)_2.6.13H_2O$ melts as has also been reported earlier[18] for a number of cases.

Moreover, the increase or decrease of T_o values with molar concentration may be understood qualitatively as

follows: The cause of supercooling may be explained in terms of the free-volume model. The dilute melts are considered to contain abundant free-volume due to the presence of lesser ions as compared to those of the concentrated melts. The glass transition temperature refers to the extent of cooling required to reach the limiting state of zero free-volume. It may be noted that the free-volume decreases successively with successive increase in the concentration of solute and therefore, less cooling is required to reach the amorphous phase in higher concentrations as compared to those in dilute solutions. Consequently, higher T_o values may be expected for the concentrated melts. Also a higher T_o value is anticipated in concentrated melts due to diminished configurational entropy of relatively compact structural alignment in such melts. Also a linear increase in the value of T_o with increasing [solute] may be explained as due to the fact that the added solute undergoes glass transition temperature at higher temperatures than that of the pure solvent. Accordingly, a linear decrease of T_o with increasing concentration of $Mg(NO_3)_2.6.1H_2O$ is observed in the case of $Ni(NO_3)_2.6.0H_2O$ - $Mg(NO_3)_2.6.1H_2O$ melts. Also an increase in the solute concentration will increase the rigidity of the resulting mixture and hence the viscosity will increase. This will, therefore, seem to be responsible for increasing the T_o values.

The exponential term "k_Y": The k_Y term computed from the VTF and that of the CEM equations has been visualised as independent of concentration in the present systems. However, the values of k_Y term has been found to vary with concentration in a number of silicate systems and that of $ZnCl_2$ - KCl. It may be noted that the exponential term remains unchanged for a system whose concentration variation does not alter the melt structure in too radical a fashion. Its values are independent of the model employed but seem to depend on the type of transport behaviour studied. Further, it is also apparently independent of the nature of the melt. Angell and Moynihan[13,14] proposed it to be a sort of universal constant and the value of k_Y taken for the viscous flow was close to 700 K while that for conductance close to 600 K. According to Cohen and Turnbull's hard-sphere model, the constancy of k_Y term may be understood in terms of its relation,

$$k_Y \text{ (VTF)} = \gamma v^*/\alpha \bar{V}_m$$

where γ is a geometric factor to correct for the overlap of the free-volume in calculating the probability of occurrence of a critical void volume v^*, α is the mean value of the coefficient of expansion from T_o to T; and $\bar{V}_m$ is the mean molecular volume. The critical void volume

v^* influences the rate of diffusion and therefore depends upon the size of the larger molecule. Despite the size of the solute molecule is equal or smaller as compared to that of the solvent the rate of diffusion will be governed by the solvent molecule, because the diffusive displacement is brought about as a result of jumping of the neighbouring solvent molecule into the void created by the transfer of solute molecule. Hence the rate of diffusion will vary as the average free volume decreases with the increase in [solute] while the critical size of the void necessary for diffusion will not change with concentration. Consequently, the critical void volume of the solvent would be similar to those of the corresponding molten mixtures. The coefficient of expansion, α varies monotonously with concentration, where the term $\gamma v^*/\alpha \bar{V}_m$ involved in the above expression must substantially be independent of the concentration of solute. On the basis of the above view the constancy in the values of k_Y term is obvious as has been found in all the cases under consideration. Angell and Brassel[33] considered it a nearly constant multiple of T_o in calcium nitrate tetrahydrate melt, and substituted DT_o for k_Y in the VTF equation where D is concentration invariant. However, any significant change in the k_Y term with concentration has not been observed in the systems studied.

On the other hand, the k_{2Y} term of the Doolittle

expression may be taken as equal to γv^* per mol which seems to be concentration independent as has been found for the k_{3Y} term of the VTF equation. This has been attributed to almost identical slopes of the linear plots (Figs. 16-19) of ln Y versus $1/(V-V_o)$ and ln $(YT^{1/2})$ versus $1/(T-T_o)$ for the two cases (Figs. 8-11).

The constancy of k_{4Y} term of equation (12) with concentration may be visualized in a manner similar to that of the k_{3Y} term of the VTF equation. This term in equation (12) was used for,

$$k_{4Y} = N \Delta\mu S_c^*/R \Delta C_p$$

where the terms have already been defined in the introduction. This equation states that the minimum configurational entropy, S_c^* which must be possessed by a region of the liquid in order to undergo co-operative rearrangement, is taken as a constant ($S_c^* = k \ln 2$, where k is the Boltzmann constant). Further it has been suggested that the $\Delta\mu/\Delta C_p$ ratio also remains constant due to the parallel changes in the energy barrier per mol of the particle, $\Delta\mu$ and the difference in the heat capacities of the glassy states and that of the liquid, ΔC_p. Therefore, the k_{4Y} term may be presumed to be an almost constant quantity as has actually been found in all the molten salt systems

studied. These findings are in accordance with those reported earlier[11,12,38-41] for a large varieties of molten salt systems, organic liquids particularly at lower temperatures and polymers.

The pre-exponential term, A_Y: The pre-exponential terms A_{5Y} and A_{4Y} computed from the free volume and the configurational entropy models are given in Tables 10-13 and 26-29, respectively. It is evident from the tables that the value of A_Y depends not only on the model employed but also on the kind of transport property studied. It depends upon the nature of the system. The A_{5Y} values obtained from the VTF equation are found to be greater than those of the CEM equation. The presence of temperature in logarithmic form in the exponential term seems to be responsible for much lower value of A_{4Y} (CEM) than that of A_{5Y} (VTF).

With a view to understand the nature of the variation of A_Y term with concentration the mean molecular mass dependence relationship, the Maxwell's relationship[42] of relaxation time and the rigidity of the system were taken into consideration. It may be noted that the values of A_{5Y} decrease linearly with concentration in the cases of $Ca(NO_3)_2.4.03H_2O$ - $MnCl_2$ and $Cd(NO_3)_2.4.18H_2O$ - $MnCl_2$ systems, while a regular increase was recorded in the cases of $Ca(NO_3)_2.4.06H_2O$ - $Co(NO_3)_2.6.18H_2O$ and $Ni(NO_3)_2.6.01H_2O$ - $Mg(NO_3)_2.6.13H_2O$ systems.

According to Cohen and Turnbull the pre-exponential term has been expressed as $A_\gamma \approx r/m^{\gamma/2}$. This indicates a direct dependence of the pre-exponential term, A_γ on the particle diameter, r and an inverse dependence on the square root of the mean molecular mass of the particle, m. Therefore, the term A_γ would increase with decrease in the average particle mass due to an increase in [solute]. The linear variation of A_γ term with solute concentration is in agreement with the $m^{-\gamma/2}$ dependence relation in the case of $Ni(NO_3)_2.6.01H_2O$ - $Mg(NO_3)_2.6.13H_2O$ system. However, such a consideration does not explain its opposite trend with increase in [solute] found for the remaining two systems. Similar discrepancy has also been observed by many workers.[14] They viewed it as the outcome of the difference in the lability of water of the hydrated ions.

The pre-exponential terms of the configurational entropy model and their nature of variation appears to be governed by some other factors. Maxwell explained the dependence of A_γ term on the relaxation time, τ and the rigidity modulus, G_∞ of the flowing entities of the system in terms of the relation,

$$\frac{1}{\tau} = G_\infty \gamma \qquad \ldots (15)$$

while the Eyring's expression for the relaxation time was given as

$$\tau = \tau_0 \exp\left[-E/RT\right] \qquad \ldots (16)$$

where τ_0 is the period of vibration of the flowing entities in the equilibrium position, E is the activation energy for relaxation; and R and T have their usual meaning. Substituting equation (15) into that of (16) one may obtain an expression for the flow properties, Y (= ϕ or Λ) in terms of G_∞ and τ,

$$Y = 1/G_\infty \tau_0 \exp\left[-E_Y/RT\right] \qquad \ldots (17)$$

Adam and Gibbs pointed out that the average transition probability, $\bar{\omega}(T)$ for the co-operative rearrangement of the flowing entities is proportional to the fraction of configurations which undergo such a transition. This may be expressed as

$$\bar{\omega}(T) \propto n'/N \qquad \ldots (18)$$

where N is the number of independent equivalent and distinguishable subsystems or configurations of macroscopic system and n', the number of configurations which undergo such a transition. Further, the transition probability for the cooperative rearrangement, $\bar{\omega}(T)$ is inversely proportional to the relaxation time, τ and thus

$$\bar{\omega}(T) \propto \frac{1}{\tau} \qquad \ldots (19)$$

The above consideration reveals the relation,

$$A_{4Y} = \frac{1}{G_\infty \tau_0} \qquad \ldots (20)$$

Consequently, the A_{4Y} term seems to depend on the modulus of rigidity of the system. With the increase of concentration the system becomes increasingly more rigid and therefore, a decrease in the average cooperative transition probability is expected. In other words, the relaxing species will have greater period of vibration in their equilibrium position as compared to those in dilute solutions.

This consideration has made it possible to understand the dependence of viscosity on the rigidity of supercooled liquids and glasses. The average relaxation time was defined as

$$\bar{\tau} = \eta / G_\infty$$

or $$\bar{\tau} = 1/G_\infty \phi \qquad \ldots (21)$$

where G_∞ is the shear modulus and ϕ represents the fluidity. It was found that, $\bar{\tau} \approx$ shear relaxation time, τ in the same equilibrium position. The temperature dependence of the mean life time, τ may also be explained by the Eyring's equation (15).

Molar intrinsic volume, V_o: The values of V_{oY} were found to be almost identical for Y = ϕ or △ as was the case with those of T_{oY} emphasising the thermodynamic nature of these parameters. Also, the values of V_o were found to be independent of temperature within the experimental range of measurement. However, Miller[43] has reported the temperature dependent intrinsic volume for the normal alkanes. This may be understood by presuming that the V_o values remain temperature independent for a hard sphere model as considered in the case of molten salt system while it becomes temperature dependent for more complex and linear molecules such as normal alkanes. Its values obtained from the extrapolation of the volume-temperature plots to T_o are close to those found from the least-squares fitting. The best fit values of V_{oY} have been found to agree with those of the expected molar volume at T_o but not at 0 K. This view led one to believe that the origin of the free volume is at T_o rather at 0 K.

The values of V_o have been found to decrease linearly with increase in the solute concentration in the cases of $Ca(NO_3)_2.4.03H_2O$ - $MnCl_2$ and $Ca(NO_3)_2.4.18H_2O$ - $MnCl_2$ systems while a linear increase has been reported in the cases of $Ca(NO_3)_2.4.06H_2O$ - $Ca(NO_3)_2.6.18H_2O$ and $Ni(NO_3)_2.6.01H_2O$ - $Mg(NO_3)_2.6.1H_2O$ melts. The decrease in the V_o

values with increasing solute concentration may be ascribed to the direct dependence of V_o on the mean molecular mass, m. It is worthy of note that in all the melts studied V_o has been found to be additive in nature. The additive nature of V_o may be attributed to the ideal behaviour of these melts with respect to the molal volume and may be given by the relation,

$$V_{o,x_i} = \sum_i x_i V_{o,i}$$

where V_{o,x_i} represents the molar intrinsic volume of the melt having the ith component of mol fraction, x_i. An increase in the V_o values with increasing [solute] in the systems mentioned above seems to be mainly determined by the additive nature of the melt while the average particle mass plays an insignificant role.

Energies of activation: The energies of activation, E_γ were calculated from the corresponding (Appendix) derivatives, $d \ln\gamma / d(1/T)$ using the computed parameters of the VTF, CEM and the MRM equations. The E_γ values thus calculated from the derivative of the VTF equation are given (Tables 33-36) as functions of temperature and concentration. The corrected activation energies, E_{corr}, are listed in Tables 37-40. These values are plotted against $[T/(T-T_o)]^2$ as shown in Fig. 27 for 69.68, 7.02, 12.49 and

TABLE 33: Activation Energies (kJ/mol) computed from VTF Equation for $Ca(NO_3)_2 \cdot 4.06H_2O$ + $Co(NO_3)_2 \cdot 6.18H_2O$ Molten Salt System

	mol % of Co^{2+}							
T/K	0.0	10.13	19.55	29.70	39.80	49.56	59.51	69.68
303.0	44.25	43.02	41.00	39.48	37.96	36.31	34.56	33.25
	(51.95)	(49.72)	(47.65)	(46.46)	(43.91)	(42.67)	(41.19)	(40.05)
308.0	41.29	40.24	38.43	37.06	35.70	34.20	32.62	31.42
	(48.49)	(46.51)	(44.65)	(43.62)	(41.29)	(40.20)	(38.87)	(37.85)
313.0	38.71	37.79	36.15	34.92	33.70	32.33	30.87	29.79
	(45.45)	(43.67)	(42.00)	(41.10)	(38.97)	(38.00)	(36.79)	(35.88)
318.0	36.42	35.62	34.12	33.01	31.91	33.65	29.31	28.31
	(40.36)	(41.15)	(39.64)	(38.85)	(36.89)	(36.02)	(34.92)	(34.11)
323.0	34.38	33.68	32.31	31.30	30.29	29.13	27.89	26.98
	(38.22)	(38.90)	(37.53)	(36.83)	(35.02)	(34.24)	(33.24)	(32.50)
328.0	32.56	31.93	30.67	29.76	28.83	27.76	26.61	25.76
	(36.29)	(36.88)	(35.63)	(35.01)	(33.33)	(32.03)	(31.72)	(31.05)

continued..

TABLE 33: continued

	mol % of Co^{2+}							
T/K	0.0	10.13	19.55	29.70	39.80	49.56	59.51	69.68
333.0	30.91	30.36	29.19	28.36	27.51	26.52	25.44	24.66
	(34.34)	(33.07)	(33.92)	(33.36)	(31.80)	(31.17)	(30.33)	(29.72)
338.0	29.42	28.93	27.85	27.09	26.30	25.38	24.37	23.65
	(32.96)	(33.42)	(32.36)	(31.87)	(30.41)	(29.84)	(29.07)	(28.51)
343.0	28.07	27.64	26.63	25.92	25.20	24.34	23.39	22.72
	(33.44)	(31.92)	(30.94)	(30.50)	(29.13)	(28.62)	(27.90)	(27.39)

Activation Energies for Fluidity data are given within parentheses.

TABLE 34: Activation Energies (kJ/mol) computed from VTF Equation for $Ca(NO_3)_2 \cdot 4.05H_2O + MnCl_2$ Molten Salt System

	mol % of Mn^{2+}					
T/K	0.0	1.05	2.02	3.50	4.99	7.02
313.0	39.00 (45.73)	39.64 (46.59)	40.38 (47.41)	41.81 (48.80)	42.61 (50.18)	44.18 (52.16)
318.0	36.68 (43.02)	37.26 (43.78)	37.93 (44.52)	39.21 (45.77)	39.93 (47.01)	41.33 (48.77)
323.0	34.62 (40.60)	35.14 (41.29)	35.75 (41.96)	36.90 (43.09)	37.55 (44.20)	38.81 (45.79)
328.0	32.77 (38.43)	33.24 (39.06)	33.79 (39.67)	34.84 (40.69)	35.44 (41.70)	36.57 (43.14)
333.0	31.11 (36.48)	31.54 (37.05)	32.04 (37.61)	33.00 (38.55)	33.54 (39.46)	34.57 (40.77)
338.0	29.60 (34.72)	30.00 (35.24)	30.46 (35.76)	31.33 (36.61)	31.84 (37.45)	32.77 (38.65)

continued..

TABLE 34 : continued

	mol % of Mn^{2+}					
T/K	0.0	1.05	2.02	3.50	4.99	7.02
343.0	28.24 (33.13)	28.60 (33.61)	29.03 (34.08)	29.83 (34.86)	30.30 (35.63)	31.15 (36.73)
348.0	26.99 (31.67)	27.33 (32.11)	27.73 (32.55)	28.46 (33.28)	28.89 (33.99)	29.68 (35.00)
353.0	25.85 (30.34)	26.16 (30.75)	26.53 (31.16)	27.21 (31.83)	27.62 (32.49)	28.34 (33.42)

Activation Energies for Fluidity data are given within parentheses.

TABLE 35: Activation Energies (kJ/mol) computed from VTF Equation for $Cd(NO_3)_2 \cdot 4.18H_2O + MnCl_2$ Molten Salt System

	mol % of Mn^{2+}					
T/K	0.0	2.50	5.35	7.88	9.83	12.49
313.0	29.53 (34.15)	29.80 (34.64)	30.72 (35.22)	31.06 (36.06)	31.84 (36.53)	32.17 (37.14)
318.0	28.07 (32.48)	28.31 (32.95)	29.17 (33.46)	29.47 (34.23)	30.19 (34.65)	30.48 (35.20)
323.0	26.75 (30.97)	26.97 (31.38)	27.76 (31.86)	28.03 (32.58)	28.70 (32.95)	28.95 (33.46)
328.0	25.55 (29.60)	25.75 (29.97)	26.49 (30.42)	26.73 (31.08)	27.36 (31.42)	27.58 (31.88)
333.0	24.46 (28.35)	24.63 (28.69)	25.33 (29.10)	25.54 (29.72)	26.13 (30.02)	26.33 (30.44)
338.0	23.46 (27.20)	23.61 (27.52)	24.27 (27.90)	24.46 (28.47)	25.01 (28.75)	25.18 (29.14)

continued..

TABLE 55: continued

	mol % of Mn^{2+}					
T/K	0.0	2.50	5.35	7.88	9.83	12.49
343.0	22.54 (26.15)	22.68 (26.44)	23.29 (26.79)	23.47 (27.33)	23.99 (27.58)	24.14 (27.94)
348.0	21.69 (25.18)	21.81 (25.45)	22.40 (25.77)	22.55 (26.28)	23.04 (26.51)	23.18 (26.84)

Activation Energies for Fluidity data are given within parentheses.

TABLE 36: Activation Energies (kJ/mol) for Fluidity computed from VTF Equation for $Ni(NO_3)_2.6.01H_2O + Mg(NO_3)_2.6.13H_2O$ Molten Salt System

	mol % of Mg^{2+}						
T/K	0.0	5.41	9.64	14.67	20.11	25.43	30.03
323.0	35.18	34.99	34.59	34.35	34.00	33.74	33.51
328.0	33.53	33.35	32.99	32.77	32.44	32.21	32.00
333.0	32.03	31.87	31.53	31.32	31.02	30.81	30.62
338.0	30.66	30.51	30.20	30.01	29.73	29.54	29.36
343.0	29.41	29.28	28.98	28.80	28.54	28.36	28.19
348.0	28.26	28.13	27.86	27.69	27.45	27.29	27.13
353.0	27.19	27.09	26.83	26.67	26.44	26.29	26.14
358.0	26.21	26.12	25.87	25.72	25.51	25.37	25.23
363.0	25.30	25.21	24.98	24.85	24.64	24.51	24.38
368.0	24.46	24.38	24.16	24.03	23.83	23.72	23.60
373.0	23.67	23.60	23.39	23.27	23.09	22.98	22.86
378.0	22.94	22.87	22.68	22.55	22.38	22.28	22.17
383.0	22.26	22.19	22.00	21.89	21.73	21.63	21.53

TABLE 37: Corrected Activation Energies (kJ/mol) as a function of Temperature for $Cu(NO_3)_2.4.06H_2O$ + $Co(NO_3)_2.6.18H_2O$ Molten Salt System

	mol % of Co^{2+}							
T/K	0.0	10.13	19.55	29.70	39.80	49.56	59.51	69.68
303.0	45.49 (53.21)	44.28 (50.98)	42.26 (48.91)	40.72 (47.72)	39.22 (45.16)	37.56 (43.93)	35.83 (42.45)	34.51 (41.31)
308.0	42.57 (49.77)	41.52 (47.78)	39.71 (45.93)	38.34 (44.90)	36.98 (42.57)	35.48 (41.48)	33.89 (40.15)	32.70 (39.13)
313.0	40.01 (46.75)	39.09 (44.97)	37.45 (43.30)	36.22 (42.40)	35.00 (40.27)	33.63 (39.30)	32.17 (38.09)	31.09 (37.18)
318.0	37.74 (44.08)	36.94 (42.47)	35.44 (40.96)	34.33 (40.17)	33.23 (38.21)	31.97 (37.35)	30.63 (36.25)	29.63 (35.43)
323.0	35.73 (41.70)	35.02 (40.24)	33.64 (38.87)	32.64 (38.17)	31.63 (36.36)	30.48 (35.59)	29.23 (34.59)	28.32 (33.84)
328.0	33.92 (39.58)	33.30 (38.25)	32.03 (37.00)	31.12 (36.37)	30.20 (34.69)	29.13 (34.00)	27.97 (33.09)	27.13 (32.41)

continued..

TABLE 37: continued

	mol % of Co^{2+}							
T/K	0.0	10.13	19.55	29.70	39.80	49.56	59.51	69.68
333.0	32.29 (37.67)	31.74 (36.45)	30.58 (35.30)	29.74 (34.75)	28.89 (33.18)	27.90 (32.56)	26.82 (31.72)	26.04 (31.11)
338.0	30.85 (35.95)	30.34 (34.82)	29.25 (33.77)	28.45 (33.28)	27.70 (31.81)	26.78 (31.25)	25.78 (30.48)	25.05 (29.91)
343.0	29.50 (34.38)	29.06 (33.35)	28.05 (32.37)	27.35 (31.93)	26.62 (30.56)	25.76 (30.05)	24.82 (29.33)	24.14 (28.82)

Corrected Activation Energies for Fluidity are given within parentheses.

TABLE 3: Corrected Activation Energies (kJ/mol) as a function of Temperature for $Ca(NO_3)_2.4.03H_2O$ + $MnCl_2$ Molten Salt System

	mol % of Mn^{2+}					
T/K	0.0	1.05	2.02	3.50	4.90	7.02
313.0	40.30 (47.03)	40.94 (47.89)	41.68 (48.71)	43.11 (50.10)	43.91 (51.48)	45.48 (53.46)
318.0	38.00 (44.34)	38.58 (45.10)	39.25 (45.84)	40.53 (47.10)	41.25 (48.33)	42.65 (50.09)
323.0	35.96 (41.94)	36.48 (42.63)	37.09 (43.30)	38.24 (44.43)	38.89 (45.54)	40.15 (47.13)
328.0	34.13 (39.79)	34.61 (40.42)	35.16 (41.03)	36.20 (42.05)	36.80 (43.06)	37.94 (44.50)
333.0	32.49 (37.87)	32.92 (38.44)	33.43 (38.99)	34.38 (39.93)	34.93 (40.85)	35.96 (42.15)
338.0	31.01 (36.13)	31.40 (36.65)	31.87 (37.16)	32.74 (38.02)	33.24 (38.86)	34.18 (40.05)

continued..

TABLE 38: continued

	mol % of Mn^{2+}					
T/K	0.0	1.05	2.02	3.50	4.99	7.02
343.0	29.66 (34.55)	30.02 (35.03)	30.45 (35.50)	31.25 (36.29)	31.72 (37.06)	32.58 (38.16)
348.0	28.44 (33.12)	28.77 (33.56)	29.17 (34.00)	29.90 (34.72)	30.34 (35.43)	31.13 (36.44)
353.0	27.32 (31.80)	27.63 (32.22)	28.00 (32.62)	28.67 (33.29)	29.08 (33.94)	29.81 (34.89)

Corrected Activation Energies for Fluidity are given within parentheses.

TABLE 39: Corrected Activation Energies (kJ/mol) as a function of Temperature for $Cd(NO_3)_2.4.18H_2O$ + $MnCl_2$ Molten Salt System

	mol % of Mn^{2+}					
T/K	0.0	2.50	5.35	7.88	9.83	12.49
313.0	30.83 (35.45)	31.10 (35.94)	32.02 (36.52)	32.36 (37.36)	33.14 (37.83)	33.47 (38.01)
318.0	29.39 (33.80)	29.64 (34.25)	30.48 (34.78)	30.79 (35.55)	31.51 (35.97)	31.80 (36.03)
323.0	28.09 (32.31)	28.31 (32.72)	29.10 (33.21)	29.37 (33.92)	30.05 (34.30)	30.29 (34.25)
328.0	26.91 (30.96)	27.11 (31.34)	27.85 (31.78)	28.09 (32.44)	28.72 (32.78)	28.94 (32.63)
333.0	25.84 (29.73)	26.02 (30.07)	26.71 (30.48)	26.91 (31.10)	27.51 (31.41)	27.71 (31.17)
338.0	24.86 (28.60)	25.02 (28.92)	25.67 (29.30)	25.87 (29.88)	26.42 (30.15)	26.59 (29.83)

continued..

TABLE 39: continued

	mol % of Mn^{2+}					
T/K	0.0	2.50	5.35	7.88	9.83	12.49
343.0	25.96 (27.57)	24.10 (27.87)	24.72 (28.21)	24.89 (28.76)	25.41 (29.01)	25.56 (28.60)
348.0	25.13 (26.62)	25.26 (26.89)	25.85 (27.22)	24.00 (27.73)	24.49 (27.96)	24.62 (27.48)

Corrected Activation Energies for Fluidity are given within parentheses.

TABLE 4: Corrected Activation Energies (kJ/mol) for Fluidity as a function of Temperature for $Ni(NO_3)_2.6.01H_2O$ + $Mg(NO_3)_2.6.13H_2O$ Molten Salt System

	mol % of Mg^{2+}						
T/K	0.0	5.41	9.64	14.67	20.11	25.43	30.03
323.0	36.52	36.33	35.93	35.69	35.34	35.09	34.86
328.0	34.89	34.71	34.35	34.13	33.80	33.57	33.36
333.0	33.41	33.25	32.91	32.71	32.41	32.19	32.00
338.0	32.06	31.92	31.60	31.41	31.13	30.94	30.76
343.0	30.83	30.70	30.35	30.22	29.96	29.79	29.62
348.0	29.70	29.58	29.31	29.14	28.89	28.73	28.57
353.0	28.66	28.55	28.29	28.13	27.90	27.76	27.61
358.0	27.70	27.60	27.36	27.21	26.99	26.86	26.72
363.0	26.81	26.72	26.49	26.35	26.15	26.02	25.89
368.0	25.99	25.91	25.69	25.56	25.36	25.25	25.13
373.0	25.23	25.15	24.94	24.82	24.63	24.53	24.41
378.0	24.51	24.44	24.24	24.13	23.95	23.85	23.74
383.0	23.85	23.78	23.59	23.48	23.32	23.22	23.12

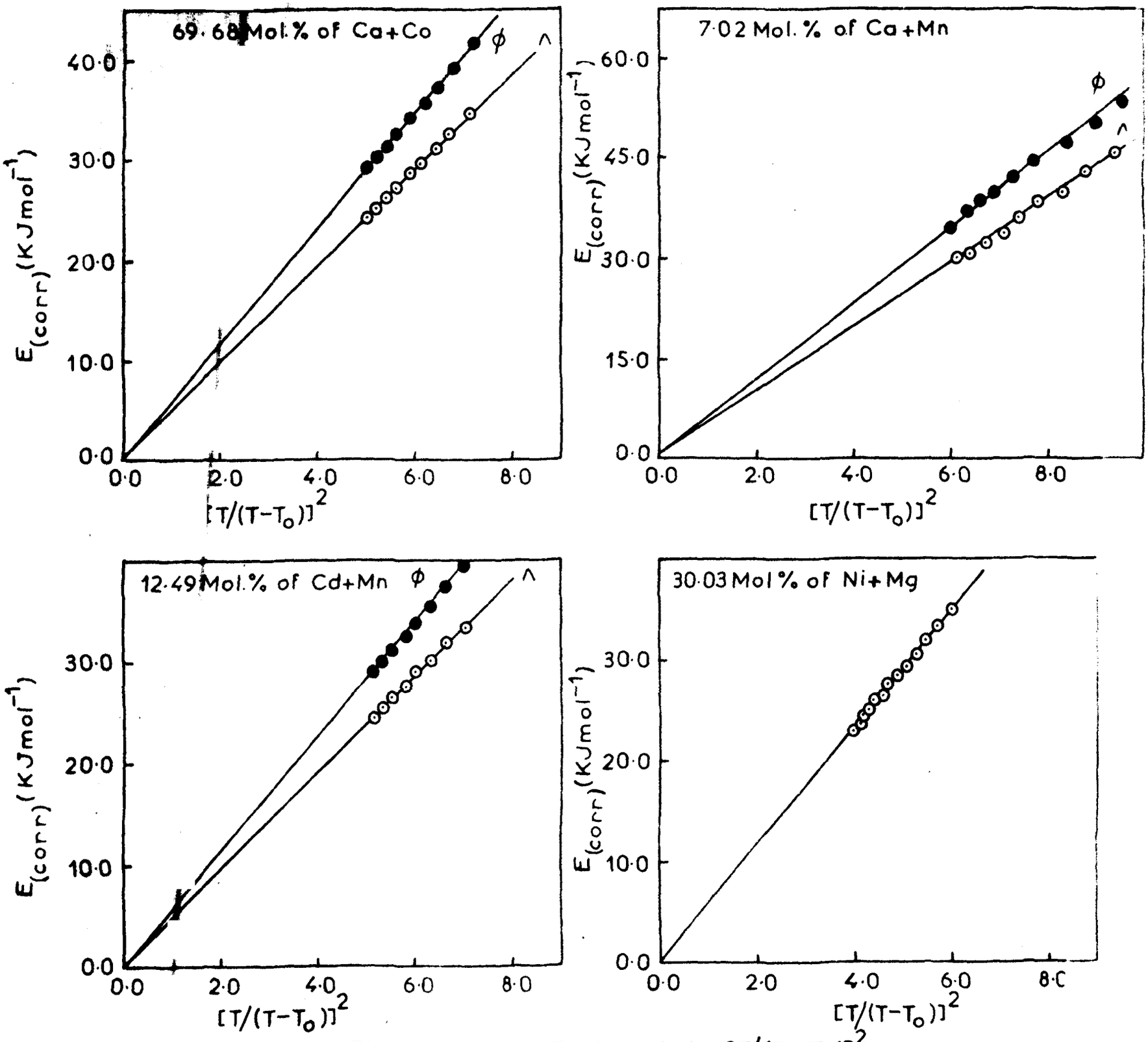

Fig.27 Plots of E_Y (corr) Vs. $[T/(T-T_o)]^2$

30.03 mol% of $Ca(NO_3)_2 \cdot 4.06H_2O$ - $Co(NO_3)_2 \cdot 6.18H_2O$, $Ca(NO_3)_2 \cdot 4.03H_2O$ - $MnCl_2$, $Cd(NO_3)_2 \cdot 4.18H_2O$ - $MnCl_2$ and $Ni(NO_3)_2 \cdot 6.01H_2O$ - $Mg(NO_3)_2 \cdot 6.13H_2O$ molten salt systems, respectively. Similar plots may also be obtained for all the concentrations of each of the systems studied. It may be noted from Fig. 27 that all the plots pass through the origin showing the sensitivity to the most probable value of T_0. It is further obvious that the selected T_0 value shows a sharp deviation in such a plot on shifting its value to ± 5 degrees. Similarly, E_γ values calculated from the corresponding derivatives of the CEM and ERM equations are listed in Tables 41-47. The experimental values of the activation energies are obtained from the tangent values of the Arrhenius plots of ln Y versus 1/T. The experimental values of E_γ are obtained only for one of the concentrated samples in each of the systems studied. For the purpose of comparison the values of the experimental E_γ and those computed from the derivatives of VTF, CEM and ERM equations, respectively, are listed together in Tables 48-51. These values for the Arrhenius region only for a single plot of each of the systems are also included in these tables. It is important to note that the energies of activation are quite sensitive to temperature in the region below the melting point of the parent solvent as compared to those in the regions above the melting point. This view is

TABLE 41: Activation Energies (kJ/mol) computed from CRM Equation for $Ca(NO_3)_2 \cdot 4.06H_2O$ + $Co(NO_3)_2 \cdot 6.18H_2O$ Molten Salt System

	mol % of Co^{2+}							
T/K	0.0	10.13	19.55	29.70	39.80	49.56	59.51	69.68
303.0	45.55 (53.26)	43.32 (49.44)	41.70 (47.70)	40.01 (46.35)	38.58 (44.52)	37.01 (43.61)	35.70 (41.64)	34.10 (39.78)
308.0	42.43 (49.56)	40.42 (46.13)	38.98 (44.58)	37.47 (43.40)	36.19 (41.77)	34.78 (40.98)	33.59 (39.20)	32.15 (37.49)
313.0	39.68 (46.32)	37.87 (43.21)	36.58 (41.83)	35.22 (40.80)	34.07 (39.32)	32.79 (38.63)	31.72 (37.03)	30.40 (35.45)
318.0	37.26 (43.45)	35.60 (40.62)	34.45 (39.39)	33.22 (38.48)	32.18 (37.14)	31.01 (36.54)	30.05 (35.07)	28.83 (33.61)
323.0	35.10 (40.92)	33.59 (38.33)	32.55 (37.21)	31.43 (36.40)	30.48 (35.19)	29.42 (34.66)	28.53 (33.31)	27.42 (31.96)
328.0	33.18 (38.65)	31.78 (36.26)	30.84 (35.25)	29.82 (34.53)	28.95 (33.42)	27.98 (32.96)	27.17 (31.73)	26.13 (30.46)

continued..

TABLE 41: continued

	mol % of Co^{2+}							
T/K	0.0	10.13	19.55	29.70	39.80	49.56	59.51	69.68
333.0	31.45 (36.61)	30.16 (34.40)	29.30 (33.49)	38.36 (32.85)	27.57 (31.83)	26.67 (31.42)	25.92 (30.28)	24.97 (29.10)
338.0	29.89 (34.77)	28.69 (32.73)	27.90 (31.89)	27.04 (31.32)	26.31 (30.38)	25.48 (30.02)	24.79 (28.96)	23.90 (27.84)
343.0	28.47 (33.11)	27.36 (31.21)	26.64 (30.44)	25.84 (29.92)	25.16 (29.05)	24.39 (28.73)	23.76 (27.75)	22.92 (26.71)

Activation Energies for Fluidity are given within parentheses.

TABLE 42: Activation Energies (kJ/mol) computed from CEM Equation for $Ca(NO_3)_2 \cdot 4.05H_2O$ + $MnCl_2$ Molten Salt System

	mol % of Mn^{2+}					
T/K	0.0	1.05	2.02	3.50	4.99	7.02
313.0	39.70 (47.17)	40.46 (47.98)	41.75 (48.89)	42.80 (50.41)	44.13 (51.91)	46.03 (54.04)
318.0	37.26 (44.25)	37.95 (44.98)	39.12 (45.80)	40.06 (47.16)	41.24 (48.50)	42.93 (50.41)
323.0	35.10 (41.66)	35.72 (42.31)	36.80 (43.05)	37.63 (44.28)	38.69 (45.49)	40.21 (47.20)
328.0	33.17 (39.34)	33.73 (39.93)	34.72 (40.61)	35.47 (41.72)	36.43 (42.82)	37.79 (44.37)
333.0	31.43 (37.26)	31.95 (37.80)	32.86 (38.42)	33.53 (39.43)	34.40 (40.43)	35.64 (41.84)
338.0	29.87 (35.39)	30.34 (35.88)	31.18 (36.45)	31.79 (37.38)	32.59 (38.29)	33.72 (39.58)

continued..

TABLE 42: continued

	mol % of Mn^{2+}					
T/K	0.0	1.05	2.02	3.50	4.99	7.02
343.0	28.45 (33.69)	28.88 (34.15)	29.66 (34.67)	30.22 (35.52)	30.95 (36.36)	31.98 (37.54)
348.0	27.16 (32.15)	27.55 (32.57)	28.29 (33.05)	28.80 (33.84)	29.47 (34.61)	30.41 (35.69)
353.0	25.98 (30.74)	26.35 (31.13)	27.04 (31.58)	27.50 (32.31)	28.12 (33.02)	28.99 (34.02)

Activation Energies for Fluidity are given within parentheses.

TABLE 43: Activation Energies (kJ/mol) computed from CEM Equation for $Cd(NO_3)_2 \cdot 4.18H_2O$ + $MnCl_2$ Molten Salt System

	mol % of Mn^{2+}					
T/K	0.0	2.50	5.35	7.88	9.83	12.49
313.0	30.98 (35.47)	31.04 (35.71)	31.78 (36.54)	31.94 (37.22)	32.59 (38.15)	33.55 (38.96)
318.0	29.38 (33.64)	29.41 (33.84)	30.10 (34.61)	30.22 (35.22)	30.81 (36.07)	31.70 (36.82)
323.0	27.93 (31.98)	27.94 (32.16)	28.57 (32.86)	28.68 (33.43)	29.22 (34.21)	30.05 (34.89)
328.0	26.62 (30.49)	26.61 (30.63)	27.20 (31.29)	27.28 (31.80)	27.78 (32.53)	28.55 (33.16)
333.0	25.42 (29.12)	25.41 (29.25)	25.95 (29.85)	26.02 (30.33)	26.48 (31.01)	27.19 (31.59)
338.0	24.33 (27.88)	24.30 (27.98)	24.82 (28.55)	24.86 (28.99)	25.29 (29.62)	25.96 (30.16)

continued..

TABLE 43 continued

	mol % of Mn^{2+}					
T/K	0.0	2.50	5.35	7.88	9.85	12.49
345.0	23.33 (26.73)	23.29 (26.82)	23.78 (27.35)	23.81 (27.76)	24.20 (28.35)	24.84 (28.85)
348.0	22.41 (25.69)	22.37 (25.76)	22.82 (26.26)	22.84 (26.64)	23.21 (27.19)	23.80 (27.66)

Activation Energies for Fluidity are given within parentheses.

TABLE 44: Activation Energies (kJ/mol) for Fluidity computed from CRM Equation for $Ni(NO_3)_2.6.01H_2O + Mg(NO_3)_2.6.15H_2O$ Molten Salt System

	mol % of Mg^{2+}						
T/K	0.0	5.41	9.64	14.67	20.11	25.43	30.03
323.0	35.75	35.60	35.43	34.94	34.80	34.45	34.21
328.0	33.95	33.82	33.67	33.21	33.09	32.78	32.55
333.0	32.32	32.21	32.08	31.65	31.55	31.25	31.05
338.0	30.84	30.75	30.63	30.23	30.14	29.87	29.68
343.0	29.50	29.41	29.31	28.93	28.85	28.60	28.43
348.0	28.26	28.19	28.10	27.74	27.67	27.44	27.28
353.0	27.13	27.07	26.98	26.65	26.58	26.37	26.22
358.0	26.09	26.04	25.96	25.64	25.58	25.38	25.24
363.0	25.13	25.08	25.01	24.71	24.66	24.47	24.34
368.0	24.23	24.19	24.13	23.85	23.80	23.62	23.50
373.0	23.40	23.37	23.31	23.04	23.00	22.83	22.72
378.0	22.63	22.60	22.55	22.30	22.26	22.10	21.99
383.0	21.91	21.89	21.84	21.60	21.56	21.41	21.32

TABLE 45 : Activation Energies (kJ/mol) computed from ERN Equation for $Ca(NO_3)_2 \cdot 4.06H_2O$ - $Ca(NO_3)_2 \cdot 6.18H_2O$ molten salt system.

	mol% Ca^{2+}							
T/K	0.00	10.15	19.55	29.70	39.80	49.56	59.51	69.68
303.0	40.41 (44.71)	39.97 (44.00)	39.55 (42.51)	38.80 (41.49)	38.00 (40.89)	36.88 (40.40)	-	-
308.0	40.08 (44.60)	39.40 (43.99)	38.76 (42.25)	37.78 (41.05)	36.79 (40.19)	35.53 (39.50)	34.39 (38.48)	-
313.0	39.20 (44.29)	38.30 (43.41)	37.47 (41.46)	36.32 (40.07)	35.18 (39.03)	33.83 (38.17)	32.62 (37.05)	31.53 (35.95)
318.0	37.82 (43.85)	36.76 (42.30)	35.80 (40.20)	34.51 (38.68)	33.29 (37.50)	31.90 (36.51)	30.65 (35.29)	29.54 (34.14)
323.0	36.06 (42.49)	34.89 (40.76)	33.84 (38.56)	32.48 (36.97)	31.22 (35.69)	29.82 (34.62)	28.58 (33.35)	27.48 (32.18)
328.0	34.04 (40.74)	32.80 (38.88)	31.71 (36.65)	30.32 (35.05)	29.06 (33.70)	27.70 (32.59)	26.50 (31.31)	25.44 (30.14)

(continued)

TABLE 45 : (continued)

	Mol% Co^{2+}							
T/K	0.00	10.13	19.55	29.70	39.80	49.56	59.51	69.68
333.0	31.85 (38.48)	30.60 (36.77)	29.51 (34.56)	28.13 (32.96)	26.90 (31.61)	25.61 (30.50)	24.46 (29.24)	23.46 (28.11)
338.0	29.60 (36.17)	28.37 (34.53)	27.31 (32.39)	25.98 (30.83)	24.81 (29.50)	23.60 (28.42)	22.53 (27.21)	21.60 (26.13)
343.0	27.37 (34.85)	26.19 (32.25)	25.18 (30.20)	23.92 (28.72)	22.82 (27.44)	21.71 (26.41)	20.72 (25.26)	19.87 (24.25)

Activation energies for fluidity are given within parentheses.

TABLE 46: Activation Energies (kJ/mol) computed from ERM Equation for $Ca(NO_3)_2 \cdot 4.05H_2O + MnCl_2$ Molten Salt System

	mol % of Mn^{2+}					
T/K	0.0	1.05	2.02	3.50	4.99	7.02
313.0	37.30 (42.75)	37.98 (43.62)	38.36 (44.51)	38.81 (44.99)	39.49 (45.60)	41.64 (46.44)
318.0	36.18 (42.03)	36.96 (42.92)	37.47 (43.81)	38.08 (44.67)	39.08 (45.38)	41.20 (46.49)
323.0	34.68 (40.85)	35.55 (41.74)	36.16 (42.61)	36.89 (43.81)	38.16 (44.60)	40.22 (45.95)
328.0	32.91 (39.29)	33.82 (40.15)	34.51 (41.00)	35.32 (42.48)	36.81 (43.33)	38.77 (44.87)
333.0	30.94 (37.44)	31.89 (38.27)	32.61 (39.08)	33.49 (40.77)	35.12 (41.66)	36.97 (43.34)
338.0	28.89 (35.39)	29.84 (36.18)	30.58 (36.95)	31.48 (38.78)	33.20 (39.69)	34.91 (41.46)

continued..

TABLE : continued

T/K	mol % of Mn^{2+}					
	0.0	1.05	2.02	3.50	4.99	7.02
343.0	26.85 (35.25)	27.76 (33.98)	28.50 (34.70)	29.39 (36.61)	31.13 (37.52)	32.71 (39.32)
348.0	24.82 (31.09)	25.72 (31.76)	26.43 (32.42)	27.30 (34.35)	29.02 (35.24)	30.46 (37.04)
353.0	22.90 (28.96)	23.76 (29.57)	24.43 (30.18)	25.26 (32.08)	26.92 (32.94)	28.22 (34.69)

Activation Energies for Fluidity are given within parentheses.

TABLE 47 : Activation Energies (kJ/mol) computed from ENM Equation for $Cd(NO_3)_2 \cdot 4.18H_2O$ - $MnCl_2$ molten salt system.

	Mol% Mn^{2+}					
T/K	0.00	2.50	5.35	7.88	9.85	12.49
313.0	29.89 (34.35)	30.02 (34.36)	30.10 (34.47)	30.13 (34.51)	30.21 (34.88)	30.31 (35.30)
318.0	28.75 (33.34)	28.97 (33.48)	29.14 (33.73)	29.27 (33.96)	29.48 (34.42)	29.72 (34.96)
323.0	27.44 (32.10)	27.72 (32.34)	27.96 (32.72)	28.16 (33.11)	28.50 (33.65)	28.85 (34.28)
328.0	26.01 (30.69)	26.33 (31.02)	26.62 (31.48)	26.88 (32.03)	27.31 (32.60)	27.75 (33.32)
333.0	24.52 (29.18)	24.86 (29.56)	25.19 (30.09)	25.48 (30.74)	25.97 (31.35)	26.48 (32.11)
338.0	23.03 (27.62)	23.37 (28.03)	23.71 (28.60)	24.01 (29.33)	24.54 (29.94)	25.10 (30.72)

(continued)

TABLE 47 : (continued)

	Mol% Mn^{2+}					
T/K	0.00	2.50	5.35	7.88	9.85	12.49
343.0	21.34 (26.05)	21.89 (26.47)	22.23 (27.06)	22.52 (27.85)	23.07 (28.42)	23.64 (29.21)
348.0	20.16 (24.52)	20.46 (24.92)	20.78 (25.51)	21.06 (26.29)	21.60 (26.86)	22.17 (27.62)

Fluidity data are given within parentheses.

TABLE 48 : Activation Energies (kJ/mol) as a Function of Temperature computed through Different Models for $Ca(NO_3)_2.4.06H_2O$ + $Co(NO_3)_2.6.18H_2O$ Molten Salt System

	69.68 mol %			
	E_η, E_Λ			
T/K	VTF	CEM	ERM	EXPTL
313.0	29.79 (35.88)	30.40 (35.45)	31.53 (35.95)	31.20 (35.82)
318.0	28.31 (34.11)	28.83 (33.61)	29.54 (34.14)	30.04 (34.66)
323.0	26.98 (32.50)	27.42 (31.96)	27.48 (32.18)	27.48 (32.48)
328.0	25.76 (31.05)	26.13 (30.46)	25.44 (30.14)	25.19 (29.98)
333.0	24.66 (29.72)	24.97 (29.10)	23.46 (28.11)	22.90 (27.48)
338.0	23.65 (28.51)	23.90 (27.84)	21.60 (26.13)	—
343.0	22.72 (27.39)	22.92 (26.71)	19.87 (24.25)	—

Activation Energies for Fluidity are given within parentheses.

TABLE 49 : Activation Energies (kJ/mol) as a Function of Temperature computed through Different Models for $Ca(NO_3)_2.4.03H_2O$ + $MnCl_2$ Molten Salt System

	7.02 mol %			
	E_η, E_Λ			
T/K	VTF	CEM	ERM	EXPTL
313.0	44.18 (52.16)	46.03 (54.04)	41.64 (46.44)	41.60 (46.20)
318.0	41.33 (48.77)	42.93 (50.41)	41.20 (46.49)	41.13 (45.76)
323.0	38.81 (45.79)	40.21 (47.20)	40.22 (45.95)	40.21 (45.29)
328.0	36.57 (43.14)	37.79 (44.37)	38.77 (44.87)	38.82 (44.83)
333.0	34.57 (40.77)	35.64 (41.84)	36.97 (43.34)	36.97 (43.90)
338.0	32.77 (38.65)	33.72 (39.58)	34.91 (41.46)	35.12 (41.60)
343.0	31.15 (36.73)	31.98 (37.54)	32.71 (39.32)	-
348.0	29.68 (35.00)	30.41 (35.69)	30.46 (37.04)	-
353.0	28.34 (33.42)	28.99 (34.02)	28.22 (34.69)	-

Activation Energies for Fluidity are given within parentheses.

TABLE 50: Activation Energies (kJ/mol) as a Function of Temperature computed through Different Models for $Cd(NO_3)_2.4.18H_2O$ + $MnCl_2$ Molten Salt System

	12.49 mol %			
	E_η, E_Λ			
T/K	VTF	CRM	ERM	EXPTL
313.0	32.17 (37.14)	33.55 (38.96)	30.13 (35.21)	31.69 (36.97)
318.0	30.48 (35.20)	31.70 (36.82)	29.54 (34.84)	29.58 (34.66)
323.0	28.95 (33.46)	30.05 (34.89)	28.67 (34.14)	28.44 (33.61)
328.0	27.58 (31.88)	28.55 (33.16)	27.57 (33.15)	27.73 (32.62)
333.0	26.33 (30.44)	27.19 (31.59)	26.30 (31.92)	26.10 (31.69)
338.0	25.18 (29.14)	25.96 (30.16)	24.92 (30.51)	—
343.0	24.14 (27.94)	24.84 (28.85)	23.47 (28.98)	—
348.0	23.18 (26.84)	23.80 (27.66)	21.99 (27.38)	—

Activation Energies for Fluidity are given within parentheses.

TABLE 51: Activation Energies (kJ/mol) for Fluidity as a Function of Temperature computed through Different Models for $Ni(NO_3)_2.6.01H_2O$ + $Mg(NO_3)_2$. $6.13H_2O$ Molten Salt System

	30.03 mol %		
T/K	VTF	CRM	EXPTL
338.0	29.36	29.68	29.39
343.0	28.19	28.43	28.28
348.0	27.13	27.28	27.17
353.0	26.14	26.22	26.06
358.0	25.23	25.24	24.96
363.0	24.38	24.34	23.85
368.0	23.60	23.50	-
373.0	22.86	22.72	-
378.0	22.17	21.99	-
383.0	21.53	21.32	-

further reinforced by comparing the computed E_γ (VTF), E_γ (CEM) and E_γ (ERM) values with those of the corresponding experimental values. Such a comparison[25] reveals a relatively better applicability of the ERM than those of the VTF and CEM equations to these systems. At this stage it may be recalled that the superiority of the ERM equation over those of the VTF and CEM stems from the fact that only the ERM equation is meant to account for the overall transport behaviour, i.e., non-Arrhenius - Arrhenius regions of each plot. The variation in the energy of activation with temperature may be understood[1,5,9,20] in the light of the free volume as well as the configurational entropy models. According to the free volume model a successive decrease in temperature causes a gradual decrease in the free volume of the system. This will consequently, require a relatively high value of the energy of activation for both the viscous and the conductance flows at lower temperature. When viewed in terms of the configurational entropy model the system which successively becomes compact as T_o approaches, the configurational entropy approaches a minimum value. The compact structure in turn, results in an increased intermolecular forces which eventually contribute to increased rigidity of the system. These consequently appear to be responsible for relatively higher activation energy at lower temperatures as has actually been found in all

the systems studied. Similar situation may also be anticipated for the behaviour of activation energies, E_Y (= ϕ or Λ) with increase in the solute concentration in the cases of $Ca(NO_3)_2.4.03H_2O$ - $MnCl_2$ and $Cd(NO_3)_2.4.18H_2O$ - $MnCl_2$ molten salt systems where E_Y values have been found to increase. However, they have been found to decrease with increase in solute concentration in the cases of $Ca(NO_3)_2.4.06H_2O$ - $Co(NO_3)_2.6.18H_2O$ and $Ni(NO_3)_2.6.01H_2O$ - $Mg(NO_3)_2.6.13H_2O$ systems. This proabably stems from the decrease in their T_o values with the solute concentration.

Thus the opposing trends encountered in the variations of E_Y values with successive increases in solute concentration appear to be guided by the corresponding T_o values which either increase with concentration as a result of increase in the compactness, intermolecular forces, and rigidity of the system or show a downward trend in order to achieve the lower T_o values of the solute as anticipated on the basis of the additive nature of T_o.

PART II

CONCENTRATION DEPENDENCE OF TRANSPORT PROPERTIES OF GLASS FORMING MELTS

INTRODUCTION

Even in extremely dilute solutions of molten salts the solute is subjected to strong interionic effects, because of close proximity of charged ions in such media. Furthermore, the fact that the majority of solutions approaching their maximum solubility become very viscous on cooling to their melting temperatures and readily supercool to the vitreous state. This has prompted to investigate the concentration dependence of transport properties. For this purpose Angell[12] employed the expression,

$$Y = A_Y T^{-1/2} \exp\left[-k_Y/Q_Y (N_o - N)\right] \qquad \ldots (22)$$

essentially based on the VTF equation. Q_Y is the slope of the linear plot of T_o versus X plot, N and N_o are the respective concentrations of the solute in equivalents per litre for the test and the glass transition concentrations, respectively. In deriving this equation the pre-exponential term, A_Y and the exponential term, k_Y have been taken as concentration invariant. Equation (22) has recently been modified by accounting for the linear variation of A_Y with concentration,

$$A_Y = A_{oY} \pm Q_{1Y} X \qquad \ldots (23)$$

to the form

$$Y = (A_{oY} \pm Q_{1Y}X) \exp\left[-k_Y/Q_Y\,(X_o - X)\right] \qquad \ldots (24)$$

in which Q_{1Y} is the slope of the plot of A_Y versus mol%, X. Though this equation describes satisfactorily the concentration dependence of transport properties in many molten salt mixtures,[18] it has a limited applicability. This equation is meaningful only within the T_o values of the two components of a mixture as the values of X_o will be either less than zero or more than 100 mol% beyond this range and are therefore physically meaningless. In view of its limited applicability, an expression based on the VTF equation was derived[44,45] at constant T/T_o (= e) values, by accounting for the linear concentration dependence of the T_o values,

$$T_o = T_{o(o)} \pm Q_{2Y}X \qquad \ldots (25)$$

where Q_{2Y} is the slope of the plot of T_o versus X, and $T_{o(o)}$ is the glass transition temperature for the pure solvent. The resulting expression is of the type

$$Y = (A_{oY} \pm Q_{1Y}X)e^{-\gamma 2}\,(T_{o(o)} \pm Q_{2Y}X)^{-\gamma 2}$$

$$\exp\left[-k_Y/(T_{o(o)} \pm Q_{2Y}X)\,(e - 1)\right] \qquad \ldots (26)$$

Equation (26) has been successfully employed to explain the concentration dependence of transport properties in many molten salt solutions.[44,45]

Similarly, another expression has been obtained[34,35] from the equation based on the configurational entropy model,

$$Y = (A'_{oY} \pm Q'_{1Y}X) \exp\left[-k'_Y/(T_{e(o)} \pm Q'_{2Y}X)e \ln e\right] \quad \ldots (27)$$

This equation has also been able to describe fairly well the concentration dependence of transport properties of molten salt systems.[34,35]

RESULTS AND DISCUSSION

The measured viscosity and electrical conductance have been found to vary significantly with variations in solute concentration for all the systems studied. The magnitude of viscosity is determined mainly by the rigid or the less mobile entities of the system while that of conductance is determined mainly by the ions of higher mobilities. Obviously the viscosity behaviour seems to show an opposite trend compared to that of the conductance as may be seen from the respective isotherms (Figs. 28,29). Similar behaviour of viscosity as well as conductance isotherms has also been reported earlier in several molten salt mixtures.[19,25,34,35,44-46] In order to explain the concentration dependence of fluidities and conductances, the best fit parameters of the VTF and the CKM equations have been considered. In all the systems studied the values of the parameters A_{3Y}, A_{4Y} and T_o have been found to vary linearly with solute concentration (Figs. 30-32), and have been expressed as

$$A_{4Y} = A_{oY} \pm Q_{1Y}X \qquad \ldots (23)$$

and

$$T_o = T_{o(o)} \pm Q_{2Y}X \qquad \ldots (25)$$

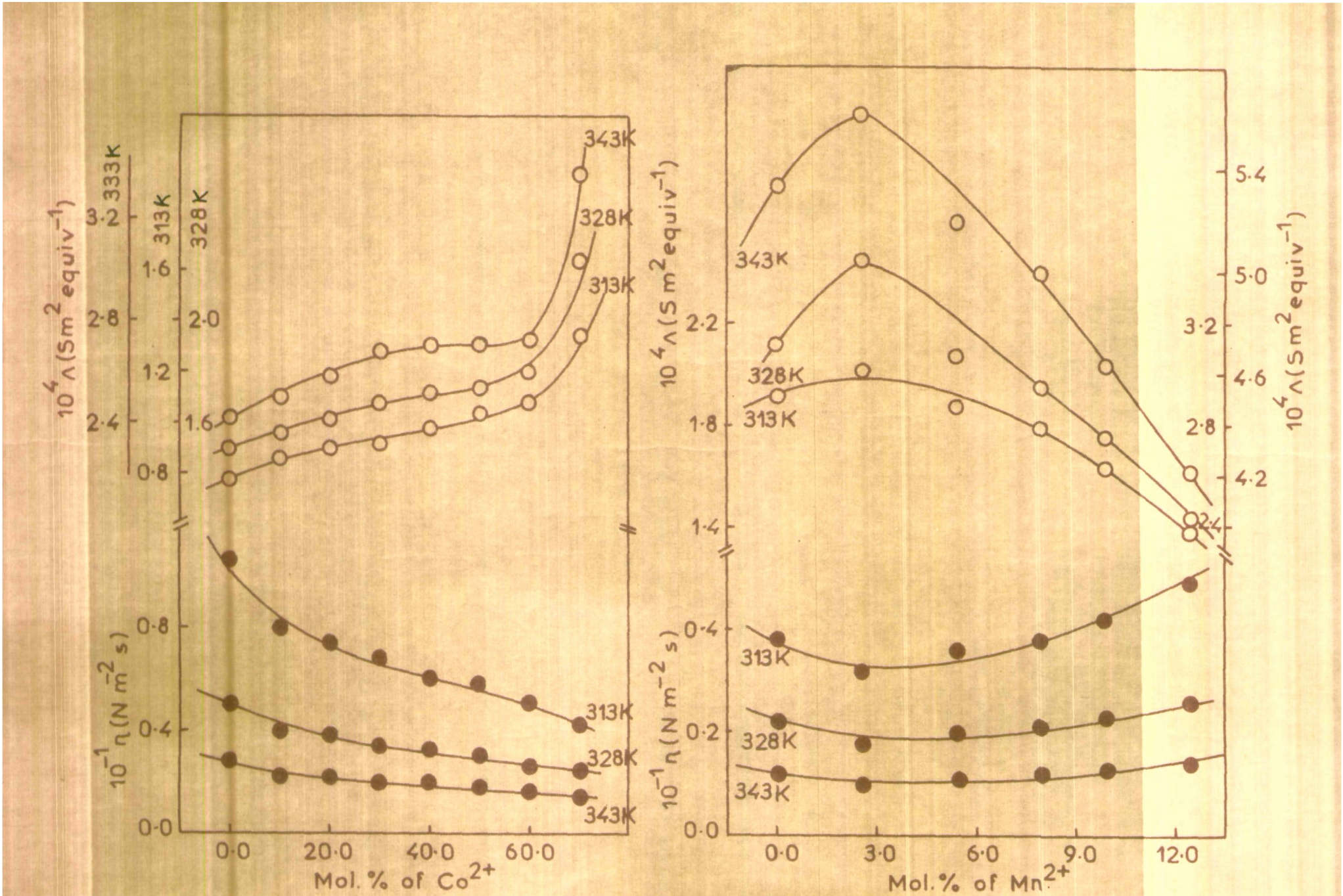

Fig.28 Concentration dependence of Viscosity and Conductance.

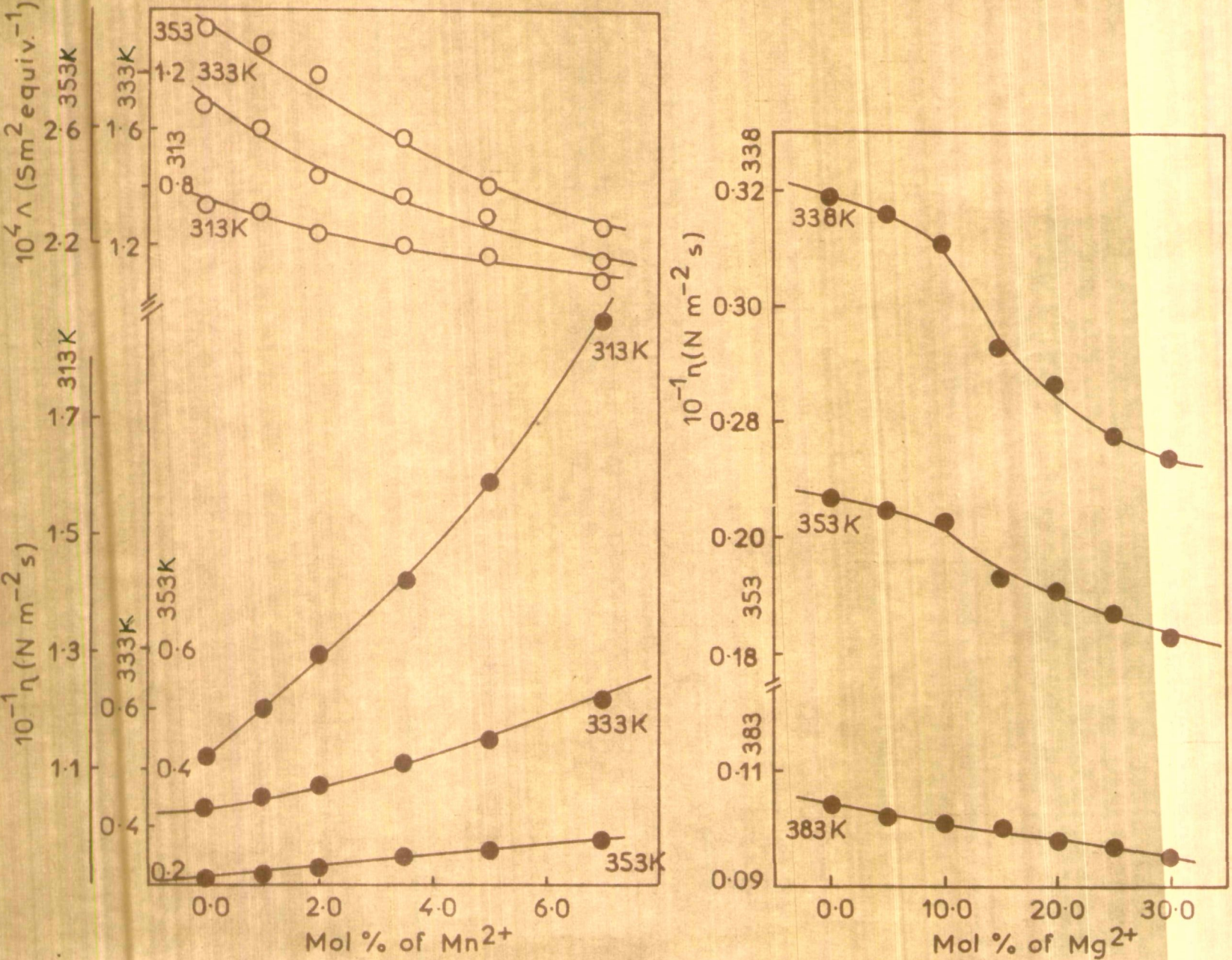

Fig.29 Concentration dependence of Viscosity and Conductance.

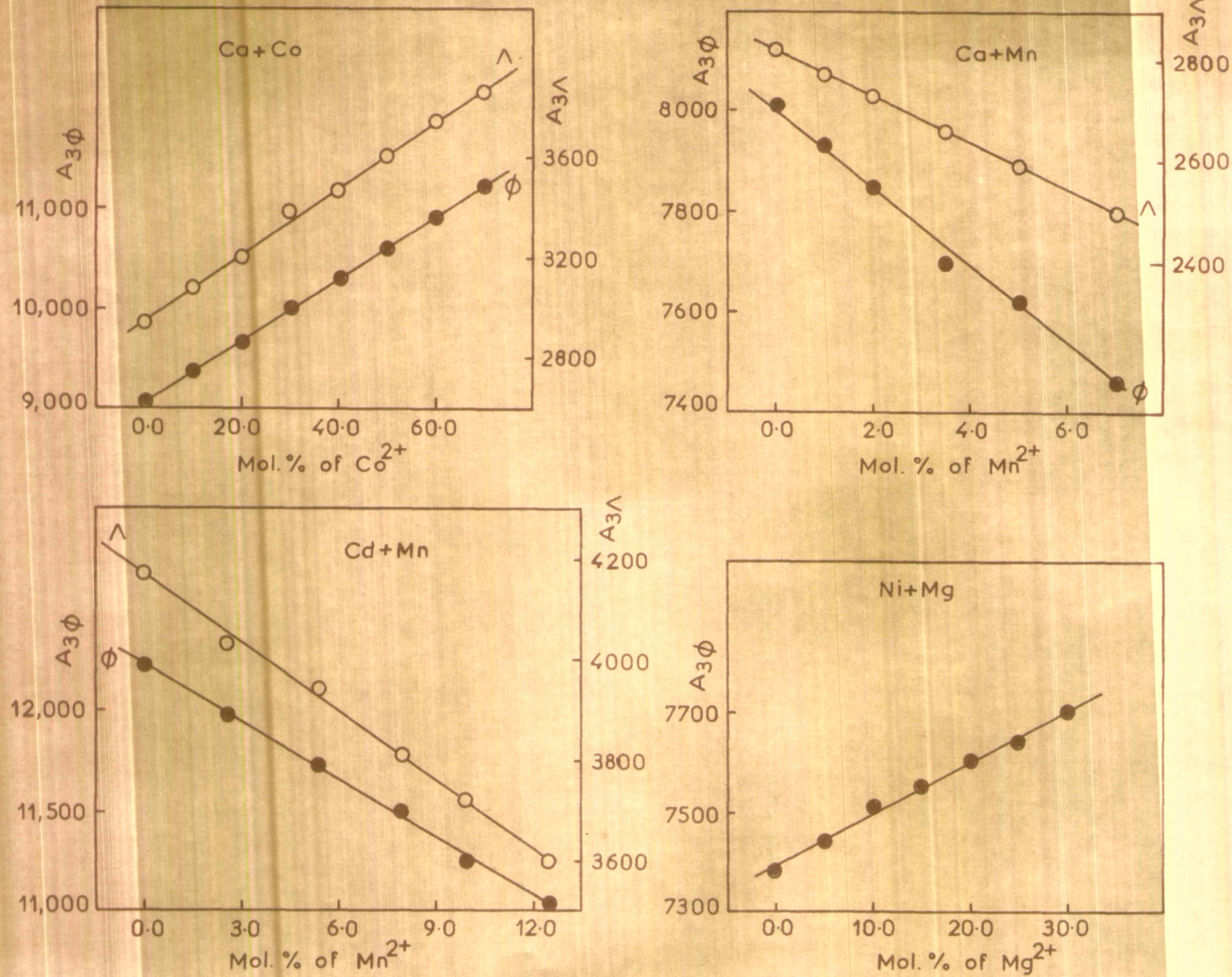

Fig. 30 Concentration dependence of $A_{3\gamma}$

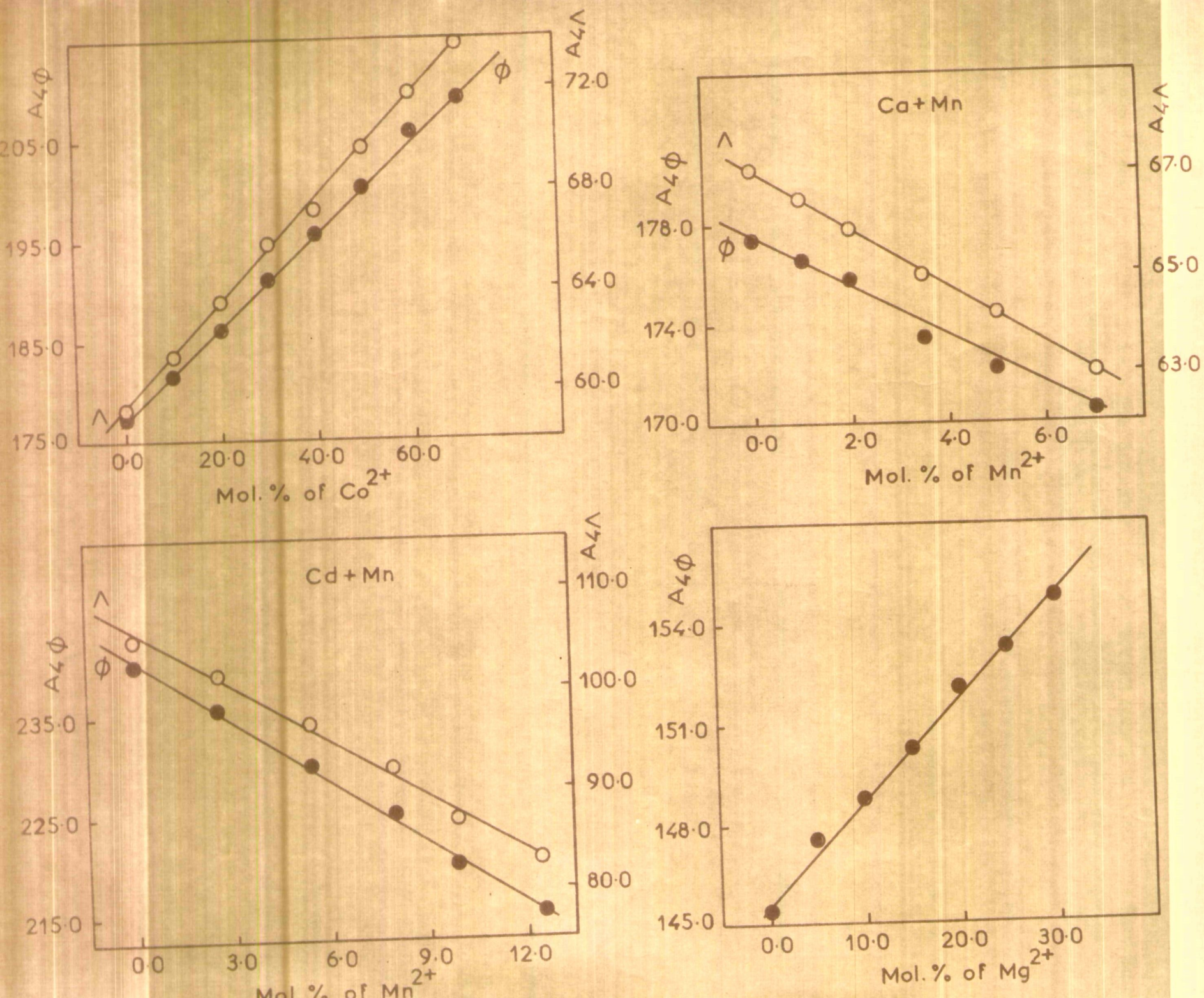

Fig.31 Concentration dependence of A_{4Y}

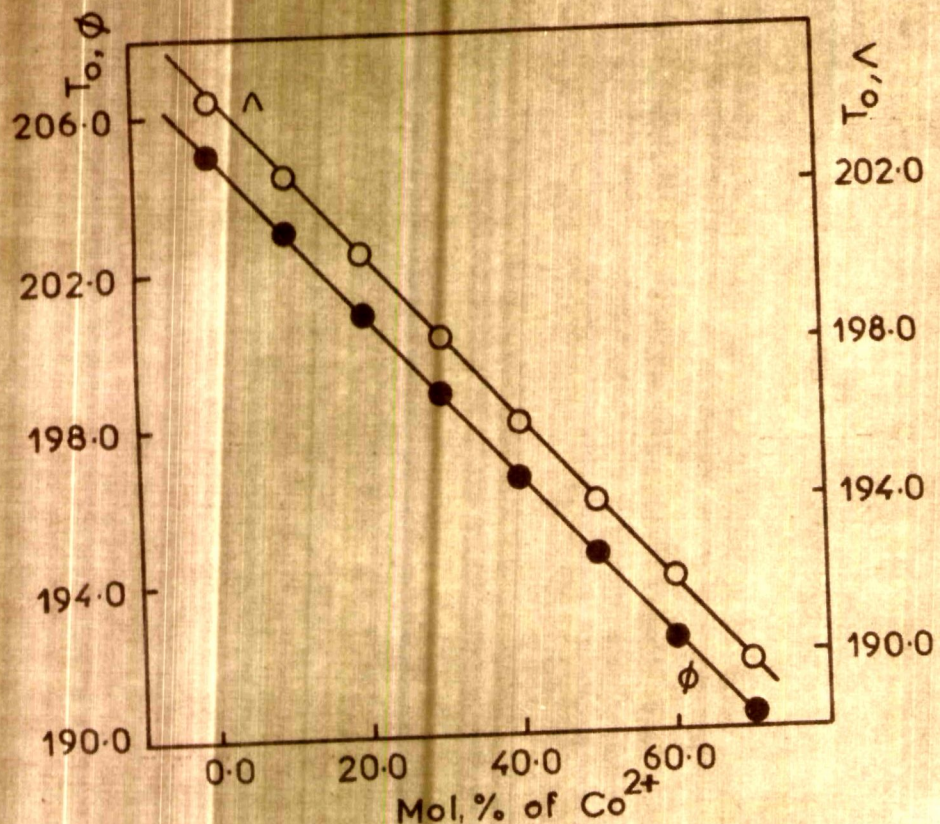

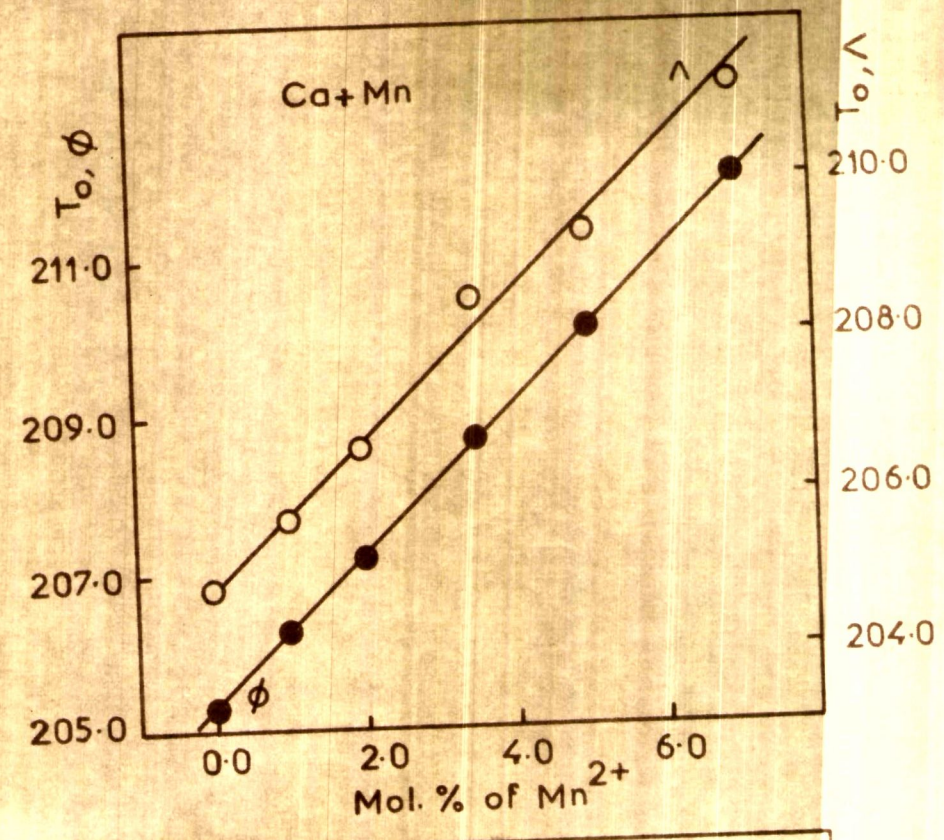

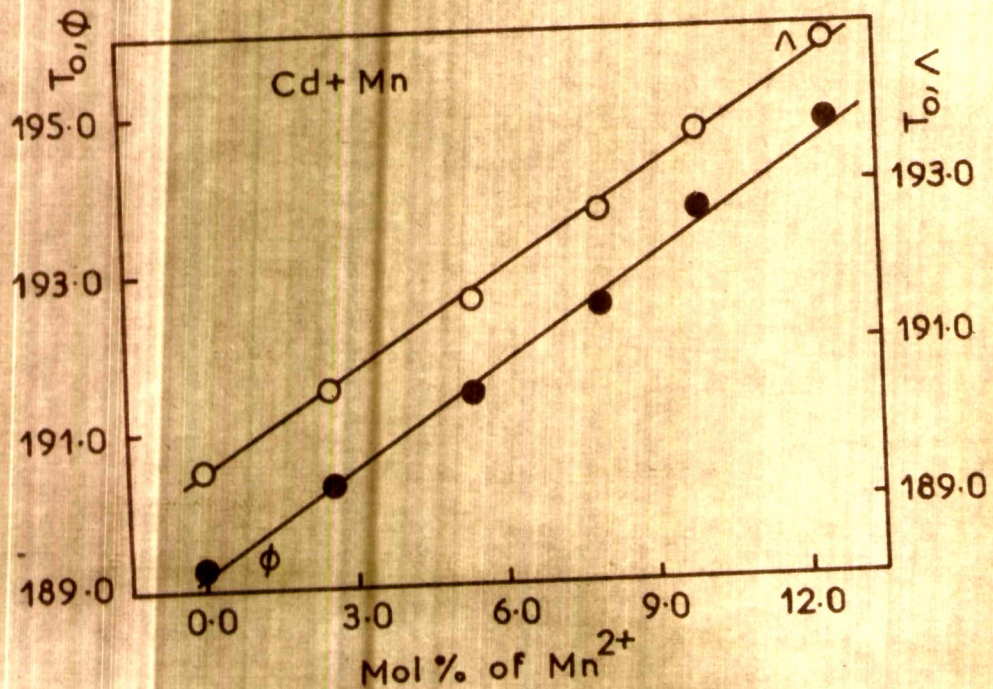

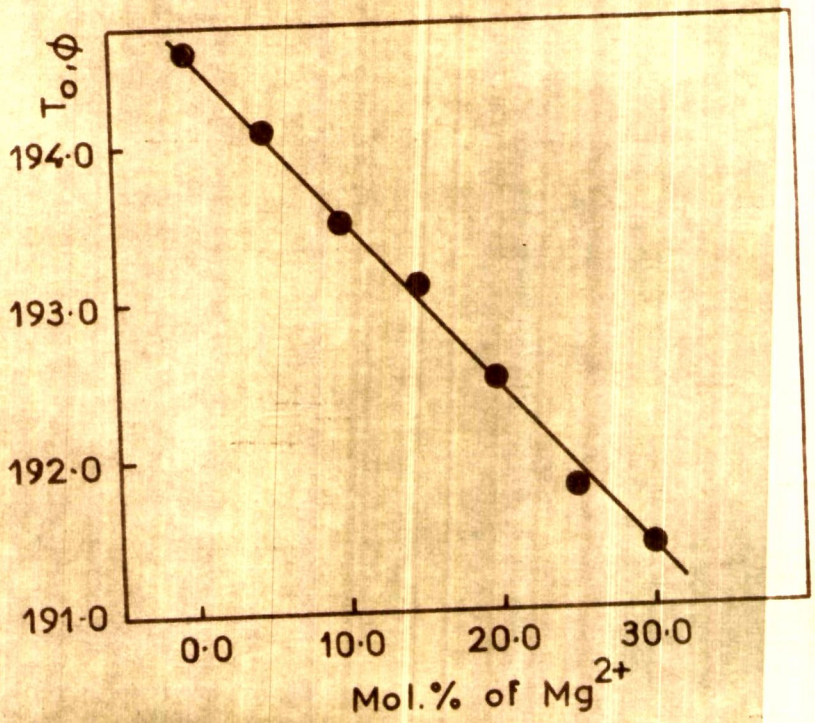

Fig.32 Concentration dependence of T_o.

given earlier. The above plots for A_{4Y} and T_o versus X were made by least-squares fitting the data to equations (23) and (25), respectively. It is interesting to note that the slopes of $A_{3\phi}$ and $A_{4\phi}$ versus concentration plots are almost similar to those of $A_{3\Lambda}$ and $A_{4\Lambda}$ versus concentration plots, respectively. The significance of such variations has already been discussed (cf. pre-exponential terms).

The concentration dependence of T_o has already been discussed in the last chapter in terms of the cohesive energy, the mean molecular mass at several concentrations and the charges in the molecular complexity.

In view of the linear dependence of the parameters A_{3Y}, A_{4Y} and T_o on concentration, the fluidity and conductance data were least-squares fitted to equations (26) and (27) for several values of constant T/T_o (= e). The corresponding temperature T lying in the experimental range and the values of e which gave reasonably good fits were selected. The best fit parameters along with the standard deviations in ln ϕ and ln Λ are listed in Tables 52 and 53. The linear plots of $1.0/\ln\left[Y\{e\,(T_{o(e)} \pm Q_{2Y}X)\}\right]^{Y2}/(A_{oY} \pm Q_{1Y}X)$ and $1/\ln\left[A'_{oY} \pm Q'_{1Y}X)/Y\right]$ against X mol% support the applicability of equation (26) and (27) in explaining the concentration dependence of such data, as shown in Appendix D (Figs. 32a and b).

TABLE 32: Computed Parameters of Isoenergic Equation

Molten Salt System	C	A_{o3Y}	Q_{1Y}	k_{3Y}	$T_{o(o)}$	Q_{2Y}	Std. dev. in ln Y
$Ca(NO_3)_2.4.06H_2O$ + $Co(NO_3)_2.6.18H_2O$	1.6	2945.0 (9050.0)	13.2 (112.7)	580.0 (679.5)	204.5 (205.0)	0.21 (0.58)	0.052 (0.066)
$Cd(NO_3)_2.4.18H_2O$ + $MnCl_2$	1.8	4165.0 (1222.0)	16.4 (95.3)	577.9 (666.7)	189.5 (189.3)	0.42 (0.44)	0.015 (0.027)
$Ca(NO_3)_2.4.05H_2O$ + $MnCl_2$	1.7	2817.0 (8005.0)	44.7 (77.7)	579.9 (670.7)	204.8 (205.3)	0.91 (0.95)	0.009 (0.051)
$Ni(NO_3)_2.6.01H_2O$ + $Mg(NO_3)_2.6.15H_2O$	1.7	(7380.0)	(10.5)	(695.0)	(194.5)	(0.11)	(0.043)

Fluidity data are given within parentheses.

TABLE 53: Computed Parameters of Isoentropic Equation

Molten Salt System	C	A_{04Y}	Q'_{1Y}	k_{4Y}	$T_{o(o)}$	Q'_{2Y}	Std. dev. in ln Y
$Ca(NO_3)_2.4.06H_2O$ + $Co(NO_3)_2.6.18H_2O$	1.6	50.1 (177.0)	0.21 (0.46)	594.5 (680.0)	205.7 (206.6)	0.20 (0.21)	0.028 (0.075)
$Cd(NO_3)_2.4.18H_2O$ + $MnCl_2$	1.8	105.0 (240.1)	1.76 (1.99)	599.1 (689.0)	191.9 (191.7)	0.42 (0.42)	0.028 (0.021)
$Ca(NO_3)_2.4.05H_2O$ + $MnCl_2$	1.7	67.1 (177.4)	0.58 (1.00)	589.8 (689.7)	206.0 (206.8)	1.04 (0.94)	0.028 (0.023)
$Ni(NO_3)_2.6.01H_2O$ + $Mg(NO_3)_2.6.15H_2O$	1.7	(145.5)	(0.33)	(692.1)	(198.0)	(0.11)	(0.018)

Fluidity data are given within parentheses.

It would be of interest to correlate[35,44,45] the parameters A_{3Y} or A_{4Y} with T_o by combining equations (25) and (25) in the following manner,

$$A_Y = [A_{oY} - (Q_{1Y}/Q_{2Y})T_{o(o)}] + (Q_{1Y}/Q_{2Y})T_o \quad \ldots (28)$$

The linear plots of A_{3Y} versus T_o (Fig. 33) support the above correlation. Similarly the parameters of the Doolittle's equation, A_{2Y} and V_{oY} have also been found[46] to vary linearly with concentration which may be expressed as

$$A_{2Y} = A''_{oY} \pm Q_{3Y}X \quad \ldots (29)$$

and $$V_{oY} = V_{o(o)} \pm Q_{4Y}X \quad \ldots (30)$$

(A'_{oY} for CBM and A''_{oY} for Doolittle)

where $V_{o(o)}$ is the molar intrinsic volume at T_o for the pure solvent, Q_{4Y} is the slope of the plot of V_o against X (Fig. 34); A''_{oY} is the value of A_{2Y} for the pure solvent and Q_{3Y} is the slope of A_{2Y} against X plot. By combining equations (29) and (30) we obtain

$$A_{2Y} = [A''_{oY} - (Q_{3Y}/Q_{4Y})V_{o(o)}] + (Q_{3Y}/Q_{4Y})V_o \quad \ldots (31)$$

Linear plots of A_{2Y} versus V_o (Fig. 35) for all the cases

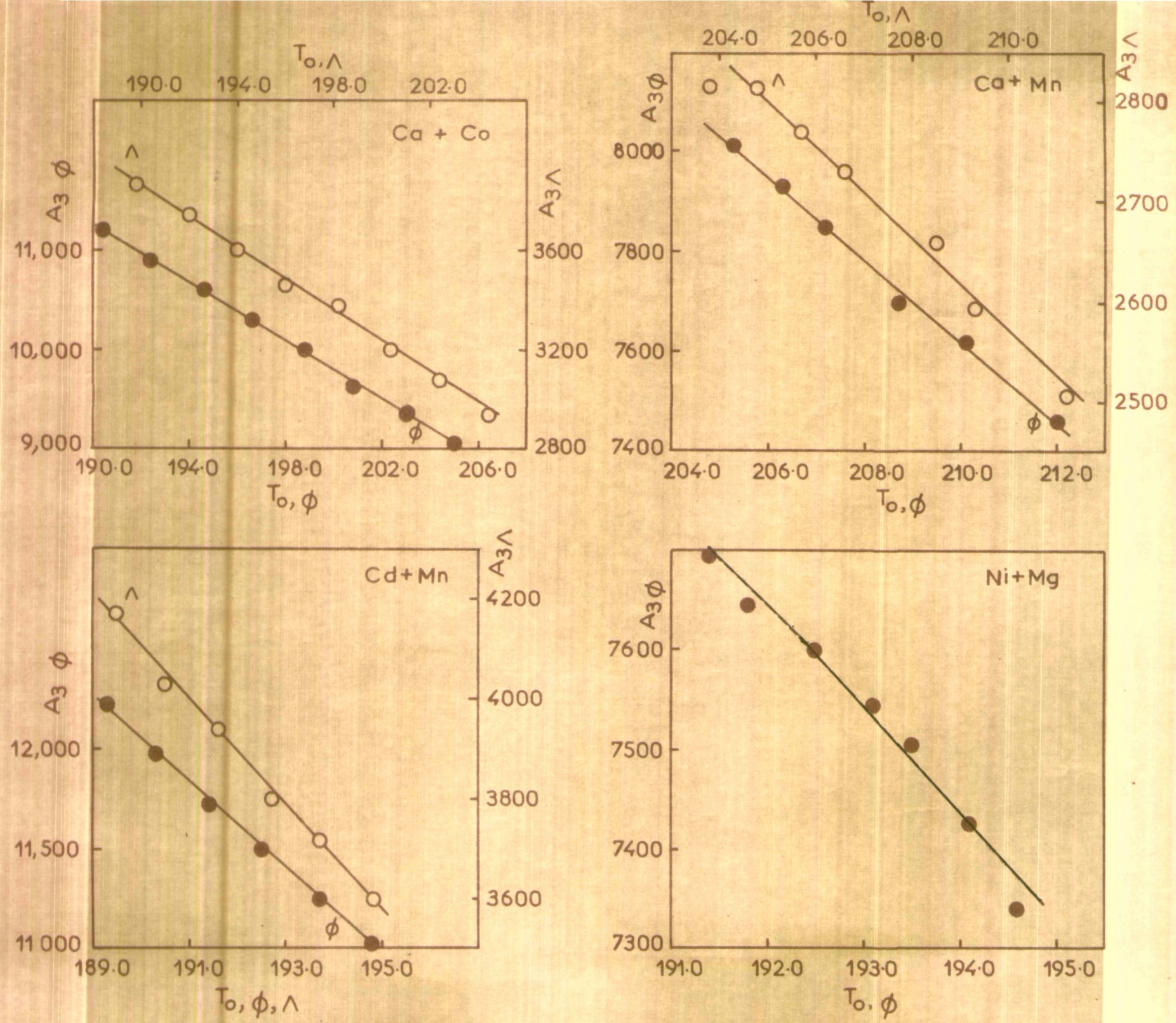

Fig. 33 Variation of A_Y against $T_{o,Y}$.

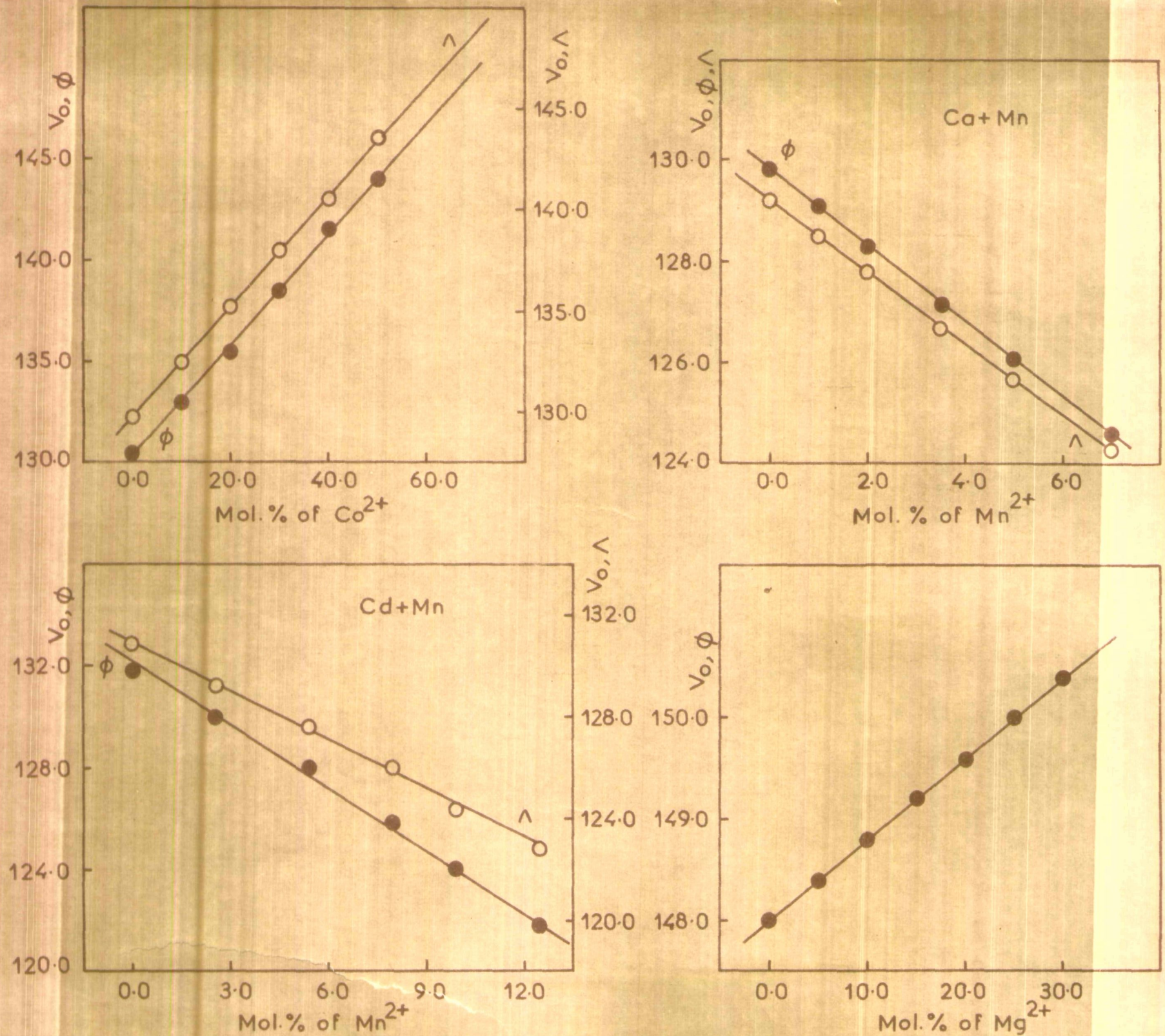

Fig. 34 Concentration dependence of $V_o^{\cdot}$

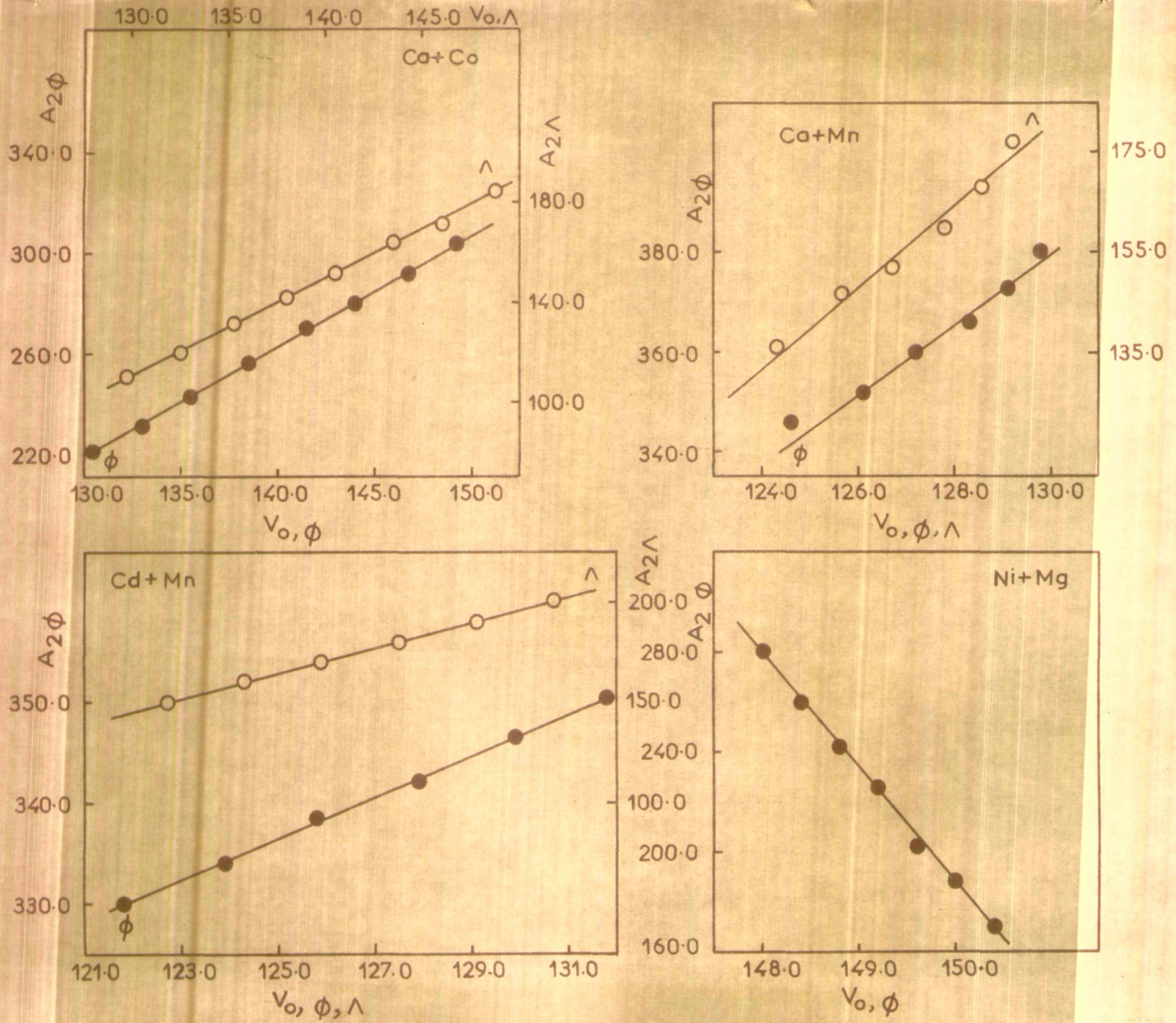

Fig.35 Variation of A_{2Y} with $V_{o,Y}$

studied support the feasibility of equation (30) in explaining such behaviours. In addition, a relationship between the V_o and the T_o has also been obtained by combining equations (25) and (30),

$$T_o = \left[T_{o(o)} - (Q_{2Y}/Q_{4Y})V_{o(o)}\right] + (Q_{2Y}/Q_{4Y})V_o \quad \ldots (32)$$

The linear plots of T_o versus V_o show the applicability of equation (32) in the present systems as shown in Fig. 36. The concentration dependence of corrected activation energies has also been examined. For this purpose E_{corr} were plotted as a function of mol% of X (Fig. 37) and the corresponding isotherm may be expressed as

$$E_{corr} = E'_{corr} + Q_{5Y}X \quad \ldots (33)$$

where E'_{corr} is the intercept and Q_{5Y} is the slope of the E_{corr} versus X plot. On the basis of the linear variation of T_o with concentration a relationship between the E_{corr} and the T_o value is obtained by combining equations (25) and (33),

$$E_{corr} = \left[E'_{corr} - T_{o(o)}\,(Q_{5Y}/Q_{2Y})\right] + (Q_{5Y}/Q_{2Y})T_o \quad \ldots (34)$$

where E'_{corr} is the value of corrected energy of activation for the pure solvent at its glass transition temperature, $T_{o(o)}$ while other parameters have their usual significance.

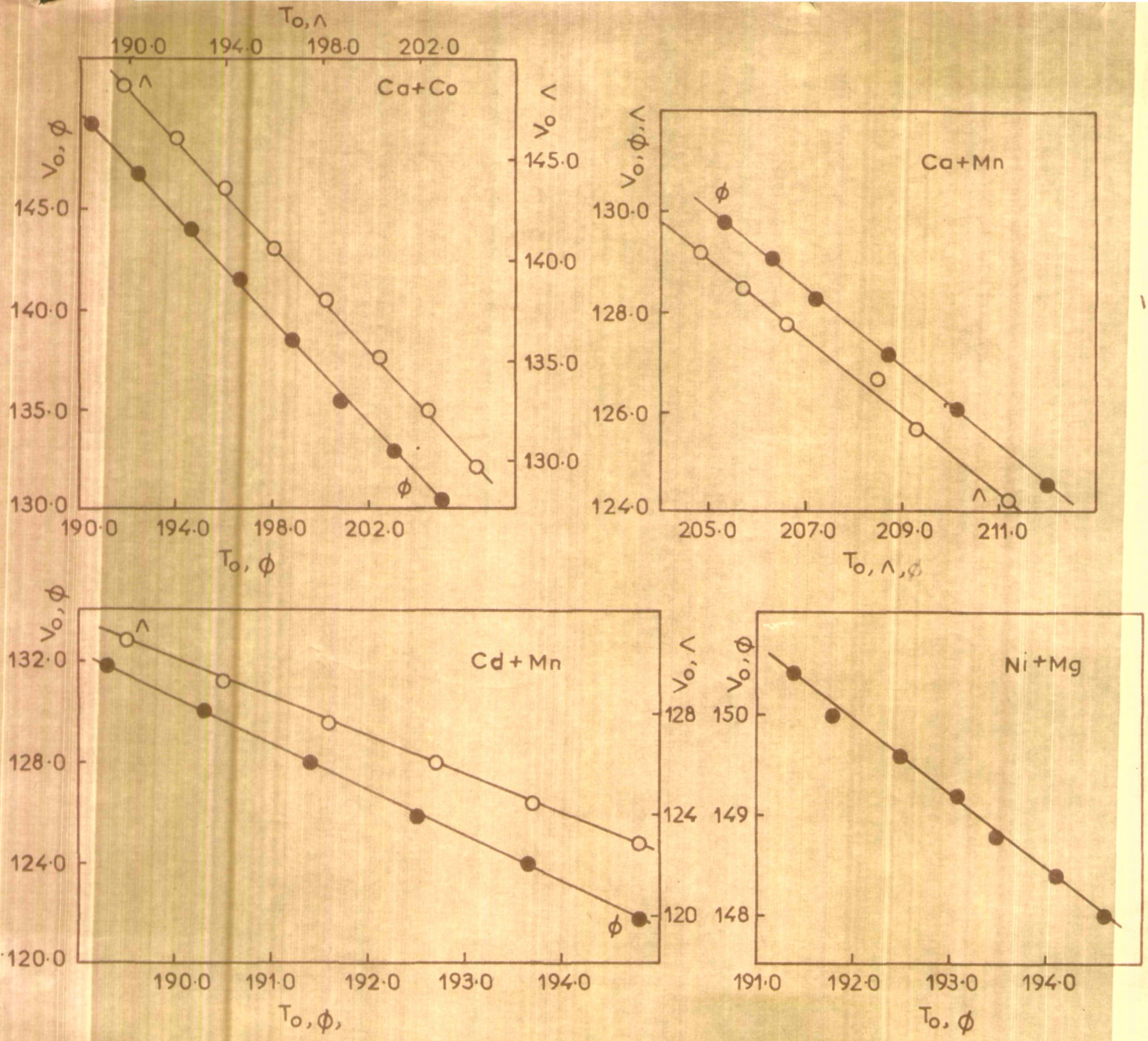

Fig. 36 Variation of V_o, γ with T_o, γ.

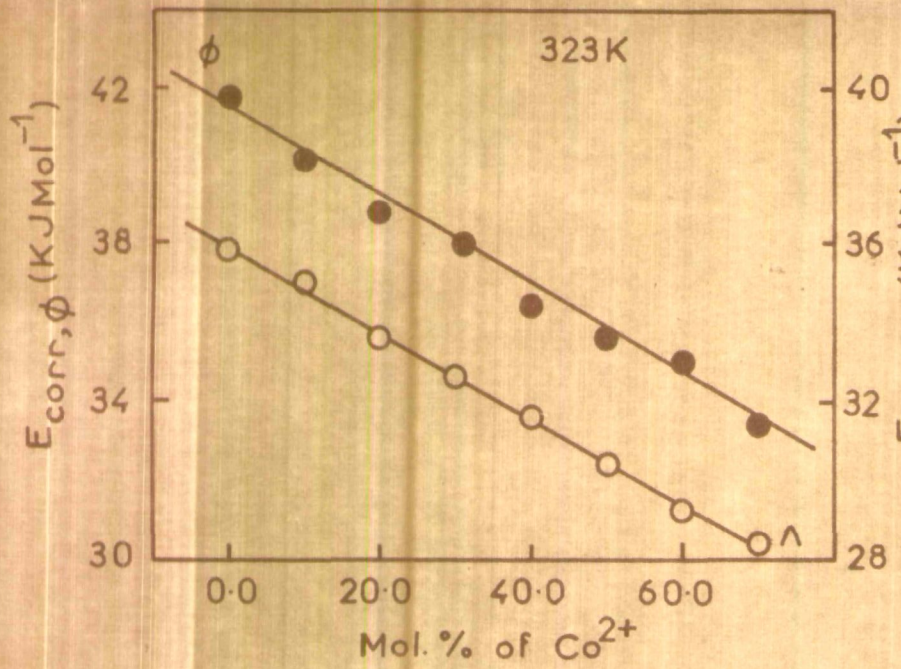

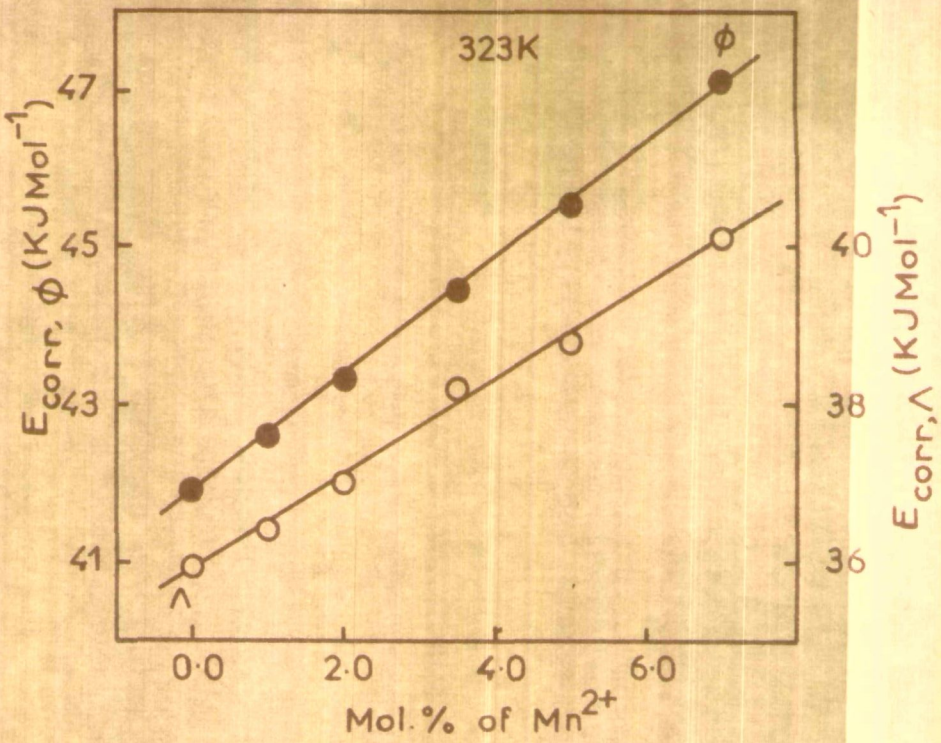

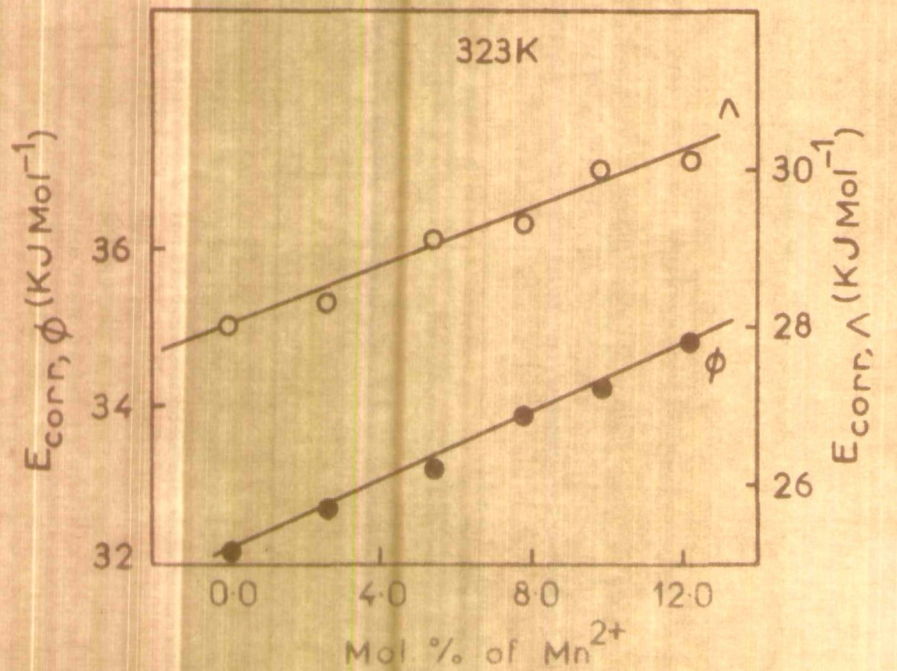

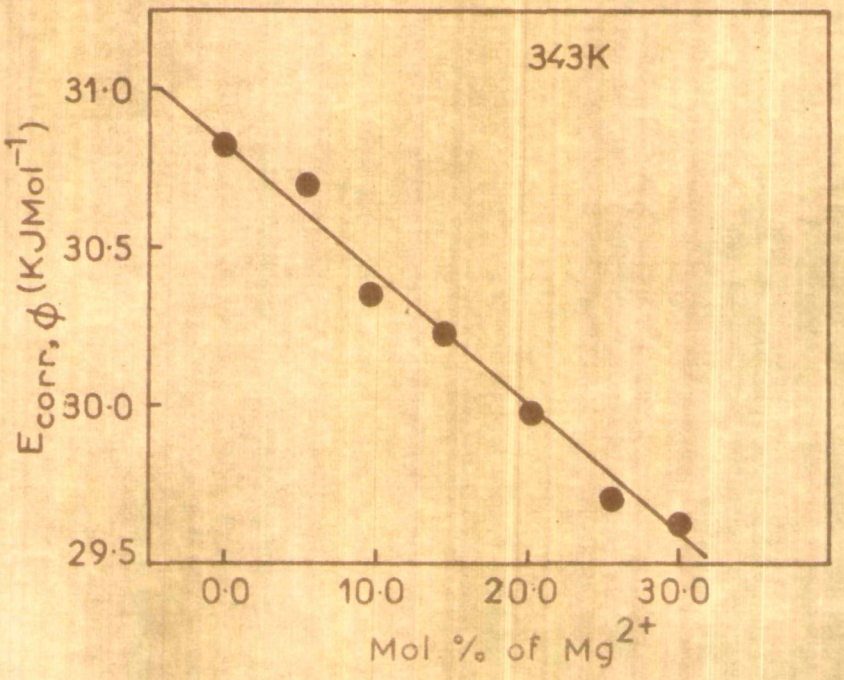

Fig. 37 Concentration dependence of Energy of Activation

In order to obtain the value of E'_{corr}, the corrected activation energies for the pure solvent were plotted against the temperature and extrapolated to $T_{e(o)}$. Such an extrapolation is possible only if the variation of E_{corr} with concentration is linear. Substituting the values of E'_{corr} in equation (33), the corresponding values of E_{corr} were computed as a function of T_e and are listed in Tables 54-57. The linear plots of E_{corr} versus T_e (Fig. 38) in the present cases provide an experimental support to equation (34).

Similarly, in view of equations (30) and (33) E_{corr} may be expected to vary linearly with increase in the values of V_e. Therefore, by combining equations (30) and (33) one may obtain the expression of the type,

$$E_{corr} = \left[E'_{corr} - V_{e(o)} \left(Q_{5Y}/Q_{4Y}\right)\right] + \left(Q_{5Y}/Q_{4Y}\right)V_e \quad \ldots (35)$$

It is seen that the plots of E_{corr} versus V_e are linear (Fig. 39) in all the systems investigated. It may be emphasised that the equations (33-35) exhibit similar trends in their variation with concentration, X, glass transition temperature, T_e and the molar intrinsic volume, V_e as have been observed in the systems studied. These correlations (equations 23-35) seem to provide bases for understanding the concentration dependence of the flow properties satisfactorily.

TABLE 54 : Computed values employed in the plots of $E_{Y(cor)}$ (kJ/mol) versus T_o (K) and $E_{Y(cor)}$ versus $10^6 x V_o$ (m^3/mol), respectively, for $Ca(NO_3)_2.4.06H_2O$ + $Co(NO_3)_2.6.18H_2O$ molten salt system

$E_{Y(cor)}$	$T_{o,Y}$	$E_{Y(cor)}$	$V_{o,Y}$
35.73	204.4	35.73	129.7
(41.70)	(205.0)	(41.70)	(130.5)
35.02	202.3	35.02	132.4
(40.24)	(202.9)	(40.24)	(133.0)
33.64	200.3	33.64	135.2
(38.87)	(200.8)	(38.87)	(135.6)
32.64	198.1	32.64	137.9
(38.17)	(198.8)	(38.17)	(138.4)
31.63	196.0	31.63	140.6
(36.36)	(196.7)	(36.36)	(141.4)
30.48	194.0	30.48	143.4
(35.59)	(194.5)	(35.59)	(144.0)
29.23	191.9	29.23	146.0
(34.59)	(192.4)	(34.59)	(146.8)
28.32	189.8	28.32	148.8
(33.84)	(190.4)	(33.84)	(149.3)

Fluidity data are given within parentheses.

TABLE 55 : Computed values employed in the plots of $E_{Y(cor)}$ (kJ/mol) versus T_o (K) and $E_{Y(cor)}$ versus $10^6 x V_o$ (m^3/mol), respectively, for $Ca(NO_3)_2.4.05H_2O$ + $MnCl_2$ molten salt system

$E_{Y(cor)}$	$T_{o,Y}$	$E_{Y(cor)}$	$V_{o,Y}$
35.96	204.8	35.96	129.2
(41.94)	(205.3)	(41.94)	(129.8)
36.48	205.7	36.48	128.5
(42.63)	(206.3)	(42.63)	(129.1)
37.09	206.6	37.09	127.8
(43.30)	(207.2)	(43.30)	(128.3)
38.24	208.5	38.24	126.7
(44.43)	(208.7)	(44.43)	(127.2)
38.89	209.3	38.89	125.7
(45.54)	(210.1)	(45.54)	(126.1)
40.15	211.2	40.15	124.3
(47.13)	(212.0)	(47.13)	(124.6)

Fluidity data are given within parentheses.

TABLE 56: Computed values employed in the plots of $E_{Y(cor)}$ (kJ/mol) versus T_o (K) and $E_{Y(cor)}$ versus $10^6 x V_o$ (m^3/mol), respectively, for $Cd(NO_3)_2.4.18H_2O$ + $MnCl_2$ molten salt system

$E_{Y(cor)}$	$T_{o,Y}$	$E_{Y(cor)}$	$V_{o,Y}$
28.09	189.5	28.09	130.7
(32.31)	(180.3)	(32.31)	(131.8)
28.31	190.5	28.31	129.1
(32.72)	(190.3)	(32.72)	(129.9)
29.10	191.6	29.10	127.5
(33.21)	(191.4)	(33.21)	(127.9)
29.37	192.7	29.37	125.9
(33.92)	(192.5)	(33.92)	(125.8)
30.05	193.7	30.05	124.3
(34.30)	(193.7)	(34.30)	(123.9)
30.29	194.8	30.29	122.7
(34.25)	(194.8)	(34.25)	(121.8)

Fluidity data are given within parentheses.

TABLE 57: Computed values employed in the plots of $E_{Y(cor)}$ (kJ/mol) versus T_o (K) and $E_{Y(cor)}$ versus $10^6 x V_o$ (m^3/mol), respectively, for $Ni(NO_3)_2.6.01H_2O$ + $Mg(NO_3)_2.6.13H_2O$ molten salt system

$E_{Y(cor)}$	$T_{o,Y}$	$E_{Y(cor)}$	$V_{o,Y}$
36.52	194.6	36.52	148.0
36.33	194.1	36.33	148.4
35.93	193.5	35.93	148.8
35.69	193.1	35.69	149.2
35.34	192.5	35.34	149.6
35.09	191.8	35.09	150.0
34.86	191.4	34.86	150.4

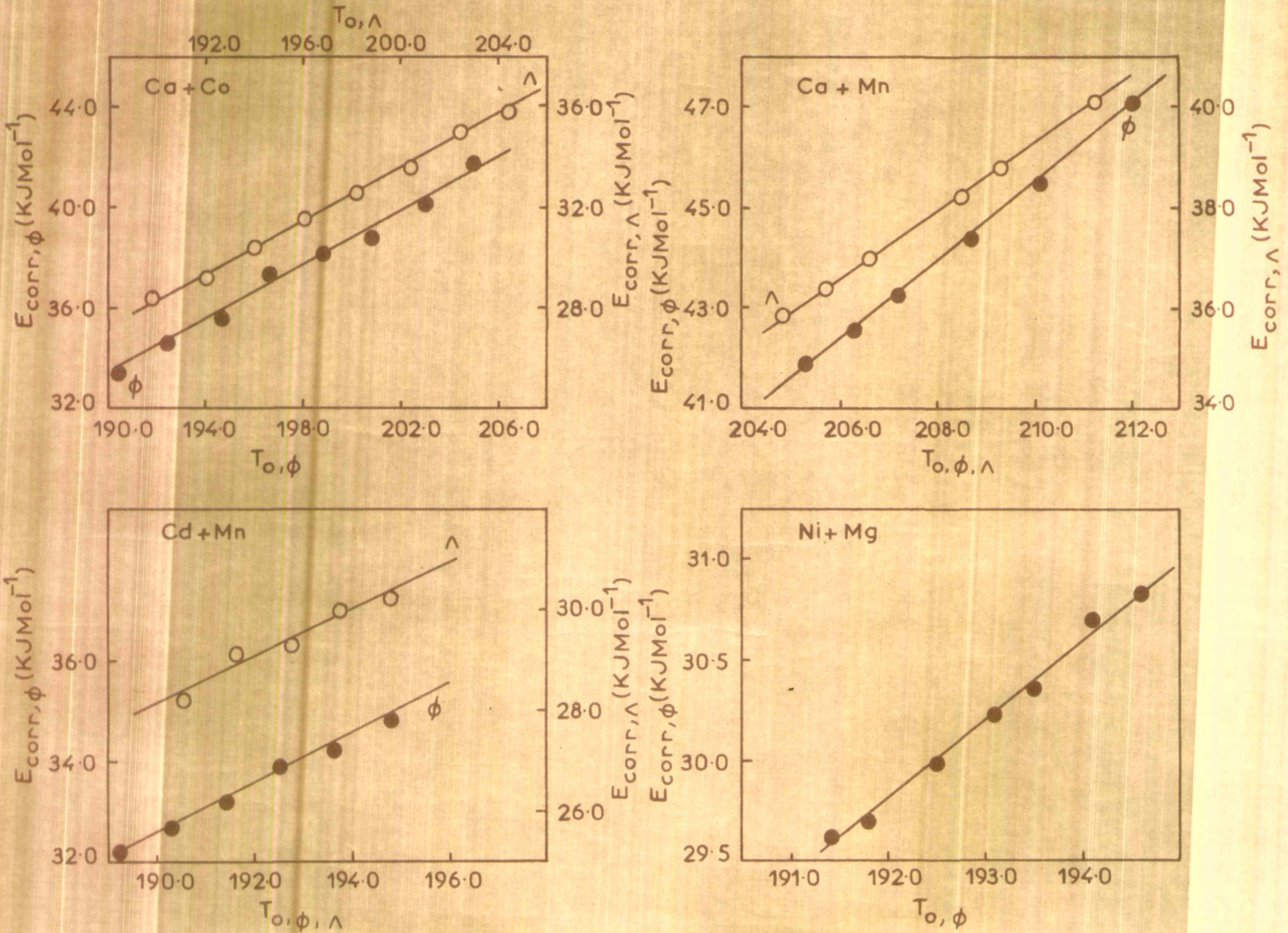

Fig. 38 Plots of $E_{corr, \phi, \wedge}$ Vs. T_o.

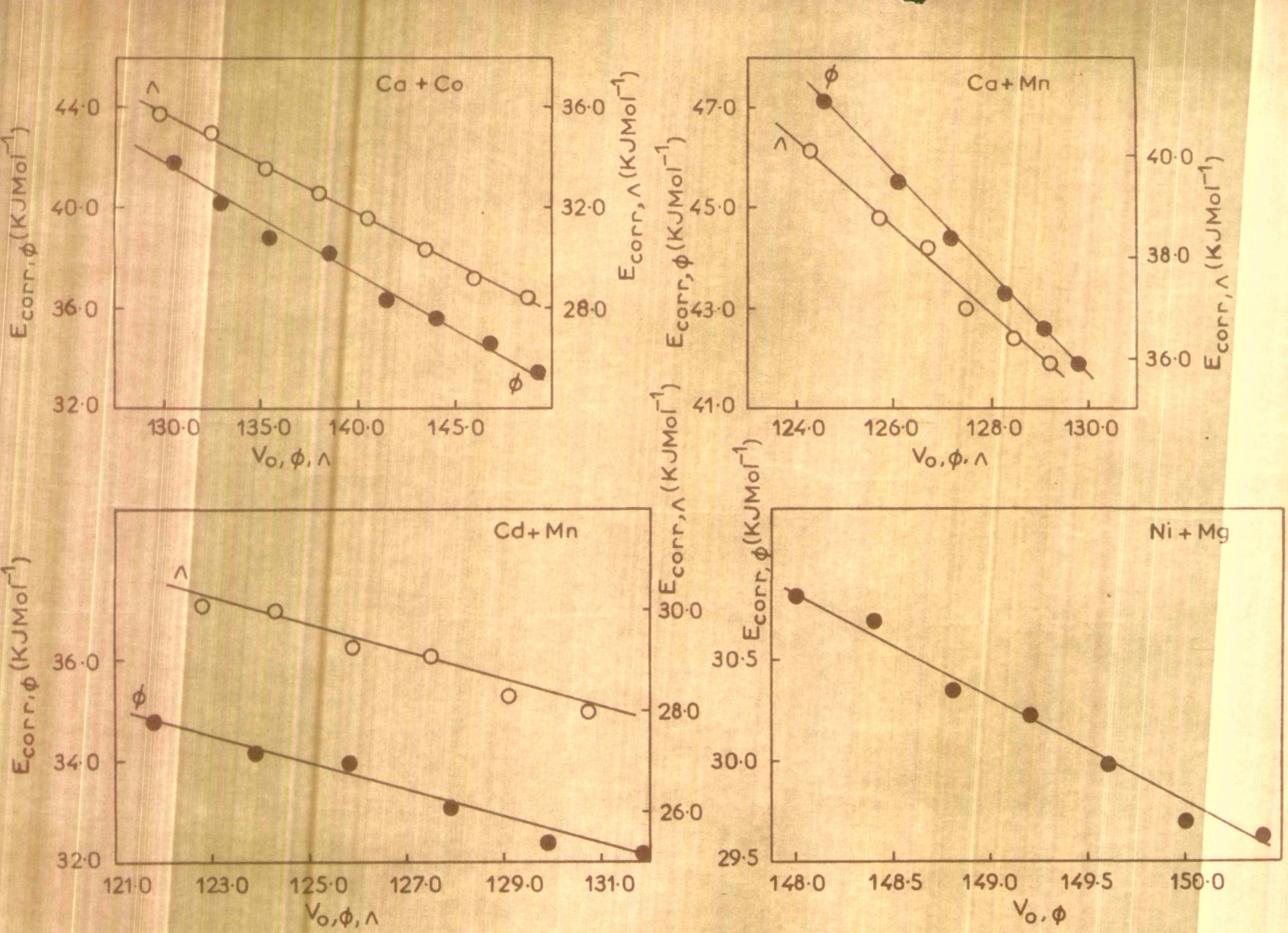

Fig.39 Plots of $E_{corr, \phi, \wedge}$ Vs. $V_{o, \phi, \wedge}$.

A P P E N D I X

APPENDIX

A. Viscosity of liquids: Let us consider a cylindrical liquid layer of area A sq. cm. moving over another similar layer at a distance of d cm. apart with a velocity difference of v cm. per sec.

The force of friction, f, required to maintain a uniform velocity gradient is given as

$$f \propto \frac{A\,v}{d}$$

or $$f = \eta \frac{A\,v}{d}$$

where η is a constant at a given temperature, depending upon the nature of the liquid and is known as the coefficient of viscosity,

$$\eta = \frac{f}{A}\left(\frac{d}{v}\right)$$

which may be defined as the force of friction between the two layers of a liquid moving past one another with different velocities. The reciprocal of viscosity is termed fluidity, ϕ.

The viscosity is expressed in the cgs unit as g/cm/sec and is denoted by "poise" and as N m^{-2}s (Newton per

square metre-sec) in the SI units. The poiseuill's equation employed for this purpose is given as

$$\eta = \pi r^4 t\ P/8V\ l$$

where V is the volume in ml. of the liquid flowing in t seconds through a narrow tube of radius r cm. and length l cm. under a hydrostatic pressure of P dynes/sq. cm. The hydrostatic pressure of a liquid column is given by

$$P = h\ \rho\ g$$

where h is the height of the column and ρ, the density of the liquid. The poiseuill's equation may, therefore, be written as

$$\eta = \pi r^4 t\ h\ \rho\ g/8V\ l$$

In actual practice the viscosity of the test liquid is measured with respect to a reference liquid. Let us take quinoline as the reference liquid; t_1 and t_2 be the times of flow of the same volume of quinoline and the test liquid through the same capillary tube, respectively, and η_1 and η_2 are their respective coefficients of viscosities then, we have,

$$\eta_1/\eta_2 = \pi r^4 t_1 h\ \rho_1 g \times 8V\ l/8V\ l \times \pi r^4 t_2 h\ \rho_2 g$$

or $$\eta_1/\eta_2 = \rho_1 t_1/\rho_2 t_2$$

where ρ_1 and ρ_2 are the densities of the reference and the test liquids, respectively.

Knowing the viscosity and density of quinoline at the required temperature and the times of fall of the two liquids, the viscosity of the test liquid can easily be calculated.

B. Calculation of Equivalent Conductance: Conductance being the reciprocal of resistance is expressed in mhos or S^{-1} where S stands for siemens. The specific conductance of a material is the reciprocal of specific resistance which is defined as the resistance of a specimen of a material of 1 cm. length and 1 sq. cm. in cross section. Thus, $K = 1/S$ where K represents the specific conductance while S denotes the specific resistance.

The equivalent conductance is calculated from the specific conductance data, equivalent weight, e, and the density ρ and is given as

$$\Lambda = \frac{Ke}{\rho} = V_e \qquad (1)$$

where V_e stands for the equivalent volume in ml. of the molten salt. Similarly, for mixtures of molten salts,

$$\Lambda = \frac{K\bar{e}}{\rho} \qquad (2)$$

where $\bar{e}$ is the mean equivalent weight calculated from the equation

$$\bar{e} = e_1 f_1 + e_2 f_2 \qquad (3)$$

where f_1 and f_2 are the equivalent fractions of component 1 and 2, respectively and e_1 and e_2 are their corresponding equivalent weights.

For W_1 gm. of component 1 mixed with W_2 gm. of component 2, the equivalent fractions are

$$f_1 = \frac{\frac{W_1}{e_1}}{\frac{W_1}{e_1} + \frac{W_2}{e_2}} \qquad (4)$$

and

$$f_2 = \frac{\frac{W_2}{e_2}}{\frac{W_1}{e_1} + \frac{W_2}{e_2}} \qquad (5)$$

By taking into account the defining relation of equivalent weight, the equivalent fraction, f, of equation (4) expressed as

$$f_1 = \frac{\frac{2W_1}{K_1}}{\frac{2W_1}{K_1} + \frac{2W_2}{K_2}} = \frac{2n_1}{2n_1 + 2n_2} \qquad (6)$$

where the M's are the molecular weights and n's the number of mols of the two components, 1 and 2.

If x be the mol fraction of component 1 mixed with (1-x) mol fraction of component 2, then

$$x = \frac{n_1}{n_1 + n_2} \quad \text{and} \quad (1-x) = \frac{n_2}{n_1 + n_2}$$

$$\frac{x}{(1-x)} = \frac{n_1}{n_2} \tag{7}$$

Substituting equation (7) into that of (6), we get

$$f_1 = \frac{2x}{2x + (1-x)} \tag{8}$$

Similarly for component 2

$$f_2 = \frac{(1-x)}{2x + (1-x)} \tag{9}$$

Thus the equation for the mean equivalent weight, $\bar{e}$ may be written as

$$\bar{e} = e_1 f_1 + e_2 f_2$$

or $$\bar{e} = \frac{2e_1 x}{2x + (1-x)} + \frac{e_2(1-x)}{2x + (1-x)} \tag{10}$$

which helps in calculating the mean equivalent weight, $\bar{e}$ for several values of the mol fraction.

C. (i) Activation Energy from the Arrhenius Equation: The Arrhenius equations for viscosity and fluidity are given as

$$Y\ (= \phi \text{ or } \lambda) = A_Y \exp\ (-E_Y/RT)$$

or
$$\ln Y = \ln A_Y - E_Y/RT \qquad (1)$$

Differentiating equation (1) with respect to the reciprocal of temperature (T^{-1}), we get,

$$\frac{d \ln Y}{d(1/T)} = -E_Y/R \qquad (2)$$

(ii) Activation Energy from the Vogel-Tammann-Fulcher (VTF) Equation: Similarly, differentiating the VTF equation,

$$Y\ (= \phi \text{ or } \lambda) = A_Y T^{-y2} \exp\left[-k_Y/(T-T_o)\right]$$

$$\ln Y = \ln A_Y - \tfrac{1}{2}\ln T - k_Y/(T-T_o)$$

with respect to the reciprocal of temperature, we get,

$$\frac{d \ln Y}{d(1/T)} = \left[\tfrac{1}{2}T - k_Y/(T-T_o)^2\right] \times T^2 \qquad (3)$$

Comparing equations (2) and (3), we get,

$$-E_Y/R = \left[\tfrac{1}{2T} - k_Y/(T-T_o)^2\right] \times T^2$$

or
$$E_Y = R\left[k_Y/(T-T_o)^2 - \tfrac{1}{2T}\right] \times T^2$$

The corrected energy may, therefore, be written as

$$E_{corr} = E_Y + \tfrac{1}{2}RT = Rk_Y \left[\frac{T}{(T-T_o)}\right]^2 \quad (4)$$

(iii) <u>Activation Energy from the Configurational Entropy Model (CEM)</u>: Similarly, we may differentiate the CEM equation,

$$Y\ (= \phi \text{ or } \Lambda) = A_Y \exp\left[-k_Y/T \ln (T/T_o)\right]$$

or $\ln Y = \ln A_Y - k_Y/T \ln (T/T_o)$ with respect to the reciprocal of temperature and get,

$$\frac{d \ln Y}{d(1/T)} = -k_Y \left[1 + \ln (T/T_o)/(\ln (T/T_o))^2\right] \quad (5)$$

Comparing equation (5) with that of (2), we get,

$$-E_Y/R = -k_Y \left[1 + \ln (T/T_o)/(\ln (T/T_o))^2\right]$$

or $$E_Y = Rk_Y \left[1 + \ln (T/T_o)/(\ln (T/T_o))^2\right] \quad (6)$$

(iv) <u>Activation Energy obtained from the computed parameters of the ERM equation</u>: The equation for viscosity based on ERM may be written as

$$\ln \eta = \ln (\theta_{\infty} A) + \left\{ \bar{E}_{\eta} + (\tfrac{1}{2}) C_{\theta\eta} \left[T_o^4 / (T_o^4 + \epsilon_{\theta\eta}^2 (T-T_o)^4) \right]^{3/2} \right\} / RT \tag{7}$$

$$\frac{\partial \ln \eta}{x} = \frac{\bar{E}_{\eta}}{R} + \frac{(\frac{1}{2}) C_{\theta\eta}}{R} \left[u + x \frac{du}{dx} \right] \tag{8}$$

$$\text{where } x = 1/T \text{ and } u = \left[\frac{T_o^4}{T_o^4 + \epsilon_{\theta\eta}^2 (T-T_o)^4} \right]^{3/2} = \left[\frac{T_o^4 x^4}{T_o^4 x^4 + \epsilon_{\theta\eta}^2 (1-T_o x)^4} \right]^{3/2} \tag{9}$$

Therefore,

$$\frac{du}{dx} = \tfrac{3}{2} \left[\frac{T_o^4 x^4}{T_o^4 x^4 + \epsilon_{\theta\eta}^2 (1-T_o x)^4} \right]^{1/2} \left[\frac{\{T_o^4 x^4 + \epsilon_{\theta\eta}^2 (1-T_o x)^4\} 4 T_o^4 x^3 - T_o^4 x^4 \{4 T_o^4 x^3 + 4 \epsilon_{\theta\eta}^2 (1-T_o x)^3 (-T)\}}{\{T_o^4 x + \epsilon_{\theta\eta}^2 (1-T_o x)^4\}^2} \right]$$

$$- \tfrac{3}{2} \left[\frac{T_o^4 x^4}{T_o^4 x^4 + \epsilon_{\theta\eta}^2 (1-T_o x)^4} \right]^{1/2} \left[\frac{4 T_o^4 x^3}{T_o^4 x^4 + \epsilon_{\theta\eta}^2 (1-T_o x)^4} - \frac{4 T_o^4 x^4 \{T_o^4 x^3 - T_o \epsilon_{\theta\eta}^2 (1-T_o x)^3}{\{T_o^4 x^4 + \epsilon_{\theta\eta}^2 (1-T_o x)^4\}^2} \right]$$

$$- \tfrac{3}{2} \left[\frac{T_o^4}{T_o^4 + \epsilon_{\theta\eta}^2 (T-T_o)^4} \right]^{1/2} \left[\frac{4 T_o^4 T^4}{T^5 \{T_o^4 + \epsilon_{\theta\eta}^2 (T-T_o)^4\}} - \frac{4 T_o^4 T^8 \{T_o^4 - T_o \epsilon_{\theta\eta}^2 (T-T_o)^3\}}{T^4 T^5 \{T_o^4 + \epsilon_{\theta\eta}^2 (T-T_o)^4\}^2} \right]$$

$$- \tfrac{3}{2} \left[\frac{T_o^4}{T_o^4 + \epsilon_{\theta\eta}^2 (T-T_o)^4} \right]^{3/2} \left[4T - \frac{4T \{T_o^4 - T_o \epsilon_{\theta\eta}^2 (T-T_o)^3\}}{T_o^4 + \epsilon_{\theta\eta}^2 (T-T_o)^4} \right]$$

$$- \frac{4 \times 3T}{2} \left[\frac{T_o^4}{T_o^4 + \epsilon_{\theta\eta}^2 (T-T_o)^4} \right]^{3/2} \left[\frac{T_o^4 + \epsilon_{\theta\eta}^2 (T-T_o)^4 - T_o^4 + \epsilon_{\theta\eta}^2 T_o (T-T_o)^3}{T_o^4 + \epsilon_{\theta\eta}^2 (T-T_o)^4} \right]$$

$$= 6T\left[\frac{T_o^4}{T_o^4 + \epsilon_{o\eta}^2 (T-T_o)^4}\right]^{3/2}\left[\frac{\epsilon_{o\eta}^2 (T-T_o)^3 (T-T_o+T_o)}{T_o^4 + \epsilon_{o\eta}^2 (T-T_o)^4}\right]$$

$$x\frac{\partial R}{\partial x} = 6\left[\frac{T_o^4}{T_o^4 + \epsilon_{o\eta}^2 (T-T_o)^4}\right]^{3/2}\left[\frac{T\epsilon_{o\eta}^2 (T-T_o)^3}{T_o^4 + \epsilon_{o\eta}^2 (T-T_o)^4}\right] \qquad (10)$$

On substituting equations (18) and (19) in equation (17) we obtain

$$\frac{\partial \ln \eta}{\partial x} = \frac{\partial \ln \eta}{\partial (1/T)} - \frac{\bar{E}_\eta}{R} + \frac{C_{o\eta}}{2R}\left[\left\{\frac{T_o^4}{T_o^4 + \epsilon_{o\eta}^2 (T-T_o)^4}\right\}^{3/2}\left\{1 + \frac{6T\epsilon_{o\eta}^2 (T-T_o)^3}{T_o^4 + \epsilon_{o\eta}^2 (T-T_o)^4}\right\}\right] \qquad (11)$$

On comparing equation (20) with equation (6) for viscosity, $\frac{\partial \ln \eta}{\partial (1/T)} = E_\eta/R$ the expression obtained is

$$E_\eta = \bar{E}_\eta + \frac{C_{o\eta}}{2}\left[\frac{1}{1 + \epsilon_{o\eta}^2 (T/T_o - 1)^4}\right]^{3/2}\left[1 + \frac{6\epsilon_{o\eta}^2 (T/T_o)(T/T_o - 1)^3}{1 + \epsilon_{o\eta}^2 (T/T_o - 1)^4}\right] \qquad (12)$$

Similar expression can be obtained for E_λ.

A P P E N D I X D

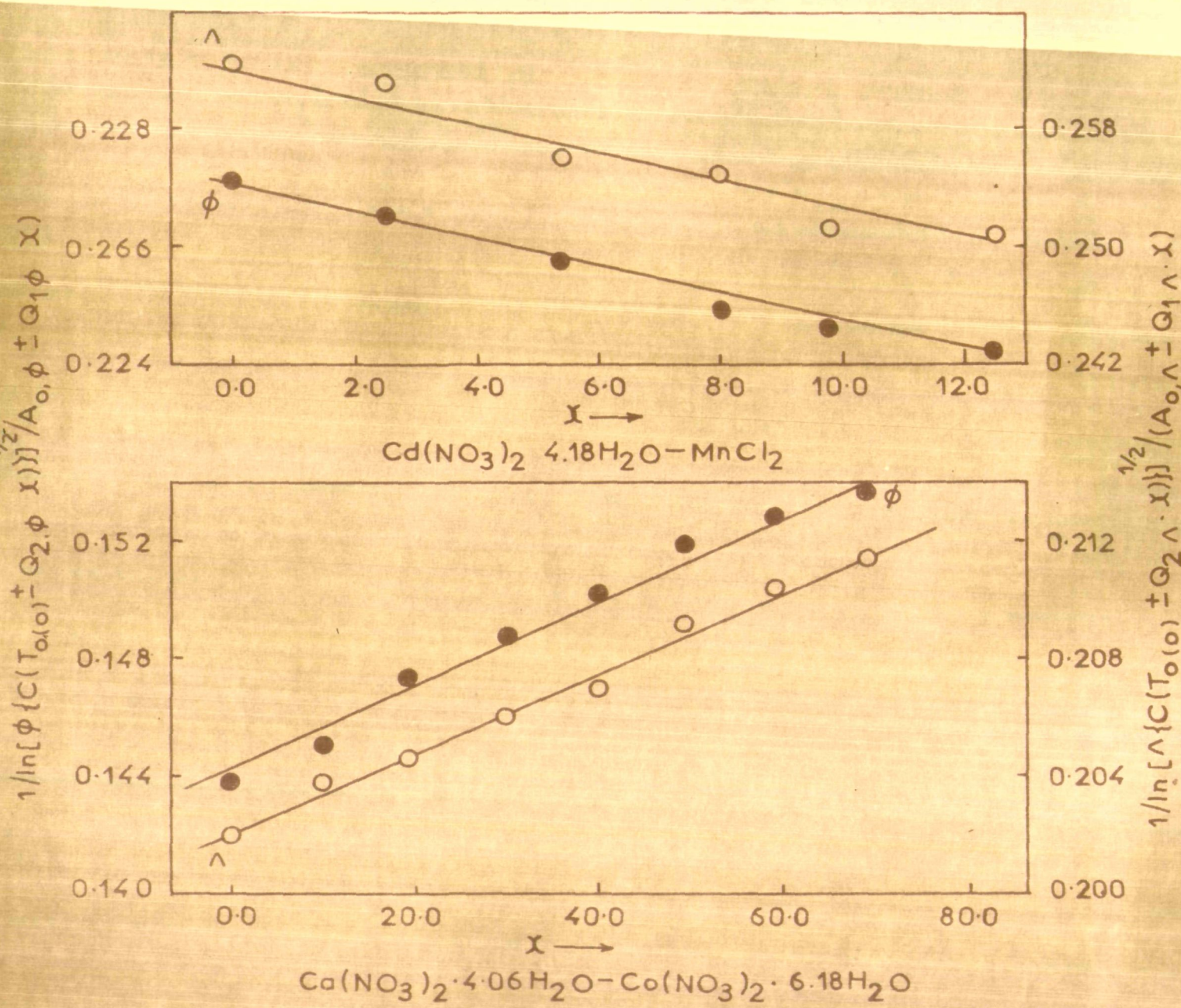

FIG. 32 (a) Plots of $1/\ln[Y\{C(T_{o(o)} \pm Q_{2Y} \cdot X)\}]^{1/2}/(A_{oY} \pm Q_{1Y} X)$ Vs X(=Mol % of solute) for $Cd(NO_3)_2 \cdot 4{\cdot}18H_2O - MnCl_2$ and $Ca(NO_3)_2\ 4{\cdot}06H_2O - Co(NO_3)_2\ 6{\cdot}18H_2O$ Molten salt systems.

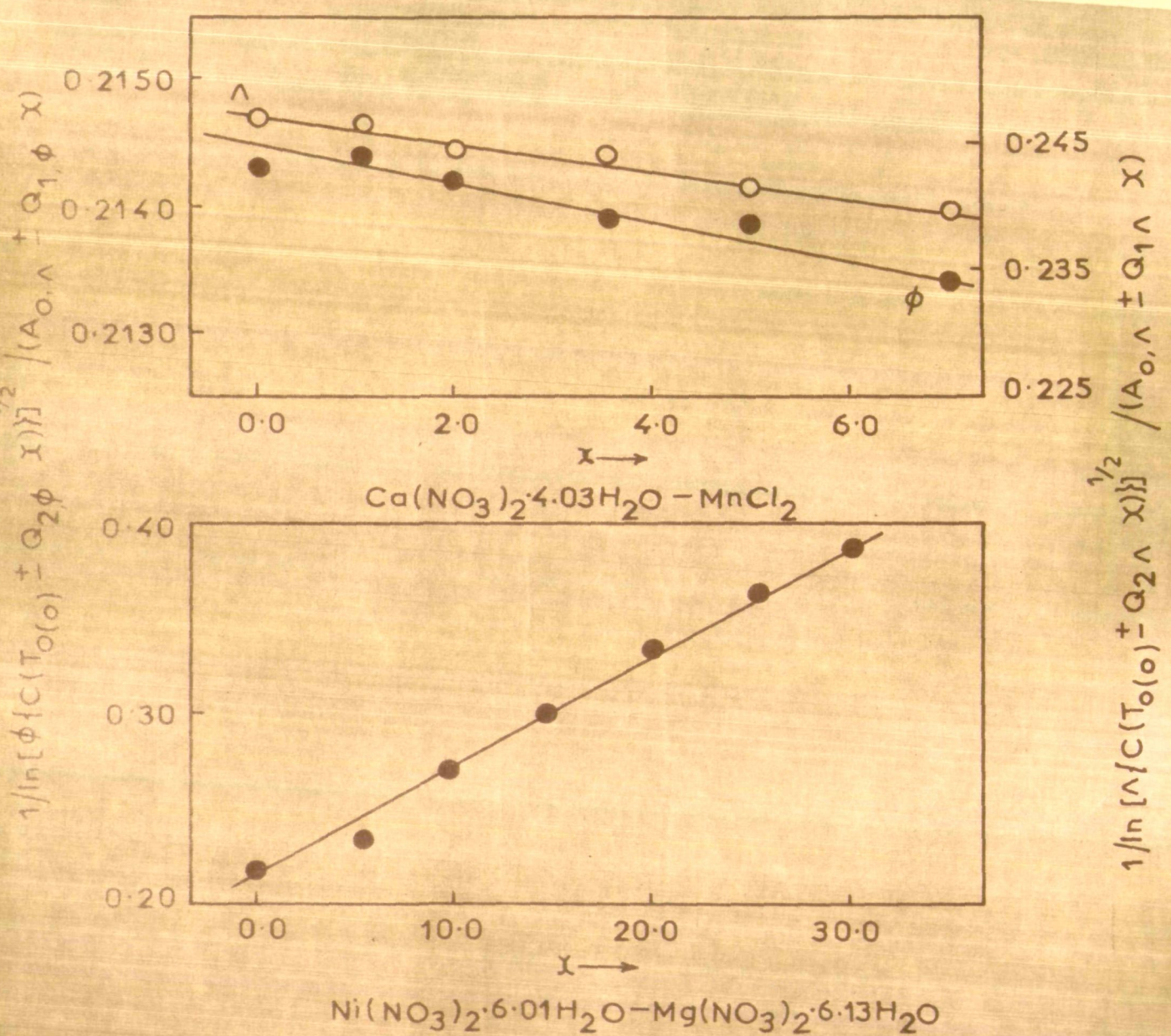

FIG 32 (a) Plots of $1/\ln[Y\{C(T_{o(o)} \pm Q_{2Y} \cdot X)\}]^{1/2}/(A_{oY} \pm Q_{1Y} X)$ Vs. X (= Mol % of solute) for $Ca(NO_3)_2 \cdot 4.03H_2O - MnCl_2$ and $Ni(NO_3)_2 \cdot 6.01H_2O - Mg(NO_3)_2 \cdot 6.13H_2O$ Molten salt system.

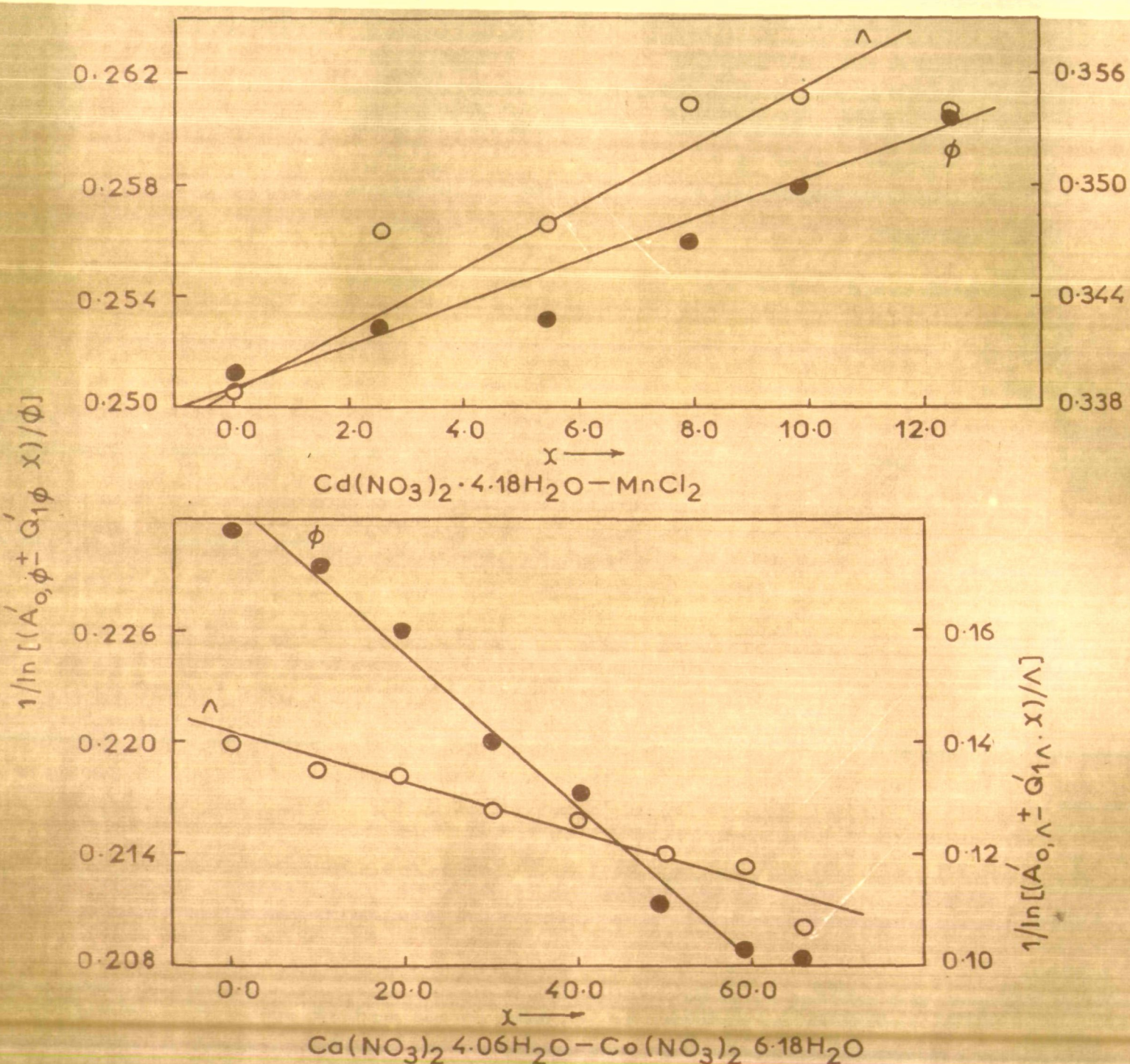

FIG. 32 (b) Plots of $1/\ln[(A'_{o,Y} \pm Q'_{1Y} X)/Y(=\phi \text{ or } \Lambda)]$ Vs. X(= Mol. % of solute) for $Cd(NO_3)_2 \cdot 4{\cdot}18H_2O - MnCl_2$ and $Ca(NO_3)_2 \cdot 4{\cdot}06H_2O - Co(NO_3)_2 \cdot 6{\cdot}18H_2O$ Molten salt systems.

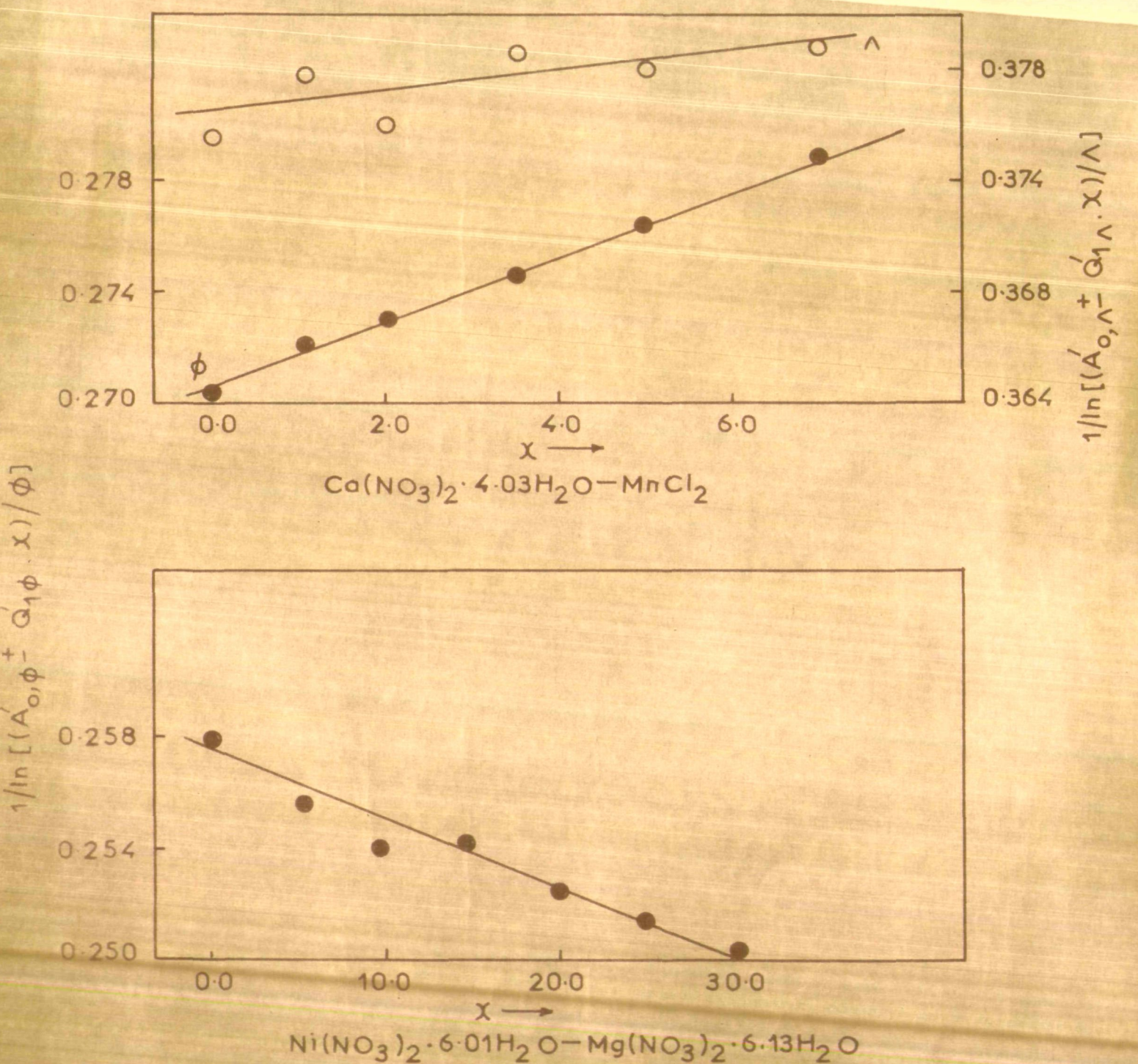

FIG. 32 (b) Plots of $1/\ln[(A'_{o,Y} \pm Q'_{1Y} \cdot X)/Y(=\Phi \text{ or } \wedge)]$ Vs. X (Mol.% solute) for $Ca(NO_3)_2 \cdot 4{\cdot}03H_2O - MnCl_2$ and $Ni(NO_3)_2 \cdot 6{\cdot}01H_2O - Mg(NO_3)_2 \cdot 6{\cdot}13H_2O$ Molten salt systems.

B I B L I O G R A P H Y

BIBLIOGRAPHY

1. D. Turnbull and M. H. Cohen, J. Chem. Phys., 29, 1049 (1958).
2. W. Kauzmann, Chem. Rev., 43, 219 (1948).
3. A. J. Batschinski, Z. Physik. Chem., 84, 644 (1913).
4. H. Eyring, J. Chem. Phys., 4, 283 (1936).
5. G. Adam and J. H. Gibbs, J. Chem. Phys., 43, 139 (1965).
6. T. G. Fox and P. J. Flory, J. Appl. Phys., 21, 581 (1950); J. Phys. Chem., 55, 221 (1951); J. Polymer Sci., 14, 315 (1954).
7. A. K. Doolittle, J. Appl. Phys., 22, 1471 (1951).
8. M. L. Williams, R. F. Landel, and J. D. Ferry, J. Am. Chem. Soc., 77, 3701 (1955).
9. M. H. Cohen and D. Turnbull, J. Chem. Phys., 31, 1164 (1959).
10. A. J. Barlow, J. Lamb, and A. J. Matheson, Proc. Roy. Soc. (London), 292, 322 (1966).
11. C. A. Angell, J. Chem. Phys., 46, 4673 (1967).
12. C. A. Angell, J. Phys. Chem., 70, 3988 (1966); ibid., 69, 2137 (1965).

13. C. A. Angell, J. Phys. Chem., 68, 1917 (1964).

14. C. T. Moynihan, C. R. Smalley, C. A. Angell, and E. J. Sare, J. Phys. Chem., 73, 2287 (1969).

15. N. Islam and M. R. Islam, Ind. J. Chem., 12, 704 (1974).

16. N. Islam, M. R. Islam, S. Ahmad, and B. Waris, Appl. Spectrosc., 29, 68 (1975).

17. N. Islam, M. R. Islam, S. Ahmad, and B. Waris, J. Am. Chem. Soc., 97, 3026 (1975).

18. N. Islam and Ismail K., J. Phys. Chem., 79, 2180 (1975); ibid., 80, 1929 (1976).

19. N. Islam, M. R. Islam, B. Waris, and Ismail K, J. Phys. Chem., 80, 291 (1976).

20. J. H. Simmons and P. B. Macedo, J. Chem. Phys., 54, 1325 (1971).

21. L. L. Sperry and J. D. Mackenzie, Phys. Chem. Glasses, 9, 91 (1968).

22. J. H. Hildebrand and R. H. Lamoreaux, J. Phys. Chem., 77, 1471 (1973); J. H. Hildebrand, Science, 174, 490 (1971).

23. H. Bloom, "The Chemistry of Molten Salts", W. A. Benjamin, Inc., New York, N.Y., 1967, p. 100.

24. H. Tweer, J. H. Simmons, and P. B. Macedo, J. Chem. Phys., 54, 1952 (1971).

25. N. Islam, S. Kumar, and K. P. Singh, J. C. S. Faraday Trans. 1, 75, 1830 (1979).

26. J. H. Kleinhekzel and H. C. Kremers, J. Am. Chem. Soc., 50, 959 (1928).

27. C. T. Moynihan, J. Phys. Chem., 70, 3399 (1966).

28. W. W. Ewing and R. J. Mikovsky, J. Am. Chem. Soc., 72, 1390 (1950).

29. C. N. Reilly, R. W. Schmid, and Fawzy S. Sadek, J. Chem. Edu., 36, 555 (1959); ibid., 36, 619 (1959).

30. C. Tanford, "Physical Chemistry of Macromolecules", John Wiley and Sons, Inc., New York, N.Y., 1961, p. 329.

31. R. E. Hester and R. A. Plane, J. Chem. Phys., 40, 411 (1964).

32. J. P. Mathieu and M. Loumsbury, Discussion Faraday Soc., 9, 196 (1950).

33. C. A. Angell and R. D. Brassel, J. Phys. Chem., 76, 3244 (1972).

34. N. Islam, S. Kumar, and K. P. Singh, Can. J. Chem., 56, 1231 (1978).

35. N. Islam, K. P. Singh, and S. Kumar, J. Electrochem. Soc., 126, 1876 (1979); Bull. Chem. Soc. Jpn., 52, 579 (1979).

36. D. Turnbull and M. H. Cohen, "Modern Aspects of the Vitreous State", J. D. Mackenzie, Ed. Butterworth's Scientific Publications, Ltd., London, 1960.

37. C. A. Angell, J. Am. Ceram. Soc., 51, 117 (1968).

38. C. A. Angell, J. Electrochem. Soc., 112, 1224 (1965).

39. C. A. Angell, J. Phys. Chem., 70, 2793 (1966).

40. J. H. Gibbs and E. A. Dimarzio, J. Chem. Phys., 28, 373 (1958); ibid., 28, 807 (1958); J. Polymer Sci., 40, 121 (1959).

41. C. T. Moynihan and C. A. Angell, J. Phys. Chem., 74, 736 (1970).

42. J. Frenkel, "Kinetic Theory of Liquids", Dover Publications, Inc., New York, N.Y., 1955, pp. 197-200.

43. A. A. Miller, J. Phys. Chem., 67, 1031 (1963).

44. N. Islam, S. Kumar, and K. P. Singh, Bull. Chem. Soc. Jpn., 51, 2712 (1978).

45. N. Islam, K. P. Singh, and S. Kumar, J. C. S. Faraday Trans. 1, 75, 1312 (1979).

46. N. Islam and A. Ali, Bull. Chem. Soc. Jpn., 53, (1980).